From IUF – Leibniz Research Institute for Environmental Medicine
at Heinrich Heine University Düsseldorf

Establishment of an Adverse Outcome Pathway-informed testing battery for predicting Parkinsonian Motor Deficits *in vitro*

Dissertation

to obtain the academic title of Doctor of Philosophy (PhD) in Medical Sciences
from the Faculty of Medicine at Heinrich Heine University Düsseldorf

submitted by
Mohamed Elgamal
(2020)

Printed with the support of the German Academic Exchange Service

As an inaugural dissertation printed by permission of the Faculty of Medicine at Heinrich Heine University Düsseldorf

Signed:
Dean: Prof. Dr. Nikolaj Klöcker
Examiners: Prof. Dr. Ellen Fritsche
PD Dr. Markus Butz

Zusammenfassung

Die Parkinson-Krankheit (PD) ist die zweithäufigste neurodegenerative Krankheit im Alter und betrifft etwa 1% der über 60-jährigen Bevölkerung. Viele epidemiologische Studien und Tierstudien unterstützen die Hypothese, dass die Exposition gegenüber Pestiziden das Risiko an Parkinson zu erkranken erhöht. Allerdings sind die Ergebnisse dieser Studien nicht eindeutig. Daher empfiehlt die europäische Behörde für Lebensmittelsicherheit (EFSA) den Einfluss von Pestiziden auf die Parkinson Krankheit durch Anwendung des ‚Adverse Outcome Pathway' (AOP) Konzepts erneut zu überprüfen. Basierend auf den Empfehlungen der EFSA, sollte in dieser Arbeit eine humane *in vitro* Batterie zur Gefahrenerkennung etablieren werden, welche auf den Wirkmechanismen (Mode-of-Action) der Parkinson Krankheit sowie auf den zugehörigen AOPs basiert. Um dieses Ziel zu erreichen, wurden zwei Testsysteme zur Untersuchung dopaminerger Neurone (DNs) etabliert. Zum einen wurden DNs durch Differenzierung humaner induzierter pluripotenter Stammzellen (hiPSCs) gewonnen. Zum anderen wurde eine humane Zellkultur aus dem Mesencephalon (LUHMES) verwendet. Mit letzterem Testsystem gelang die Etablierung verschiedener Assays, welche die Schlüsselereignisse (Key Events; KEs) der Parkinson-AOPs abbilden. Die Untersuchung dieser KEs basiert auf der Bestimmung der Zell Viabilität durch Messung der Reduktaseaktivität und der Adenosintriphosphat (ATP) Produktion, der Bestimmung der proteasomalen Aktivität, der Messung von Zytotoxizität, sowie der Identifizierung von Apoptose. Mit Hilfe von zwei Modelsubstanzen für Parkinson, Rotenon und Paraquat, konnte so eine Testbatterie basierend auf LUHMES Zellen etabliert werden. Zur Sicherstellung der Spezifität der Batterie wurden die Negativsubstanzen Saccharin und Diethylenglycol getestet. Des Weiteren wurde der konzentrations- und zeitabhängige Effekt der häufig verwendeten Organophosphat-Pestizide (Chlorpyrifos, Parathion, Malathion und Dichlorovos) sowie deren Oxon-Metabolite untersucht. Veränderungen des intrazellulären Metaboloms während der LUHMES Differenzierung und der Exposition mit Pestiziden wurden mit Hilfe der Kernspinresonanzspektroskopie bestimmt. Alle Organophosphat-Pestizide sowie deren Metabolite verursachten Zytotoxizität und reduzierten die Zell Viabilität. Dabei sind die Aktivitätsprofile von Chlorpyrifos und Parathion vergleichbar mit Rotenon, während die von Malathion und Dichlorovos vergleichbar mit Paraquat sind. Es wurden außerdem eindeutige metabolische Veränderungen durch die Differenzierung und die Exposition mit Pestiziden hervorgerufen, was den Mehrwert der Metabolomanalyse für die Gefahrenerkennung verdeutlicht. Zusammenfassend konnte gezeigt werden, dass sich Substanzeffekte auf frühe KEs der Parkinson Krankheit in einer auf LUHMES Zellen basierenden Testbatterie identifizieren lassen. Jedoch müssen weiterführende Arbeiten zeigen, ob diese Effekte spezifisch für dopaminerge Neurone sind.

Summary

Parkinson's disease (PD) is the second most common neurodegenerative disorder of the elderly affecting approximately 1% of the population older than 60 years old. Numerous epidemiological and animal studies have supported the hypothesis that exposure to pesticides can increase the risk for developing PD, however, the results of these studies are not conclusive. Therefore, the European Food Safety Authority (EFSA) recommended the reassessment of the hypothesis that some pesticides may cause Parkinsonian motor deficits (PMD) using the adverse outcome pathway (AOP) concept. Based on the recommendations of EFSA, this work aimed to establish an AOP-informed and mode-of-action-based human *in vitro* test battery for hazard identification. Therefore, two test systems were established to obtain dopaminergic neurons, i.e. differentiated human induced pluripotent stem cells (hiPSCs) and Lund human mesencephalic (LUHMES) cells. A test battery based on dopaminergic neurons differentiated from LUHMES cells was successfully established. This human cellular model was used to establish assays based on key events (KEs) of the proposed AOPs using two model compounds for PMD, rotenone and paraquat. Those KEs are represented by the assessment of cell viability based on reductase activity and adenosine triphosphate (ATP) production, proteasomal activity, cytotoxicity and apoptosis. In order to determine the specificity of this test battery, the negative compounds saccharin and diethylene glycol were tested. The concentration- and time-dependent effects of the commonly used organophosphate pesticides chlorpyrifos, parathion, malathion and dichlorvos, as well as their oxon metabolites were investigated using this test battery. Moreover, changes of the metabolome during neuronal differentiation and in response to pesticides on differentiated LUHMES cells were assessed. All organophosphate pesticides and their metabolites affect at least cytotoxicity and cell viability based on reductase activity and ATP levels in the test battery. Thereby, the activity profiles of chlorpyrifos and parathion are similar to that of rotenone, while the effects of malathion and dichlorvos resemble paraquat responses. Furthermore, clear metabolome changes were detected during the neuronal differentiation of LUHMES cells and after exposure to pesticides, which indicate the potential value of implementing this approach for the toxicological assessments in the future. Notably, LUHMES cells seem to be a suitable model to identify if a compound affects early KEs of the AOP leading to PMD. However, future work needs to shed light on the specificity of the effects for dopaminergic neurons.

List of abbreviation

°C	Degree Celsius	**CTG assay**	Cell Titer-Glo assay
95% CI	95% confidence interval	**CYP2B enzyme**	Cytochrome p450 2B subfamily (CYP2B) enzyme
Ala	alanine	**DAT**	Dopamine transporter
ANOVA	Analysis of variance	**ddH_2O**	Double distilled water
AO	Adverse outcome	**DMEM**	Dulbecco's Modified Eagle Medium
AOP	Adverse outcome pathway	**DMSO**	Dimethyl sulfoxide
Asp	Aspartate	**DNA**	Deoxyribonucleic acid
ATCC	American-Type-Culture-Collection	**EFSA**	European Food Safety Authority
ATP	Adenosine triphosphate	**ENO2**	Neuron-specific enolase
BCA assay	Bicinchoninic acid assay	**ETC**	Electron transport chain
BDNF	Brain-derived neurotrophic factor	**$FADH_2$**	Flavin adenine dinucleotide
BSA	Bovine serum albumin	**FCS**	Fetal calf serum
CI	Mitochondrial complex I	**FGF**	Fibroblast growth factor
CII	Mitochondrial complex II	**FGF8b**	Fibroblast growth factor-8b
CIII	Mitochondrial complex III	**GDNF**	Glial cell line-derived neurotrophic factor
CIV	Mitochondrial complex IV	**GIRK**	G protein-gated inwardly rectifying potassium channels
CV	Mitochondrial complex V	**Gln**	Glutamine
Ca^{2+}	Calcium	**Glu**	Glutamate
cAMP	Cyclic adenosine monophosphate	**Gly**	Glycine
cDNA	Copy DNA	**GPC**	Glycerophosphocholine
Cit	Citrate	**GSH**	Glutathione
CS	CS Corpus striatum	**hiPSCs**	Human induced pluripotent stem cells
CTB assay	CTB assay Cell Titer Blue assay	**HR ^{1}H NMR**	High-resolution proton magnetic resonance spectroscopy

IATA	Integrated approaches for testing and assessment	**PMD**	Parkinsonian motor deficits
IC50	Half maximal inhibitory concentration	**P-value**	Probability value
ICC	Immunocytochemistry	**qRT-PCR**	Quantitative real time polymerase chain reaction
iPSC	Induced pluripotent stem cells	**RNA**	Ribonucleic acid
IVIVE	In vitro in vivo Extrapolation	**ROS**	Reactive oxygen species
KER	Key events relationship	**Rpm**	Revolutions per minute
KEs	Key events	**SAG**	Smoothened agonist
KSR	Knockout serum replacement	**SDs**	Standard deviations
Lac	Lactate	**SEM**	Standard error of mean
LDH	Lactate dehydrogenase	**SK channels**	Small-conductance calcium-activated potassium channels
LUHMES cells	Lund human mesencephalic cells	**SN**	Substantia nigra
MIE	Molecular initiating event	**Suc**	Succinate
ML	Milliliter	**TCA cycle**	Tricarboxylic acid cycle
MoA	Mode of action	**tCho**	Total choline
MPP+	1-methyl-4-phenylpyridinium	**TGF β3**	Transforming growth factor-β3
MPTP	1-methyl-4-phenyl-1,2,3,6-tetrahydropyridine	**TH**	Tyrosine hydroxylase
Myo	Myo-Inositol	**TSP**	3-(Trimethylsilyl) propanoic acid
n. d.	Not detected	**Tyr**	Tyrosine
NAA	Naphthaleneacetic acid	**UKN**	University of Konstanz
NADH	Nicotinamide adenine dinucleotide	**UPP**	Ubiquitin proteasome pathway
NSP	Nigrostriatal pathway	**Val**	Valine
PBS	Phosphate Buffered Saline	**WOE**	Weight of evidence
PC	Phosphocholine	**αKG**	Alpha-ketoglutarate
PCR	Polymerase chain reaction	**µg**	Microgram
PD	Parkinson’s disease	**µL**	Microliter
Phe	Phenylalanine	**µM**	MicroMolar

Table of contents

1 Introduction

1.1 Parkinson's disease

Parkinson's disease (PD) is a progressive degenerative disorder of the central nervous system that primarily affects motor systems. Resting tremors of the hands are recognisable signs of the disease in affected individuals, with time as the disorder develops the symptoms include general shaking, slow movement and difficulty to walk (Parkinson, 2002; Marino *et al.*, 2019). In the advanced stages, the disease includes wide spectrum non-motor symptoms including dementia and behavioural difficulties, such as depression (Poewe, 2008).

PD is the second most common neurodegenerative disorder in the elderly. Approximately 1% of those over 60 years of age are diagnosed with this debilitating disease (Hirtz *et al.*, 2007). In 2012, Khedr *et al*. in their suggested prevalence of PD was higher among rural populations, for example Egypt, in comparison to the industrialized countries. This observation correlates with exposure to pesticides being one reported factor for the development of the disease (Rösler *et al.*, 2018).

To date, there are no curative options available for PD or reverse the disease progression. However, one or a combination of therapeutic agents, surgery and physiotherapy may help to ameliorate the symptoms (Toulouse and Sullivan, 2008; Oertel, 2017). It is estimated the annual cost of PD is around 20000 US dollars. Much of the cost is related to the clinical management of the disease, i.e. medications, surgical intervention, deep brain stimulation and physiotherapy. However, PD also imposes indirect costs, i.e. the economical cost to the individual and the family, including decreased work efficiency, loss of working hours and the need for the family to provide support and care for the affected family member (Dowding *et al.*, 2006; Kowal *et al.*, 2013; Bovolenta *et al.*, 2017; Martinez-Martin *et al.*, 2019).

1.2 Pathophysiological changes in Parkinson's disease

The commonly observed symptoms of Parkinsonian motor deficits (PMD) such as tremors, bradykinesia and rigidity are generally accepted to be due to the degeneration of dopaminergic neurons that project from the substantia nigra (SN) to corpus striatum (CS), as reviewed by Alexander, (2004).

Reported evidence implies the sub-optimum functioning of the mitochondria, which are the powerhouse of a cell, is a contributing factor for the PD syndrome (Siekevitz, 1957; Winklhofer and Haass, 2010). A series of biochemical reactions within the mitochondria, known as the tricarboxylic acid cycle (TCA cycle) yield a number of reduced co-enzymes that are oxidized by the electron transport chain (ETC) to yield energy in the form of adenosine triphosphate (ATP; Stenesh, 1998). In addition, these series of chemical reactions yield reactive oxygen species (ROS) which are degraded by functional mitochondrial complex (CI). It is generally accepted a consequence of CI dysfunction is decreased energy production, in the form of reduced ATP and increased oxidative stress, as previously reviewed (Lazarou *et al.*, 2009; Zhao *et al.*, 2019).

Therefore, CI dysfunction is associated with failure of energy production and oxidative stress (Raha and Robinson, 2000). Consistent with these observations, an adult male injected with the synthetic analogue of meperidine called 1-methyl-4-phenyl-1,2,3,6-tetrahydropyridine (MPTP) would develop PMD like characteristics (Davis *et al.*, 1979). This is because MPTP is a potent CI inhibitor and thereby reduces intracellular ATP levels (Ramsay *et al.*, 1986; Nicklas *et al.*, 1987). Furthermore, investigators have reported inducing PD like syndrome in animals administered MPTP (Bové and Perier, 2012). Moreover, observations imply the impairment of the CI is restricted to the SN and other regions of the brain of patients with PD are unaffected (Schapira *et al.*, 1990; Devi *et al.*, 2008).

As well as being the powerhouse, mitochondria also play a role in controlling apoptotic pathways (Van Loo *et al.*, 2002). The activation of the proapoptotic and inactivation of antiapoptotic proteins resulting in the translocation of Bax proteins into the mitochondria. These events stimulate the release of cytochrome c into the cytoplasm to induce the cleavage of caspase 3/7, which is ATP dependent, as reviewed by Wang and Youle, (2009). In 1996, Mochizuki *et al.* observed the degeneration of dopaminergic neurons in the SN of PD patients as reflected by the apoptotic process.

Demonstration of α-synuclein protein aggregates in the brain cell inclusions is generally accepted to be the gold standard for neuropathological evaluation of PD (Stefanis, 2012). These α-synuclein aggregates are degraded by the ubiquitin proteasome pathway (UPP), an observation supported by the finding that impairment of the UPP leads to the aggregation and accumulation of α-synuclein. The net result of this impairment is degeneration of dopaminergic neurons in the SN, ultimately

leading to motor impairment, which is the hallmark of PD (McNaught and Jenner, 2001; McNaught *et al.*, 2004; Bentea *et al.*, 2015).

Briefly, the ubiquitinated proteins are recognized by a very large multicatalytic protease complex called the 26S proteasome as proteins destined for degradation to small peptides. The 26S complex comprises a central barrel-shaped 20S proteasome with a 19S regulatory particle at either or both its ends. The 20S proteasome is a hollow cylinder containing the mechanisms of protein degradation. It is constructed from four stacked hollow rings, each of which contains seven distinguishable but related subunits. The two outer α rings are identical as are the two inner β rings. Three of the subunits in the β rings contain the proteolytic active sites, which are positioned on the interior surface of the cylindrical structure. The outer α subunits of the 20S particle surround a narrow, central and gated pore which are the entry and exit points of the substrates and products, respectively. Substrate entry is itself a complex process catalyzed by the 19S unit. The UPP ensures compartmentalization of proteolysis and prevents nonspecific destruction of cellular proteins as previously reviewed (Lecker et al., 2006; Leestemaker and Ovaa, 2017).

1.3 Pesticides as a potential risk factor in Parkinson's disease

Of the patients diagnosed with PD, 5-15% are to well-identified genetic mutations. For the remainder, the causal agents are unidentified. This group of PD patients are classified as idiopathic PD. One causal agent, as mentioned above, maybe exposure to pesticides (Klein and Westenberger, 2012; Ball *et al.*, 2019).

Pesticides are used worldwide in the agricultural sector to maximise crop production. It is estimated that the annual global usage of pesticides is around two million tonnes. This usage is expected to increase to 3.5 million tonnes in 2020 (Sharma *et al.*, 2019). The worldwide use of pesticide is shown in Fig.1.

Among the numerous pesticides used within agriculture for nearly one century is rotenone (Clark, 1929). This pesticide is known to be a potent CI inhibitor and is used for inducing PD like syndrome in animal models (Talpade *et al.*, 2008; Cannon *et al.*, 2009). Another commonly used herbicide is paraquat as a redox cycler with a chemical structure similar to the active metabolite of MPTP (Shimizu *et al.*, 2001; Somayajulu-Niţu *et al.*, 2009). Animals administered paraquat have been reported to have

decreased dopaminergic contents in the nigrostriatal pathway (NSP) and induced motor impairment (Liou *et al.*, 1996; Brooks *et al.*, 1999). Similarly, administration of one of the following organophosphate pesticides, chlorpyrifos, parathion, malathion and dichlorvos to animals induced a variable degree of affecting the dopaminergic neurons in SN and fibres in CS leading to motor impairment (Zhu *et al.*, 2001; Binukumar *et al.*, 2010; Deveci and Karapehlivan, 2018; Mohammadzadeh *et al.*, 2018). These animal model data were supported by a study assessing the correlation between the risk of PD and pesticides (Tanner *et al.*, 2011). These authors suggested that CI inhibitors and oxidative stressors, e.g. rotenone and paraquat, respectively increased the risk of PD.

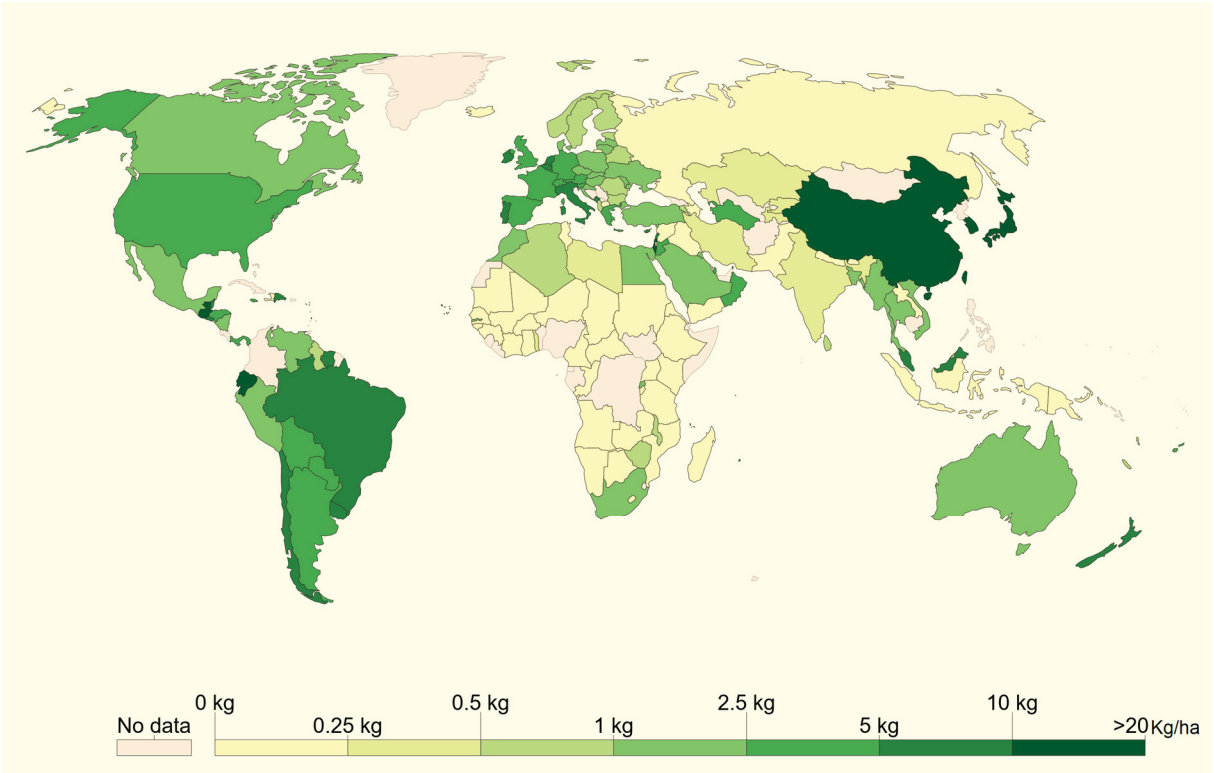

Fig.1: Worldwide pesticide use. The map displays the average pesticides' application per unit of cropland from 1990 to 2017. The map was adapted from Roser (2020). Ha, hectare, Kg: kilogram.

A meta-analysis of published data between 1985 and 2011 demonstrated a significant increase in the risk of PD with occupational exposure to pesticides. Although it was noted that the correlation was variable and inconsistent (Van Maele-Fabry *et al.*, 2012). A more recent meta-analysis by other investigators has reported a higher risk of PD with exposure to pesticides (Gunnarsson and Bodin, 2017). Overall data implies the

risk of PD is greater with occupational than the non-occupational exposure to pesticides. Furthermore, the risk of PD increases among individuals occupational exposure to organophosphate pesticides (Allen and Levy, 2013) including chlorpyrifos, malathion and parathion. In keeping with these observations, investigators have reported a prolonged exposure to pesticides is associated with a higher risk of PD (Narayan *et al.*, 2017). These data of increased risk of PD is supported by a study among Egyptians exposed to pesticides (Rösler *et al.*, 2018). In addition, a review by European Food Safety Authority (EFSA) of the studies conducted between 2006 and 2012 whilst revealing an association between exposure to pesticides and the risk of developing PD, the correlation was not absolute (Ntzani *et al.,* 2013). The summary of the association of PD with exposure to pesticides is presented in table 1.

Table 1: Association of PD with pesticides

Pesticide/Pesticide class	OR/RR *(95% CI)*
Pesticide mixture[1]	1.28 (1.03 – 1.59)
Pesticide mixture[2]	1.67 (1.42 – 1.97)
Pesticide mixture[3]	1.66 (1.40 – 1.96)
Organophosphate pesticides[3]	1.07 (0.71 – 1.62)
Malathion[3]	1.17 (0.72 – 1.90)
Parathion[3]	1.03 (0.66 – 1.63)
Organophosphate pesticides[4]	1.29 (0.92 – 4.04)
Pesticide mixture[5]	7.09 (1.12 – 44.01)
CI inhibitors[6]	1.7 (1.0 – 2.8)
Rotenone[6]	2.5 CI: (1.3 – 4.7)
Oxidative stressors[6]	2.0 (1.2 – 3.6)
Paraquat[6]	2.5 (1.4 – 4.7)
Pesticide mixture[7]	1.58 (1.35 – 2.85)
Paraquat[7]	1.32 (1.10 – 1.60)

95% CI: 95% confidence interval, OR: odds ratio, RR: relative risk.
References: (Van Maele-Fabry *et al.*, 2012)[1], (Gunnarsson and Bodin, 2017)[2], (Allen and Levy, 2013)[3], (Narayan *et al.*, 2017)[4], (Rösler *et al.*, 2018)[5], (Tanner *et al.*, 2011)[6], (Ntzani *et al.,* 2013)[7].

1.4 The adverse outcome pathway concept

The adverse outcome pathway (AOP) concept is a framework that organizes a series of events needed to induce toxic effects after exposure to a compound. The first step of the toxicity is termed as a molecular initiating event (MIE), by which the compound interacts with the organism resulting in the initiation of the adverse effects due to the toxicity process. The key events (KEs) describe the progression of the toxicity process.

The early KEs are the changes occurring at the cellular levels, while the later KEs are the changes that can be observed at tissue or organ levels. Finally, the adverse outcome (AO) is the effect at the level of an organism or population in the form of alteration of function or occurrence of disease (Ankley *et al.*, 2010; Villeneuve *et al.*, 2014). In an AOP, predictive relationships between the KEs, the KE relationships (KERs), are formed. Thereby, the weight of evidence (WOE) approach is used to reflect the level of confidence of the KER. This is conducted through gathering and organising the scientific evidence supporting KER by evaluating biological plausibility and empirical support between the KEs (upstream and downstream KEs). The inconsistencies and uncertainties among the assembled information and evidence are part of evaluating the WOE of KER (OECD, 2015).

The AOP concept was introduced in the scientific community to provide a conceptual framework for the ecotoxicological risk assessment based on the mode of action (MoA) and to increase the speed and accuracy of this assessment (Ankley *et al.*, 2010; Kleinstreuer *et al.*, 2016). Since the AOP concept explains the link of MIE with AO through KEs, it is used as a basis for organizing the assays dependent on the MIE and KEs in an Integrated Approaches for Testing and Assessment (IATA) for compounds screening (Ockleford *et al.*, 2017).

AOP is helpful during the decision making by the regulatory agencies. Though, risk assessment cannot be only dependent on AOP. It should be integrated with all available data including *in silico*, *in vivo* and toxic kinetic in an IATA approach. Importantly, AOP is not a testing strategy or a computational model, but it is highly beneficial for integrated gathering evidence which can be helpful for planning testing strategies. AOP is not MoA analysis, however, it systemically describes how a chemical induces an AO, thereby being chemical agnostic yet MIE-specific (Villeneuve *et al.*, 2014).

1.5 Using the adverse outcome pathway to support the notion that the pesticides exposure increases the risk of Parkinson's disease

Association between the exposure to pesticides and PD was reported by a number epidemiological studies, however, the causality has not been confirmed (Tanner *et al.*, 2011; Van Maele-Fabry *et al.*, 2012; Gunnarsson and Bodin, 2017). Therefore, two AOPs were developed to provide mechanistic understandings of pesticide exposure

causing PMD (Ockleford *et al.*, 2017). The first AOP was used to describe the link of the CI inhibitors to the PMD. The MIE of CI inhibitors is binding to the CI causing its inhibition (KE1) and mitochondrial dysfunction (KE2). The KE3 is impaired protein degradation leading to degeneration of dopaminergic neurons in NSP (KE4) and neuroinflammation (KE5). Finally, the AO at the level of the organism is the PMD. The second AOP describes the redox-cycling of a chemical initiated by electrons released by the ETC (MIE) leading to PMD. The KE1 is the generation of free oxygen radicals within the mitochondria leading to mitochondrial dysfunction. The impairment of the protein degradation (KE2) resulting in dopaminergic neurodegeneration of NSP (KE3) and neuroinflammation (KE4) leading to the development of AO (Fig.2; Ockleford *et al.*, 2017). The WOE of the mechanistic association of the KERs based on the biological plausibility and empirical support is ranked as weak, moderate or strong (Bal-Price *et al.*, 2018).

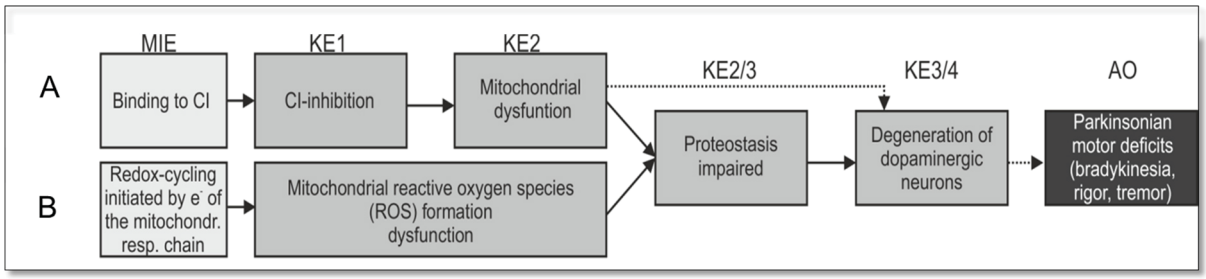

Fig.2: AOP scheme. A) the molecular initiating event (MIE) of the mitochondrial complex I (CI) inhibitors, like rotenone, is binding to the CI (AOP1), B) while other compounds classes like paraquat initially affect redox-cycling (AOP2) adapted from (Ockleford *et al.*, 2017). AO: adverse outcome, AOP: adverse outcome pathway, KEs: key events.

The WOEs of KERs between the binding to CI and its inhibition and between CI inhibition and mitochondrial dysfunction are rated strong according to the biological plausibility and empirical support (Bal-Price *et al.*, 2018). While, the WOE of KER linking MIE of the chemical redox cyclers with the mitochondrial dysfunction is rated strong according to biological plausibility and moderate according to empirical support (Ockleford *et al.*, 2017). The WOEs of KERs linking the mitochondrial dysfunction with impaired proteostasis and impaired proteostasis with dopaminergic degeneration are moderate according to biological plausibility and strong according to empirical support. The WOE of KER between mitochondrial dysfunction and degeneration of dopaminergic neurons is ranked strong according to the biological plausibility and empirical evidence (Terron *et al.*, 2018). Modified Bradford– Hill's criteria were used for evaluating the WOE of KERs. If lines of evidence are available concerning the

causative link between MIE, KEs and AO, they would be represented in a quantitative way. This would be helpful for decision making in the regulatory context (Ockleford *et al.*, 2017).

1.6 Cellular models of Parkinson's disease

1.6.1 Cancer cell line

The neuroblastoma SH-SY5Y cell line is one of the most commonly used cell lines for modelling PD. It has also been used for modelling other neurological disorders. Neuronal differentiation of the SH-SY5Y cell line varies from one day to three weeks (Xicoy *et al.,* 2017). The undifferentiated SH-SY5Y cells express a low level of the dopaminergic markers. Once neuronal differentiation occurs, the expression profile of the neuronal markers changes according to the differentiation protocols the cell line is subjected to (Adem *et al.*, 1987; Presgraves *et al.*, 2003; Lopes *et al.*, 2010). However, it should be noted SH-SY5Y cell line is of oncogenic decent and this may warrant caution in any data resulting from its use in any PD studies (Kovalevich and Langford, 2013; Lopes *et al.*, 2017).

1.6.2 Human induced pluripotent stem cells (hiPSCs)

In 2007, Takahashi *et al.* reported the establishment of induced pluripotent stem cells (iPSCs) from mouse fibroblast and reprogrammed human somatic cell hybrid (Yu *et al.*, 2007). This development enabled scientists to overcome the obstacles resulting from ethical consideration of human using embryonic stem cells (Colman, 2013). Using the hiPSCs for disease modelling is clearly preferable when investigating human disorders. Their human origin overcomes any physiological and genetic differences between human and rodent cell lines, as well as other species. Furthermore, the hiPSCs were developed by reprogramming somatic cells, which are more representative of normal cellular mechanisms than tumour cell lines (Lopes *et al.*, 2017). But it should be noted that the many different hiPSCs differentiation protocols lead to a variety of different neuronal subtypes (Fritsche *et al.*, 2018; Nimtz *et al.*, 2020). Some of these protocols describe the differentiation of hiPSCs to dopaminergic neurons (Hartfield *et al.*, 2014; Fernández-Santiago *et al.*, 2015). Among these differentiation protocols, Zhang *et al.,* (2014a) described the dopaminergic differentiation of hiPSCs to subtypes of dopaminergic neurons in SN. Differentiation of

hiPSCs allows *in vitro* investigation of the pathological changes, the effects of genetic mutations and the difference in susceptibility to environmental contaminants depending on if the donor is PD patient or healthy individual (Ryan *et al.*, 2013; Suzuki *et al.*, 2017). One disadvantage in hiPSCs differentiation protocols to generate dopaminergic neurons is the time taken to differentiate them which reduces throughput and increases costs (Swistowski *et al.*, 2010; Hartfield *et al.*, 2014; Tofoli *et al.*, 2019). More importantly, the major disadvantage is the lack of reproducibility of the differentiation process. This may be a consequence of the source of hiPSCs and handling issues (Mahajani *et al.*, 2019). Despite these limitations, hiPSCs remain the preferred cells in disease modelling studies (Shi *et al.*, 2017; Doss and Sachinidis, 2019).

1.6.3 The Lund human mesencephalic (LUHMES) cells

LUHMES cells are a subclone of MESC2.10 cells derived from the ventral mesencephalon of an 8 weeks old human fetus. LUHMES cells are myc-immortalized (tet off) and their proliferation is inhibited upon addition of tetracycline (Lotharius *et al.*, 2005; Schildknecht *et al.*, 2009). LUHMES cells can be induced to differentiate to generate dopaminergic neurons on exposure to cyclic adenosine monophosphate (cAMP) and glial cell line-derived neurotrophic factor (GDNF). The differentiated LUHMES cells have long neurites, show electrical activity and express dopaminergic and synaptic markers. Importantly because LUHMES cells are human immortalized cells, the data generated has greater translational impact compared to tumour or rodent cells (Scholz *et al.*, 2011). Furthermore, Schildknecht *et al*., (2013) reported generation of genetically-modified LUHMES cells which stably express genetic mutations. This may enable investigators to better understand the PD genetic-environmental interaction. LUHMES cells also have the advantage that they can be used to study the effects of drugs and chemical compounds (Tong *et al.*, 2017). However, because LUHMES cells are pure neuronal cell line lacking the glial cells limits their use in the investigation of neuroinflammation (Scholz *et al.*, 2011).

1.7 Aim of the thesis

Systematic literature reviews and meta-analyses suggest that exposure to pesticides might be associated with an increased risk for developing PD. However, this association shows a variable degree of heterogeneity and inconsistency (Tanner *et al.*,

2011; Van Maele-Fabry *et al.*, 2012; Gunnarsson and Bodin, 2017). To better understand this association, EFSA recommended the reassessment of the hypothesis that pesticides can cause PMD using the AOP concept. Thus, two AOPs were developed that provide mechanistic understandings for pesticide exposure causing PMD, i.e. 1) 'Inhibition of the CI of nigra-striatal neurons leads to PMD and 2) 'Redox-cycling of a chemical initiated by electrons released by the ETC leading to PMD (Ockleford *et al.*, 2017). Based on these two AOPs, the aim of this thesis was to establish a human, AOP-informed and MoA-based *in vitro* test battery for hazard assessment of pesticides leading to PMD.

Therefore, the following objectives were addressed in this thesis:

1) Establishment of a test system for assessing early KEs of the two AOPs.

2) Set-up of a test battery of test methods measuring the effects of pesticides on AOP-informed early KEs.

3) Chemical testing with the test methods using a test set of pesticides and negative compounds.

2. Materials and methods

2.1 Material

2.1.1 Laboratory equipment

Table 2: Laboratory equipment

Laboratory equipment	Supplier
Autoclave	KSG GmbH, Neukirchen-Vluyn, Germany
Heating blocks	Thermo Fisher Scientific, Carlsbad, USA Panasonic, Hamburg, Germany
Incubators	Heraeus, Cologne, Germany Thermo Fisher Scientific, Carlsbad, USA Sanyo, Moriguchi, Japan
Light-optical microscope	Olympus, Düsseldorf, Germany
ThermoCell Mixing block	Bioer, UK
Multimode microplate reader	Tecan, Männedorf, Switzerland
Polymerase chain reaction (PCR) cycler	Qiagen, Hilden, Germany
Refrigerators/Freezers	Liebherr, Biberach, Germany Thermo Fisher Scientific, Carlsbad, USA
Table-top centrifuge	Thermo Fisher Scientific, Carlsbad, USA
Weighting scale	Sartorius, Göttingen, Germany

2.1.2 Consumables

Table 3: Consumables

Consumables	Supplier
6-Well Plates	Sarstedt, Nümbrecht, Germany
24-Well Plates	Sarstedt, Nümbrecht, Germany
96-Well Plates	Sarstedt, Nümbrecht, Germany

96- white Well Plates	Brand, Wertheim, Germany
Culture dishes, Ø 100 x 20 mm	Greiner Bio-One, Frickenhausen, Germany
Nunc EasYFlask 75cm2	Thermo Fisher Scientific, Roskilde, Denmark
Nunc EasYFlask 175cm2	Thermo Fisher Scientific, Roskilde, Denmark
Parafilm	Pechiney, Paris, France
Pipette Tips, 10 µL, 100 µL and 1000 µL	Biozym, Hessisch Oldendorf, Germany
PCR tubes, 0.1 mL 4-tubes	Biozym Biotech Trading GmbH, Vienna, Austria
Tubes, 15 mL	Sarstedt, Nümbrecht, Germany
Tubes, 50 mL	Sarstedt, Nümbrecht, Germany

2.1.3 Cell culture media and supplements

Media composition for hiPSCs

Table 4: Medium components for hiPSC culture

Medium components	Supplier
mTeSR1 basal medium (#05850)	Stemcell Technology, Grenoble, France
DMEM medium (#10829018)	Thermo Fisher Scientific, Paisley, UK
Knockout serum replacement (KSR; #10828010)	Thermo Fisher Scientific, Paisley, UK
Neurobasal medium (#21103049)	Thermo Fisher Scientific, Grand Island, USA
5x supplement (#HPRG740)	Thermo Fisher Scientific, Grand Island, USA
Non-essential amino acid stock solution (100x; 11140050)	Thermo Fisher Scientific, Grand Island, USA
Mercaptoethanol stock (100x; #ES-007-E)	Millipore, Darmstadt, Germany
N2 supplement (#17502048)	Thermo Fisher Scientific, Grand Island, USA

B27 supplement (50x; #17504044)	Thermo Fisher Scientific, Grand Island, USA
Glutamax stock solution (100x; #35050061)	Thermo Fisher Scientific, Grand Island, USA
Penicillin/ampicillin stock solution (100x; #P06-07100)	Pan Biotech, Munich, Germany
N6,2′-O-Dibutyryladenosine 3′,5′-cyclic monophosphate sodium salt (#D0627)	Sigma-Aldrich, Steinheim, Germany
Fibroblast Growth Factor-8b (FGF8b; #SRP4053)	Sigma-Aldrich, Steinheim, Germany
Glial cell line-derived neurotrophic factor (#G1777)	Sigma-Aldrich, Steinheim, Germany
Smoothened agonist (SAG; #566660)	Millipore, Darmstadt, Germany
Brain-derived neurotrophic factor (BDNF; #248-BD-005)	R&D Systems, Minneapolis, USA
Transforming growth factor-β3 (TGF β3; #SRP3171)	Sigma-Aldrich, Steinheim, Germany
CHIR99021(#4423/10)	R&D Systems, Minneapolis, USA
LDN193189 (#SML0559)	Sigma-Aldrich, Steinheim, Germany
Purmorphamine (#sc-202785)	Santa Cruz, Texas, USA
Ascorbic acid (#A5960)	Sigma-Aldrich, Steinheim, Germany
Accutase (#A11105-01)	Thermo Fisher Scientific, Grand Island, USA
Matrigel (#356231)	BDBiosciences, Heidelberg, Germany
Laminin (#L2020)	Sigma-Aldrich, Steinheim, Germany
Poly-L-ornithine (#P4538)	Sigma-Aldrich, Steinheim, Germany
Fibronectin (#F0635)	Sigma-Aldrich, Steinheim, Germany

Table 5: Cell culture medium composition of hiPSCs

Medium	Composition
MTeSR1 serum-free medium	mTeSR1 basal medium 5x supplement Penicillin/ampicillin stock solution (100x)

KSR differentiation medium	DMEM medium Knockout serum replacement (KSR) Non-essential amino acid stock solution (100x) Penicillin/ampicillin stock solution (100x) Mercaptoethanol stock (100x)
N2 differentiation medium	DMEM media N2 supplement (100x) Pnicillin/ampicillin stock solution (100x)
B27 differentiation medium	Neurobasal medium B27 supplement (50x) Glutamax stock solution (100x) Penicillin/ampicillin stock solution (100x)

Table 6: Cell culture medium components of hiPSC with supplements

Days	Medium	Growth Factors
D (-2- -1)	**MTeSR1 medium**	
D (0)	**KSR medium**	LDN-193189 (100 nM) SB431542 (10 µM)
D (1-2)	**KSR medium**	FGF8b (50 ng/ml) LDN-193189 (100 nM) Purmorphamine (2 µM) SAG (0.25 µM) SB431542 (10 µM)
D (3-4)	**KSR medium**	CHIR99021 (3 µM) FGF8b (50 ng/ml) LDN-193189 (100 nM) Purmorphamine (2 µM) SAG (0.25 µM) SB431542 (10 µM)
D (5-6)	**KSR medium (75%)** **N2 medium (25%)**	CHIR99021 (3 µM) FGF8b (50 ng/ml) LDN-193189 (100 nM)

		Purmorphamine (2 µM) SAG (0.25 µM)
D (7-8)	**KSR medium (50%)** **N2 medium (50%)**	CHIR99021 (3 µM) LDN-193189 (100 nM)
D (9- 10)	**KSR medium (25%)** **N2 medium (75%)**	CHIR99021 (3 µM) LDN-193189 (100 nM)
D (11-12)	**B 27 medium**	Ascorbic acid (0.2 mM) BDNF (10 ng/mL) cAMP (0.1 mM) CHIR99021 (3 µM) GDNF (10 ng/mL) TGF β3 (1 ng/ml)
D (13-45)	**B 27 medium**	Ascorbic acid (0.2 mM) BDNF (10 ng/mL) cAMP (0.1 mM) GDNF (10 ng/mL) TGF β3 (1 ng/ml)

BDNF: brain-derived neurotrophic factor, cAMP: cyclic adenosine monophosphate, FGF8b: fibroblast Growth Factor-8b, GDNF: glial cell line-derived neurotrophic factor, SAG: smoothened agonist, TGF β3: transforming growth factor-β3.

Table 7: Medium components for LUHMES cell culture

Medium component	Supplier
Advanced Dulbecco's Modified Eagle (DMEM)/F-12 medium (#12634028)	Thermo Fisher Scientific, Grand Island, USA
N6,2′-O-Dibutyryladenosine 3′,5′-cyclic monophosphate sodium salt (#D0627)	Sigma-Aldrich, Steinheim, Germany
Recombinant Human FGF basic/FGF2, 145 aa TC Grade Protein CF (FGF; # 4114-TC-01M)	R&D Systems, Minneapolis, USA
Recombinant Human GDNF (#212-GD-050)	R&D Systems, Minneapolis, USA
L- glutamine (#G7513)	Sigma-Aldrich, Steinheim, Germany

N2 supplementation (#17502048)	Thermo Fisher Scientific, Grand Island, USA
Tetracycline (#T7660)	Sigma-Aldrich, Steinheim, Germany

Table 8: Media composition for LUHMES cell culture

Medium	Composition
Proliferation medium	Advanced DMEM/F12 medium L-glutamine (2 mM) 1× N2 supplement FGF (40 ng/ml)
Differentiation medium	Advanced DMEM/F12 medium L-glutamine (2 mM) 1× N2 supplement GDNF (2 ng/ml) cAMP (1 mM) Tetracycline (1 µg/ml)
Freezing medium	Proliferation medium 20% Fetal calf serum (FCS) 10% (v/v) 10% DMSO (v/v)

cAMP: cyclic adenosine monophosphate, FGF: fibroblast Growth Factor, GDNF: glial cell line-derived neurotrophic factor.

Table 9: Cell culture components

Cell culture component	Company
Fibronectin bovine plasma (#F1141)	Sigma-Aldrich, Steinheim, Germany
Phosphate Buffered Saline (PBS, #L 1825)	Biochrom, Berlin, Germany
Poly-L-ornithine hydrobromide (#P3655)	Sigma-Aldrich, Steinheim, Germany
Trypsin-EDTA (0.05%) with phenol red (#11590626)	Thermo Fisher Scientific, Paisley, UK

Table 10: List of chemicals

Chemicals	Company
Chlorpyrifos (#C11600000)	LGC standards
Chlorpyrifos oxon (#C11603000)	Dr Ehrenstorfer GmbH, Augsburg, Germany
Dichlorvos (#45441)	Sigma-Aldrich, Steinheim, Germany
Dimethyl sulfoxide (DMSOc)	Carl Roth GmbH + Co. KG, Karlsruhe, Germany
Epoxomicin (#sc-200298)	Santa Cruz, Texas, USA
Malaoxon (#36142)	Sigma-Aldrich, Steinheim, Germany
Malathion (#36143)	Sigma-Aldrich, Steinheim, Germany
Paraoxon-ethyl (#36186)	Sigma-Aldrich, Steinheim, Germany
Paraquat chloride (#sc-257968)	Santa Cruz, Texas, USA
Parathion ethyl (#C15880000)	LGC standards
Rotenone (#sc-203242)	Santa Cruz, Texas, USA
Staurosporine (#S4400)	Sigma-Aldrich, Steinheim, Germany

2.1.4 Cell biological and molecular assays

Table 11: Cell biological and molecular assays

Assay	Company
Bicinchoninic acid (BCA) assay	Thermo scientific, Rockford, USA
Caspase-Glo® 3/7 Assay	Promega, Madison, USA
CellTiter-Blue Assay	Promega, Madison, USA
CytoTox-ONE Assay	Promega, Madison, USA
CellTiter-Glo® Luminescent Cell Viability Assay	Promega, Madison, USA
PCR-Purification Kit	Qiagen, Hilden, Germany
Proteasome-Glo™ Chymotrypsin-Like Cell-Based Assay	Promega, Madison, USA
QuantiTec Reverse Transcription Kit	Qiagen, Hilden, Germany
QuantiFast SYBR Green PCR Kit	Qiagen, Hilden, Germany
RNeasy Mini Kit	Qiagen, Hilden, Germany

2.1.5 Software

Table 12: List of computer software

Computer software	Application
GraphPad Prism 8.21	Data evaluation, statistics and graphical representation
icontrol 1.9	Measurement of cell-based assays: cytotoxicity, viability, apoptosis, proteasomal activity, ATP levels and protein quantification
Mestrenova version 8.0.1-10878	Processing and analyzing the High-resolution proton magnetic resonance spectroscopy (^{1}H NMR) spectra
Microsoft Excel 2019	Data evaluation
RotorGene 1.7	Measurement and data evaluation of qRT-PCR

2.2 Methods

2.2.1 Cell culture and differentiation of hiPSCs

Differentiation of hiPSCs to dopaminergic neurons was conducted according to the protocol published by Zhang *et al.,* (2014a). The details of the differentiation protocol are summarized in Fig.3. Six-well plates were coated with matrigel diluted in DMEM/F12 medium (1:40) and left overnight at 4°C. On the next day, the coated plates were left to equilibrate at room temperature and matrigel solution was aspirated. The hiPSCs were seeded at a density of 3.6 x 10^4 cells/cm^2 in 6-well plates corresponding to 3.6 x 10^5 cells/well (2 mL of mTeSR1 media per well). One day later, the media was aspirated and 2 mL of mTeSR1 were added to allow the hiPSC to grow before the start of the differentiation process. One day later (D0), the whole of the media was aspirated and 2 mL of KSR differentiation media containing LDN-193189 (100 nM) and SB431542 (10 µM) were added. On D1 and D2, the media was removed followed by addition of 2 mL of KSR differentiation media containing FGF8b (50 ng/ml), LDN-193189 (100 nM), purmorphamine (2 µM), SAG (0.25 µM) and SB431542 (10 µM). On D3 and D4, after removal of the media, 2 mL of KSR differentiation media containing

CHIR99021 (3 µM), FGF8b (50 ng/ml), LDN-193189 (100 nM), purmorphamine (2 µM), SAG (0.25 µM) and SB431542 (10 µM) were added to each well. On D5 and D6, the media was removed and replaced by a mixture of differentiation media (75% KSR and 25% N2 media) containing CHIR99021 (3 µM), FGF8b (50 ng/ml), LDN-193189 (100 nM), purmorphamine (2 µM) and SAG (0.25 µM). On D7 and D8, after removing the media, 2 mL of a mixture of differentiation media (50% KSR and 50% N2 media) containing CHIR99021 (3 µM) and LDN-193189 (100 nM) were added. On D9 and D10, the ratio of the composition of the differentiation media was changed to (25% KSR and 75% N2 media) containing CHIR99021 (3 µM) and LDN-193189 (100 nM). After removal of the media, 2 ml of the new media were added to each well. On D11 and D12, 2 mL of B27 differentiation media containing ascorbic acid (0.2 mM), BDNF (10 ng/mL), cAMP (0.1 mM), CHIR99021 (3 µM), GDNF (10 ng/mL) and TGF β3 (1 ng/ml) were added after removal the media. For the rest of the differentiation (D13-D20), the media was substituted by 2 mL of the B27 differentiation media containing ascorbic acid (0.2 mM), BDNF (10 ng/mL), cAMP (0.1 mM), GDNF (10 ng/mL) and TGF β3 (1 ng/ml) on a daily basis.

On D20, cells were replated in 6-well plates coated with poly-L-ornithine, laminin and fibronectin. 1 mL of poly-L-ornithine (15 µg/mL) in phosphate-buffered saline (PBS) was added to every well and was left overnight at 37°C. On the next day, poly-L-ornithine containing solution was removed and washed three times with distilled sterile water. The plates were left to dry under the laminar flowbench. 1 mL of laminin (1µg/mL) in PBS was added to every well and was left overnight at 37°C. On the next day, laminin containing solution was removed and washed three times with distilled sterile water. The plates were left to dry under the laminar flow bench. Finally, 1 mL of fibronectin (2 µg/ml) dissolved in PBS was added to every well and was left overnight at 37°C. On the next day, the plates were stored at 4°C. On D 20, the media was removed and 1 mL of warm accutase was added to every well of the plates containing cells. The plates were incubated at 37 °C for 5 min. The cells were detached by gentle pipetting up and down. The cell suspension was then transferred to a 15 mL falcon tube containing neurobasal media and was centrifuged at 1200 revolutions per minute (rpm) for 3 minutes. The supernatant medium was removed and the cell pellet was resuspended in B27 medium. The fibronectin containing solution was then removed from the coated 6-well plates and was washed twice with PBS. The cells were replated and seeded at a density of 2 x 10^5 cells/cm^2 in six-well plates corresponding to 2 x 10^6

cells/well. On D21, the media was removed to remove the dead cells and 2 mL of the new media were added. The media was exchanged every other day. This differentiation protocol was repeated three times using the NIH-11 and IMR-90 (WiCell) cell lines and was followed by morphological analysis by phase-contrast microscope and mRNA expression analysis.

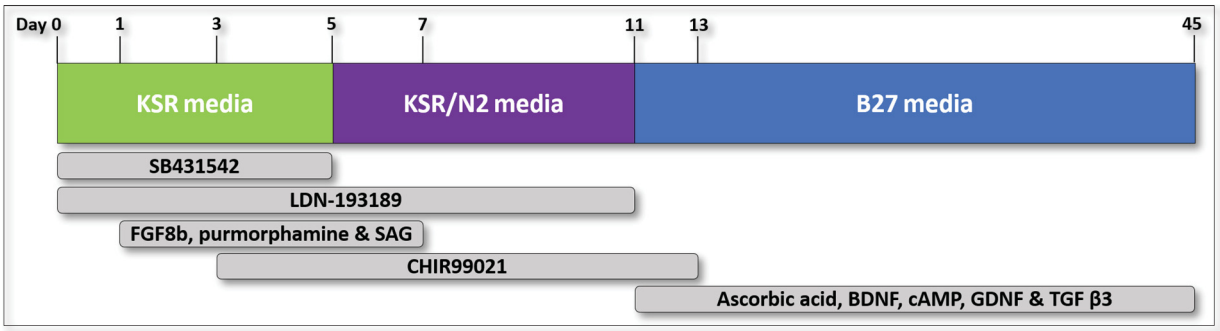

Fig. 3: Experimental set-up for differentiation of hiPSC to dopaminergic neurons. This figure was adapted from Zhang *et al.*, (2014a). BDNF: brain-derived neurotrophic factor, cAMP: cyclic adenosine monophosphate, FGF8b: fibroblast Growth Factor-8b, GDNF: glial cell line-derived neurotrophic factor, SAG: smoothened agonist, TGF β3: transforming growth factor-β3.

2.2.2 Cell culture and differentiation of LUHMES cells

Proliferation of LUHMES cells

LUHMES cells were kindly provided by Prof. Dr. Leist (University of Konstanz, Germany). These cells were generated by immortalization of fetal mesencephalon cells with a v-myc retroviral vector controlled by tetracycline (tet-off). For growing the undifferentiated LUHMES cells, as previously described (Scholz *et al.*, 2011), Nunc EasYFlask 75 cm^2 and 175 cm^2 cell culture flasks were coated with poly-L-ornithine (50 ng/ml) and fibronectin (1.5 µg/ml) overnight at 37°C. On the second day, the coating solution was aspirated and the flasks were washed once with distilled sterile water. The flasks were left to dry under the laminar flow bench. LUHMES sells were grown at a density of 3×10^6 or 6×10^6 cells into coated plastic cell culture T75 and T175 flasks, respectively, in proliferation media in an adherent manner. The proliferation media consisted of advanced DMEM/F12 medium, L-glutamine (2 mM), N2 supplement (1×) and FGF (40 ng/ml). The proliferating LUHMES cells grew at 37°C in humidified air having 5% CO_2.

Passaging of LUHMES cells

When the confluence of the cells reached 70% to 80%, usually after two days of incubation, they were split. The medium was removed and the LUHMES cells were washed once with PBS. The LUHMES cells were incubated at 37 °C with 2 mL or 4 ml of trypsin-EDTA (0.05%) in cell culture T75 and T175 flasks, respectively, for 30 to 60 seconds. The cells were detached by gentle tapping and subsequently flushing with 25 mL advanced DMEM/F12 medium. Then, the cell suspension was transferred to a 50 mL falcon tube and was centrifuged at 1200 rpm for five minutes. The supernatant medium was removed and the cell pellet was resuspended in advanced DMEM/F12 medium. The 3×10^6 or 6×10^6 cells were seeded in coated cell culture T75 and T175 flasks, respectively, in proliferation media and were split every two days (at 70 to 80% confluence).

Cryopreservation of LUHMES cells

For cryopreservation, the proliferating LUHMES cells were washed once with PBS and incubated with trypsin-EDTA (0.05%) for 30 to 60 seconds at 37°C. The cells were detached by gentle tapping followed by flushing with the advanced DMEM/F12 medium. The cell suspension was transferred to a 50 mL falcon tube and was centrifuged at 1200 rpm for five minutes. Supernatant was discarded and the cell pellet was resuspended in freezing medium at a density of 3×10^6/mL. The freezing media was composed of proliferation medium, 20% FCS (v/v) and 10% DMSO (v/v). One mL of freezing media containing cells was rapidly transferred to cryo tubes. The tubes were stored in pre-cooled (4°C) freezing-container filled with 100% technical isopropanol. The cells were stored in -80°C for 24 hours. On the next day, the LUHMES cells were transferred to liquid nitrogen for long-term storage.

LUHMES cells were thawed at 37°C until only a small piece of ice was seen in the cryo tube. The cells were transferred into a 50 mL falcon tube containing 25 mL advanced DMEM/F12 and were centrifuged at 1200 rpm for five minutes. The supernatant was discarded and LUHMES cells were seeded into a coated plastic cell culture T75 flask in proliferation media.

Differentiation of LUHMES cells

For differentiation of LUHMES cells into dopaminergic neurons, cells were seeded at a density of 4 × 10^6 or 8 × 10^6 cells into a coated plastic cell culture T75, or T175 flask, respectively, and cultured with proliferation media for one day (pre-differentiation day). The next day, the proliferation medium was removed and differentiation medium was added for another two days. The differentiation media consist of advanced DMEM/F12 medium, L-glutamine (2 mM), N2 supplement (1×), GDNF (2 ng/mL), cAMP (1 mM) and tetracycline (1 µg/ml). On the second day of differentiation, the cells were split as described for proliferating LUHMES cells with an extended incubation time with trypsin-EDTA (0.05%) of three minutes. The cells were seeded in coated 6, 24 and 96-wells plates at a density to 1.2-1.5 × 10^6, 300-400 × 10^3 and 35-50 x 10^3 cells/well, respectively.

2.2.3 Molecular characterization by qRT-PCR

For molecular characterization of the neuronal differentiation of hiPSC, RNA was isolated on day 1 and day 25 of differentiation. For LUHMES cells, RNA of the proliferating and differentiating cells on day 4 and 6 was isolated. Quantitative real time polymerase chain reaction (qRT-PCR) was done using the QuantiFast SYBR Green PCR Kit in the Rotor Gene Q cycler, as described in detail below. For the hiPSCs, the expression of the dopaminergic neuron marker tyrosine hydroxylase (TH) and dopaminergic transporter (DAT), the marker of the dopaminergic neuron subtype of SN, the G protein-gated inwardly rectifying potassium (GIRK) channels and progenitor cell marker (SOX2) was assessed. For LUHMES cells, the expression of the genes coding for pan neuronal marker neuron-specific enolase 2 (ENO2) and dopaminergic neurons (TH and DAT) was evaluated.

RNA isolation

TheRNeasy Mini Kit was used for RNA isolation according to the instruction of the manufacturer. The RNA concentrations were measured using the nanodrop.

Reverse transcription of RNA into cDNA

Transcription of cDNA to RNA was done with 500 ng of RNA using the QuantiTect Rev Transcription Kit according to the manufacturer's instruction. To remove the genomic DNA, 12 µl of the double distilled water (ddH_2O) with the RNA template were added to 2 µl of gDNA wipeout buffer (7x). This mixture was incubated for two minutes at 42°C to remove gDNA. Afterward, 1 µl of reverse transcriptase and 5 µl of MasterMix solution were added and then centrifugated at 2000 rpm for 30 seconds. Then, the cDNA was synthesized as shown in details in table13.

Table 13: Reverse transcription of RNA into cDNA

Process	Temperature	Duration
gDNA removal	42°C	2 minutes
cDNA synthesis	42°C	30 minutes
End reaction	95°C	3 minutes
Cooling	4°C	∞

Quantitative real-time PCR

According to the manufacture's instruction, the Rotor Gene Q cycler was used to conduct qRT-PCR, as shown in table 14. The number of cycles needed to reach the pre-defined fluorescence intensity were determined as C_t values. The Ct values of the gene of interest was normalized to the expression of the housekeeping gene (β-actin) that is stably expressed in cells (dCt values; see formula below). To assess the relative expression of the gene of interest between the different time points, the dC_t values of the samples at the different time points where normalized to the control (ddCt; see formula below).

Table 14: Quantitative real-time PCR cycles

Task	Temperature	Duration	Number of cycles
Denaturation	95°C	7 minutes	1x
Denaturation	95°C	10 seconds	47x
Annealing	60°C	35 seconds	
Elongation	72°C	20 seconds	
Melting	75 - 99°C		1x

$dC_t = C_t$ (gene of interest) – dC_t (housekeeping gene)

$ddC_t = dC_t$ (control) – dC_t (sample)

Table 15: Oligonucleotides used for qRT-PCR

Oligonucleotide primers	Sequence
β-actin	FW: 5’ CAGGAAGTCCCTTGCCATCC 3’ RV: 5’ ACCAAAAGCCTTCATACATCTCA 3’
DAT	FW:5' GAAGATCTGCCCCATACTGAA 3' RV:5' GCGATGATGACGTTGTAGAAGA 3'
GIRK	FW:5' TTGTTCAGTCTTGCTCCGTT 3' RV:5' AGTCATGGATTCTGTCAGCTTG 3'
ENO2	FW: 5’ AGCTGAGAGCTTTCGGGATG 3’ RV: 5’ TCCAAGGCTTCACTGTTCTCC 3’
SOX2	FW: 5’ GGGAAAGTAGTTTGCTGCCTC 3’ RV: 5’ AGAGAGGCAAACTGGAATCAGG 3’
TH	FW:5' TTCTCGCAGGACATTGGC 3' RV:5' CTTACACAGCCCGAACTCC 3'

DAT: dopamine transporter, ENO2: neuron-specific enolase 2, GIRK: G protein-gated inwardly rectifying potassium channel, SOX2: SRY-box containing gene 2, TH: tyrosine hydroxylase.

2.2.4 Immunocytochemical staining

For immunocytochemical (ICC) staining, LUHMES cells were fixed with 4% paraformaldehyde for 30 minutes. This was followed by washing three times with PBS. The cells were then incubated with βIII-tubulin antibody (rabbit; 1:200), as a neuronal marker diluted in PBS containing 0.1% Triton X and 1% bovine serum albumin (BSA) overnight at 4°C. After incubation with primary antibody, the cells were washed three times with PBS and then incubated with anti-rabbit IgG-Alexa®546 (1:500) in combination with phalloidin-Alexa®488 (1:70), as a cytoskeletal marker and Hoechst 33258 (1:100) as a nuclear marker for 60 minutes. Finally, the cells were washed in PBS and imaged on a confocal laser scanning microscope TCS SP8 in CECAD imaging facility in Cologne.

2.2.5 Cell biological assays

To identify if a compound affects the early KEs of PMD, cell biological assays to detect these KEs were used. As a readout for mitochondrial dysfunction, cell viability based on the metabolic activity and ATP levels was assessed by the Cell Titer Blue (CTB) and the Cell Titer-Glo (CTG) assays, respectively. For differentiating between the different types of cell death, necrosis or apoptosis, the following two essays were selected. For membrane integrity of differentiated LUHMES cells, the lactate dehydrogenase (LDH) levels in the culture medium as an indicator of necrosis were measured by the CytoTox-ONE™ Homogeneous Membrane Integrity Assay. Caspase 3/7 activity as an indicator of apoptosis, was assessed by Caspase-Glo® 3/7. Finally, to assess the effects on the proteasome, the activity of the chymotrypsin-like subunit of proteasome 20S was assessed by Proteasome-Glo™ Chymotrypsin-Like Cell-Based Assay.

Assessment of cytotoxicity using the CytoTox-ONE™ Homogeneous Membrane Integrity Assay

The CytoTox-ONE assay detects the cell membrane damage by measuring the level of LDH. This is an indirect measure of necrosis. The CytoTox-ONE reagent contains lactate, NAD+ and resazurin. LDH is a catalyst for the oxidation of lactate to pyruvate stimulating the conversion of resazurin to fluorescent resorufin. The fluorescent signals are proportional to the LDH levels.

The CytoTox-ONE reagent was prewarmed for 15 minutes before the start of the experiment. 5 µl of Triton X-100 9% solution per well of 96-well plate were added to the positive control wells to reach the final concentration of 0.43%. These positive control wells with lysed cells give the maximum response of the assay. The plates were incubated for 20 minutes in a cell culture incubator. 50 µl of the differentiation media from each well were transferred to a new 96-well plate. 50 µl of the CytoTox-One reagent were added to each well. The plates were incubated for 1.5 hours at 37°C and the amount of LDH in the medium was measured with a multimode microplate reader (Tecan) at the wavelengths 540Ex/590Em.

Assessment of cell viability using the Cell Titer Blue assay

The CTB assay measures the cellular metabolic activity by quantifying the function of cellular reductases. Thereby, the substrate resazurin is reduced to fluorescent resorufin by metabolically active cells and used as an indicator for viable cells.

Differentiation media and CTB reagent were pre-warmed. CTB reagent was mixed with differentiation media 1:3 (x µL CTB-reagent + 2x µL medium). 50 µl of the media were transferred to another 96-well plate to be used in the CytoTox-ONE Homogeneous Membrane Integrity Assay. 33.3 µl of this dilution were added to 50 µl of differentiation media. 83.3 µl of this final dilution were then added to each well containing 50 µl medium (1:4). The plates were incubated for 1.5 hours at 37° C and 5% CO_2 and then measured with a multimode microplate reader (Tecan) at the wavelengths 560 Ex/590Em.

Assessment of apoptosis using the Caspase-Glo® 3/7 Assay

This assay was used to assess apoptosis by measuring luminescence-based caspase 3/7 activities and was multiplexed with the CytoTox-ONE Homogeneous Membrane Integrity and CTB assays in one experimental run. The Caspase-Glo reagent contains tetrapeptide sequence DEVD, luciferase, and cell lysis. After cleavage of the DEVD containing substrate by caspases, the luciferase reaction occurs producing signals which are proportional to the activity of the caspases.

From every well, 50 µl of the differentiation media were transferred to another transparent plate for LDH measuring. Then, the cell viability was assessed after adding the CTB reagent and incubation for 1.5 hours. Subsequently, 83.3 µl of differentiation media containing the CTB reagent were removed and 50 µl of the pre-warmed Caspase-Glo reagent were added. To lyse the cells, the plates were shaken with the orbital shaker for 20 minutes at 350 rpm. Then, the content was transferred to white-walled plates by a multichannel pipette. The luminescence was measured after 30 minutes using the luminescence function of a multimode microplate reader (Tecan).

Assessment of proteasomal activity using Proteasome-Glo™ Chymotrypsin-Like Cell-Based Assay

The activity of the chymotrypsin-like activity subunit of the 20 S proteasome was assessed using Proteasome-Glo™ Chymotrypsin-Like Cell-Based Assay. The assay

reagent contains succinyl-leucine-leucine-valine-tyrosine-aminoluciferin, which is cleaved at 20S proteasome. After that, the luciferase reaction resulted in generation of the luminescent signals. These signals are proportional to the activity of the chemotrypsin-like subunit of proteasome 20S.

Prior to conducting the experiment, the proteasome-Glo reagent was left for 15 minutes to equilibrate to room temperature. 50 µl of the differentiation media was removed and 50 µl of the reagent was added. The plates then were shaken with the orbital shaker for 20 minutes at 350 rpm for lysing the cells and mixing with the assay reagent. Using a multichannel pipette, the content was transferred to white-walled plates. The luminescent signals were measured after 30 minutes using the luminescence function of a multimode microplate reader (Tecan).

Assessment of ATP levels using the Cell Titer-Glo® Luminescent Cell Viability Assay

CTB assay measures the reduction of resazurin to fluorescent resorufin. Therefore, it indicates the amount of reduction equivalents (nicotinamide adenine dinucleotide (NADH)/ flavin adenine dinucleotide ($FADH_2$)) delivered by glycolysis or the TCA cycle. Thus, it indicates the amount of actively metabolizing cells. ATP is mainly produced within mitochondria and therefore dependent on the activity of the ETC, as reviewed by Zhao *et al.*, (2019). Therefore, the ATP levels is used as a more direct readout for mitochondrial activity. Additionally, it can be used as another indicator for cell viability. The assay reagent contains beetle luciferin. The reaction of ATP with the beetle luciferin produces luminescent signals which are proportional to the ATP levels.

Before conducting the experiment, the CTG reagent was left for 15 minutes to equilibrate to room temperature. 50 µl of the differentiation media were removed and 50 µl of the reagent were added. Shaking of the plates was conducted with the orbital shaker for 20 minutes at 350 rpm. Later, the content was transferred to white-walled plates by a multichannel pipette. Using the luminescence function of a multimode microplate reader (Tecan), the luminescence was measured.

2.2.6 Compounds testing

For compounds testing, LUHMES cells were differentiated for 6 days without compound exposure. The cells were exposed to the compounds on day 6 for 6, 24 and 48 hours (Fig.4). The cell viability based on the metabolic activity and ATP level, cytotoxicity, apoptosis and proteasomal activity were assessed as described in section 2.2.5.

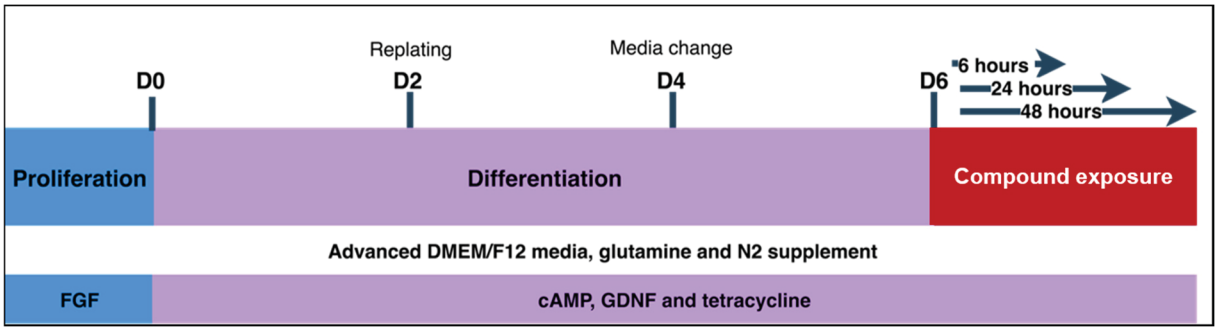

Fig.4: Experimental set-up for differentiation of Lund human mesencephalic (LUHMES) cells to dopaminergic neurons and compound exposure. LUHMES cells were induced to differentiate to dopaminergic neurons by addition of tetracycline to inhibit the proliferation and addition of cyclic adenosine monophosphate (cAMP) and glial cell-derived neurotrophic factor (GDNF). Differentiated LUHMES cells were exposed to chemicals at day 6 of differentiation for 6, 24 and 48 hours.

First, the LUHMES cells were exposed to serial concentrations of the model compounds. The first model compound is rotenone as a representative for the CI compounds described in the AOP1. Rotenone was also as an assay specific positive compound in the CTB and CTG assay. The second model compound is paraquat which disturbs the redox cycling and represents the compounds of the AOP2. Epoxomicin is a potent inhibitor of the activity of 20 S proteasome and was selected as a positive control in Proteasome-Glo™ Chymotrypsin-Like Cell-Based Assay. Staurosporine is a potent inducer of caspase 3 and was used as a positive control for apoptosis in Caspase-Glo® 3/7 Assay (Table 16).

After setting up the testing battery with the model and positive compounds, the next step was to test for the specificity by adding negative compounds. Serial concentrations of saccharin and diethylene glycol were applied to the cells. For investigating the toxicity of the organophosphate pesticides, the cells were exposed to serial concentrations of chlorpyrifos, parathion, malathion and dichlorvos. Chlorpyrifos oxon, paraoxon and malaoxon are the metabolites of chlorpyrifos, parathion and malathion, respectively. Due to the fact that LUHMES cells cannot metabolize the selected pesticides (Eaton *et al.*, 2008; Miksys and Tyndale, 2013; Tong *et al.*, 2017),

serial concentrations of chlorpyrifos, paraoxon and malaoxon were applied to the cells (Table 16).

Table 16: Compounds testing

Compound classes	Compounds	Concentrations [µM]
Model compounds	Rotenone	0, 0.016, 0.08, 0.4, 2, 10 and 50
	Paraquat	0, 20, 50, 100, 500, 1000 and 5000
Negative compounds	Saccharin	0, 4.11, 12.34, 37.03, 111.11, 333.33 and 1000
	Diethylene glycol	0, 4.11, 12.34, 37.03, 111.11, 333.33 and 1000
Assay specific positive compounds	Epoxomicin	0, 0.069, 0.206, 0.617, 1.852, 5.556, 16.667 and 50
	Staurosporine	0, 0.0032, 0.016, 0.08, 0.4, 2 and 10
Organophosphate pesticide	Chlorpyrifos	0, 1, 3.1, 9.3, 27.8, 83.3 and 250
	Parathion	0, 163.84, 204.8, 256, 320, 400 and 500
	Malathion	0, 65.84, 98.77, 148.15, 222.22, 333.33 and 500
	Dichlorvos	0, 15.63, 31.25, 62.5, 125, 250 and 500
Metabolites of the organophosphate pesticide	Chlorpyrifos oxon	0, 0.27, 0,82, 2.47, 7.41, 22.22, 66.67 and 200
	Paraoxon	0, 65.84, 98.77, 148.15, 222.22, 333.33 and 500
	Malaoxon	0, 65.84, 98.77, 148.15, 222.22, 333.33 and 500

2.2.7 Metabolomics

In order to characterize the effects of neuronal differentiation in LUHMES cells and the metabolomic consequences of compounds' exposure, the water-soluble metabolome was assessed using the HR ^{1}H NMR. First, cytotoxicity of both model compounds and organophosphate pesticides on LUHMES cells was assessed. The following concentrations were identified as the concentrations reducing the viability by 50 percentage after 48 hours of exposure: rotenone (1.5 µM), paraquat (50 µM),

chlorpyrifos (35 µM) and parathion (350 µM). Prior to exposure, LUHMES cells were differentiated for 6 days, as described in section 2.2.2.

Samples of undifferentiated, differentiating (day two, four, six, and eight), and compound-treated LUHMES cells on culture dishes were incubated with trypsin-EDTA (0.05%) for three minutes under standard cell-culture conditions. Then, the cells were detached by flushing with ice-cold advanced DMEM/F-12 medium media and transferred into a 15 mL tube. The cell suspension was centrifuged at 1200 rpm for five minutes at 4°C. After removal of the supernatant, the pellet was washed once with 5 mL ice-cold PBS. After a second centrifugation step, the cell pellet was resuspended in 5 mL PBS. Of that, 500 µL were transferred into a fresh 15 mL tube and used for the assessment of the total protein content for sample normalization. The remaining 4.5 mL were centrifuged at 1200 rpm for 5 minutes at 4°C and the cell pellet was stored at -80 °C or directly used for metabolite extraction.

In order to stop all intracellular metabolic reactions, 4 mL pre-chilled methanol were added to the pellets on ice. The samples were vortexed and incubated for 15 minutes on ice. Afterwards, 4 mL chloroform were added, vortexed, and incubated on ice for ten minutes. Subsequently, 4 mL ddH_2O were added, vortexed, and incubated at 4 °C overnight to enable phase separation.

The next day, the samples were centrifuged at 3500 rpm for 25 minutes at 4°C without a brake. Next, the upper water-methanol phase (8 mL) was separated from the lower chloroform phase and distributed equally into four 2 mL Eppendorf tubes. The methanol was evaporated in an Eppendorf concentrator for three hours. Afterwards, the samples were pooled, deep-frozen in liquid nitrogen, and lyophilized overnight. Dried samples were stored at -80°C until measurement.

The lyophilizates were resuspended in 20 mM phosphate buffer (pH 7.0) containing 10% D_2O and 3-(Trimethylsilyl) propanoic acid (TSP) as an internal standard. ^{1}H NMR spectra were acquired on a Bruker AVANCE III HD 700 spectrometer equipped with a 5 mm HCN TCI cryo-probe operating at 700 MHz (16.4 Tesla). The data was obtained using excitation sculpting for water suppressing and the following acquisition parameters: 25°C sample temperature, 9800 Hz sweep width, 3.2 s repetition time and time-domain data points of 32 K and 256 transients. Mestrenova software was used to

process and analyze the HR ^{1}H NMR spectra. Equal concentrations of TSP in each sample were used as an internal standard for normalization.

Bicinchoninic acid (BCA) assay

For protein quantification, the BCA assay was used according to the manufacturers' instructions. In brief, 25 µl cell lysate and 25 µl of serial BSA dilutions (0.1, 0.25, 0.5, 0.75, 1 and 2 mg/ml) were added to a 96-well plate. A total of 200 µl of the working reagent were added to every well. The working reagent was prepared by mixing the BCA reagent A with B with a ratio of 50:1 (50x µL BCA reagent A + 1x µL BCA reagent B). The plates were left on an orbital shaker for 30 seconds at 350 rpm followed by an incubation at 37°C for 30 minutes. Absorbance was measured at 562 nm on a multimode microplate reader (Tecan).

2.2.8 Statistical analyses

Using GraphPad Prism software, means and standard errors of mean (SEMs) were calculated from three independent experiments performed in triplicates, and normalized to the media or solvent control, for the cytotoxicity assay to the maximum cell death lysis control, or for neuronal differentiation to the undifferentiated cells. For significance analysis of concentration response data, a one-way analysis of variance (ANOVA) followed by Dunnett's post hoc test was performed. Thereby the data from each compound concentration were compared to the respective media, solvent or lysis control, and probability value (P-value) < 0.05 was considered significant.

For calculating the half maximal inhibitory concentration (IC_{50}) and the 95% confidence interval of the compound's effects, the sigmoidal dose-response curve fitting was conducted. Therefore, a four-parameter logistic nonlinear regression model was used and the upper and lower values were set to 100% and 0%, respectively.

All metabolomic data represent the means and standard deviations (SDs) of three biological replicates. Significance was calculated using a one-sided t-test, a P-value of $p<0.05$ was considered significant. For the experiments assessing the metabolomic changes of differentiating LUHMES cells, the data was normalized to undifferentiated LUHMES cells. For the experiments evaluating the metabolomic consequences of compounds' exposure, the results of treated cells were normalized to the results of the cells exposed to the medium with solvent control.

3 Results

3.1 hiPSC and LUHMES cells differentiation into dopaminergic neurons

The first objective of this thesis was to establish a test system that reflects PMD related adverse events in a dopaminergic system. In order to overcome the ethical consideration and difficulty of obtaining human neurons, neuronal differentiation of hiPSC and LUHMES cell lines was carried out.

3.1.1 Neuronal differentiation of hiPSCs

Human iPSCs are generated by reprogramming of human somatic cells (Yu *et al.*, 2007). Several protocols describe the induction of these cells into dopaminergic neurons (Hartfield *et al.*, 2014; Fernández-Santiago *et al.*, 2015). Since the goal of this thesis was to establish a testing battery for hazard assessment of pesticides leading to PMD, the assays included within the battery should be based on the subtypes of dopaminergic neurons found in the SN. Zhang *et al.*, (2014a) described the differentiation into subtypes of dopaminergic neurons *in vivo* located in the SN. This is the reason for selecting this protocol.

To establish a protocol for the differentiation of dopaminergic neurons from hiPSCs (IMR90 (WiCell)) and NIH-11 cell lines were differentiated according to the protocol published by Zhang *et al.*, (2014a). The experimental set-up for the differentiation of hiPSCs into dopaminergic neurons is summarized in Fig.3 in the section 2.2.1.

Morphological analyses

The differentiation of hiPSCs was monitored by morphological analysis using a phase-contrast microscope. The phase-contrast images of the differentiating hiPSCs showed an increase of confluency to 100% within the first 6 days of differentiation. Between day 6 and day 19, the cells grew in multiple layers and formed cell aggregates (Fig.5 A-C). After splitting at day 20, the cells grew slower and formed neurites. However, on day 25 and 29, inconsistencies were detected between different wells since neurons with different lengths of neurites were observed (Fig.5 E, F), while the cells showed morphological characteristics that indicated cell death on other wells (Fig.5 D).

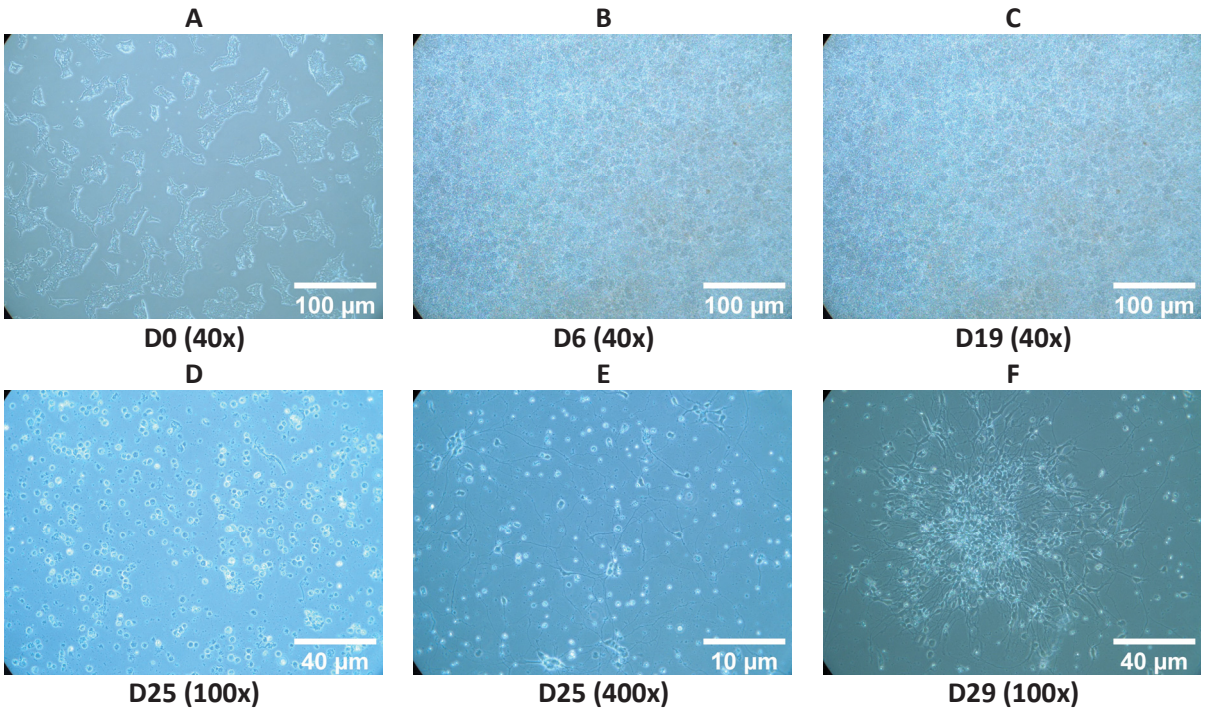

Fig.5: Differentiation of hiPSCs into dopaminergic neurons. Representative images of (A) hiPSCs on the first day of differentiation. Increasing cell density and cell growth in multiple layers were observed on day 6 (B) and 19 (C) of differentiation. Cell death was observed on day 25 (D) of differentiation. Neurons with long neurites were detected on day 25 (E) and day 29 (F) of differentiation.

To prevent the high confluency, the cell number was reduced from 3.6 x 10^4 cells/cm^2, to 1.8 x 10^4 cells/cm^2 and 1.2 x 10^4 cells/cm^2 on the plating day (Fig.6 A-C). Yet, the cells continued to grow in multiple layers and the confluency issues were not solved. Besides, the inconsistencies between the wells displayed in, cellular detachment was observed on day 25 and 27 resulting in only a few neuronal cells left on day 27 (Fig.6 D-I).

mRNA expression analyses

For molecular characterization of neuronal differentiation of hiPSCs, RNA was isolated from undifferentiated hiPSCs and from differentiated cultures on day 25. The expressions of dopaminergic neuron specific markers (TH, DAT and GIRK channel) and the progenitor cell marker (SOX2) were analyzed using qRT-PCR. They showed increased expression of TH by 910.17 folds and GIRK channel by 17.75 folds compared to control. However, there was no significant change in expression of SOX2 (0.85) or DAT (1.64) on day 25 of differentiation compared to undifferentiated cells (Fig.7).

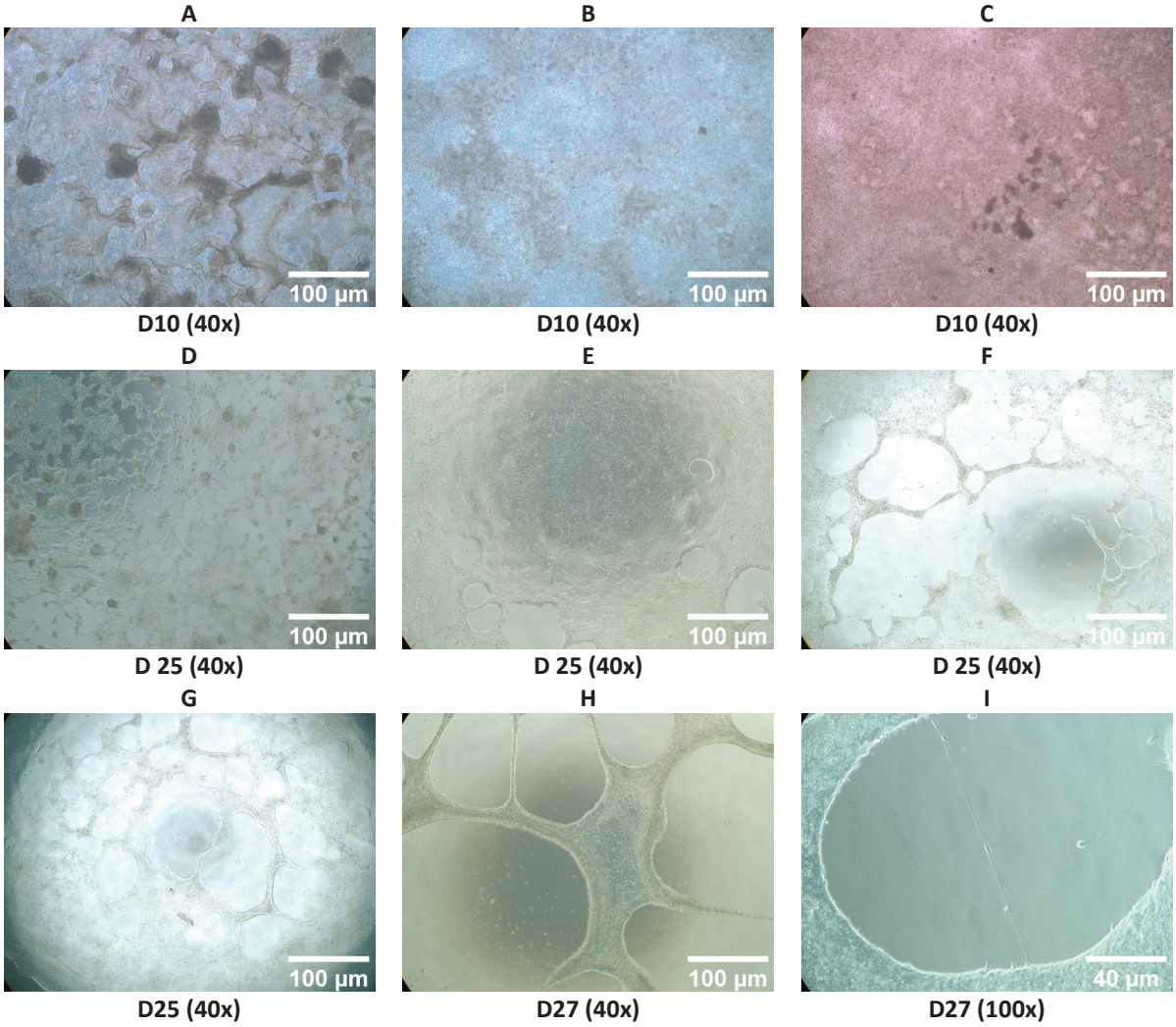

Fig.6: The obstacles of hiPSC differentiation into dopaminergic neurons. Representative images of cells growing in multiple layers on day 10 with density of 3.6 x 10^4 cells/cm^2 (A), 1.8 x 10^4 cells/cm^2 (B) and 1.2 x 10^4 cells/cm^2 (C). (D - G) Cell detachment on day 25 of differentiation in 24-well plates (D, E), 8 chamber slides (F) and 96-well plates (G). Cell detachment and arrangement in bundles with few neuronal branches on day 27 of differentiation (H, I).

The morphological evaluation of differentiated hiPSCs indicates that differentiated cells on day 25 are of the neuronal lineage. The expression of the rate-limiting enzyme for dopamine synthesis, TH, indicates the presence of dopaminergic neurons. Additionally, the increased expression of the GIRK channel indicates the differentiation to a subtype of dopaminergic neurons *in vivo* located in the SN. However, the expression of DAT was not changed during differentiation. Since DAT is responsible for the transport of dopamine from the synaptic cleft to neurons (Overk and Mufson, 2010), this may indicate that the hiPSC-derived dopaminergic neurons are not able to take up dopamine. The expression of the progenitor marker SOX2 was not affected indicating that the cells are still in a state of early differentiation.

Although the differentiation protocol seems to produce dopaminergic neurons, the lack of reproducibility and inconsistencies between wells does not allow the use of these cells for compound testing in a medium-throughput set up. Other limitations are the long differentiation time of 25- 45 days as well as the limited amount of material gained after differentiation.

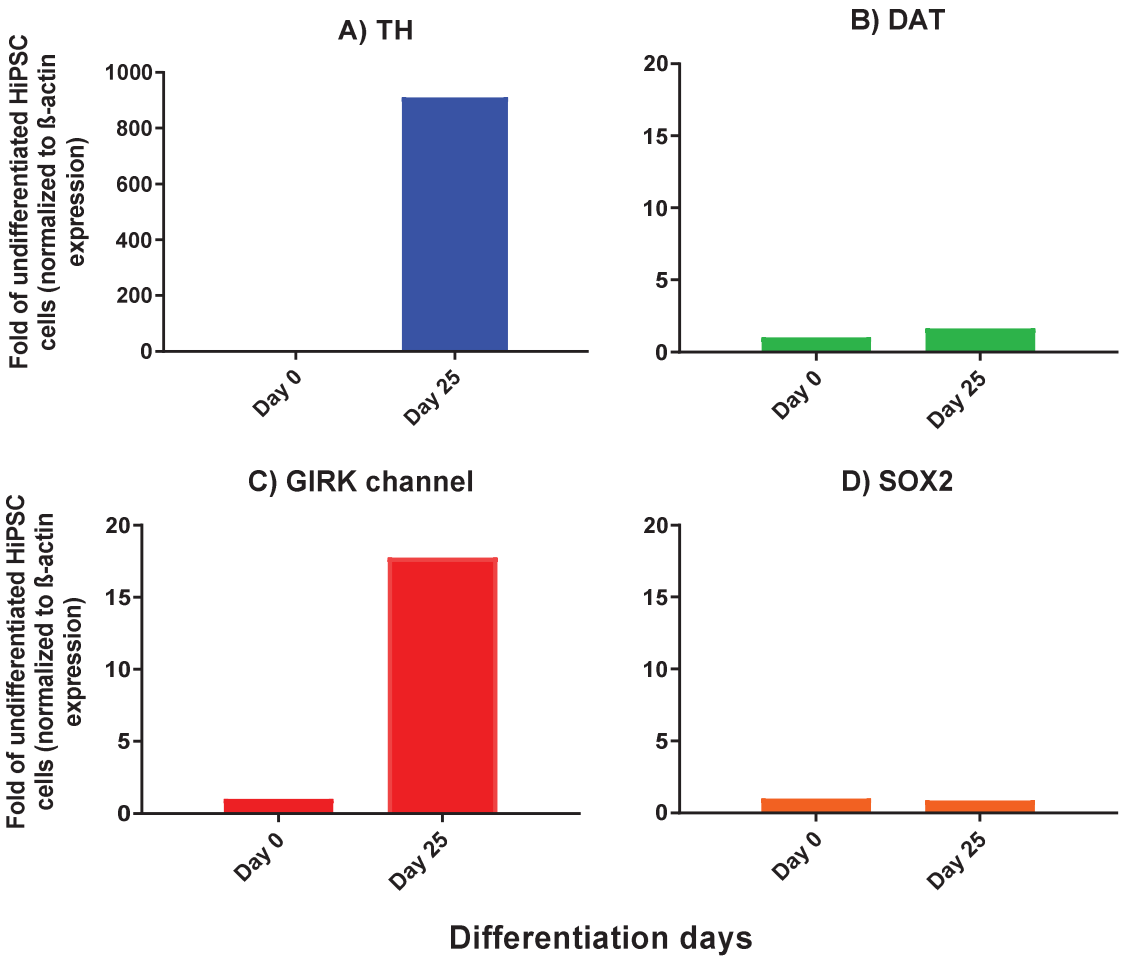

Fig.7: qRT-PCR analyses of neuronal differentiation of hiPSCs. Human iPS cells were differentiated for 25 days. The mRNA expression of dopaminergic neurons markers (A; TH, B; DAT), a dopaminergic neuron subtype of the SN (C; GIRK channel) and progenitor cells (D; SOX2) on day 0 (undifferentiated cells) and day 25 of differentiation was analyzed using qRT-PCR. Data are shown as fold of expression of these markers on day 25 compared to undifferentiated cells (expression of specific markers was normalized to ß-actin expression). Data from one experiment is shown (n=1). DAT: dopamine transporter, GIRK channel: G-protein-coupled inwardly rectifying potassium channel, TH: tyrosine hydroxylase, SN: substantia nigra, Sox2: SRY-box containing gene 2.

To circumvent these disadvantages, the usability of a testing battery based on LUHMES cells was evaluated. These cells allow the generation of a larger number of

dopaminergic neurons within a shorter period of time and have previously been used for compound testing (Tong *et al.*, 2017). Therefore, they are a suitable alternative for hiPSC-derived dopaminergic neurons.

3.1.2 Neuronal differentiation of LUHMES cells

To establish a protocol for the generation of dopaminergic neurons from LUHMES cells, the cells were differentiated according to the protocol by Scholz *et al.*, (2011). LUHMES cells are human cells that can be differentiated into dopaminergic neurons within six days, which is faster than the neuronal differentiation of hiPSCs. LUHMES cells express general dopaminergic markers (DAT, dopamine receptor D_2 and TH) and more importantly markers for the dopaminergic neuron subtypes found in the SN (GIRK). Therefore, using LUHMES cells to set up the testing was a promising approach.

Morphological analyses

LUHMES cells were differentiated for 6 days. The phase contrast images of differentiating LUHMES cells showed an increasing confluence to up to 70 - 80% over the first two days of differentiation (Fig.8 A-B). After splitting and seeding in 24-well plates, the cells started to assume a neuronal morphology with neurites (Fig.8 C). On day 6 of differentiation, neuronal networks were formed (Fig.8 D-F).

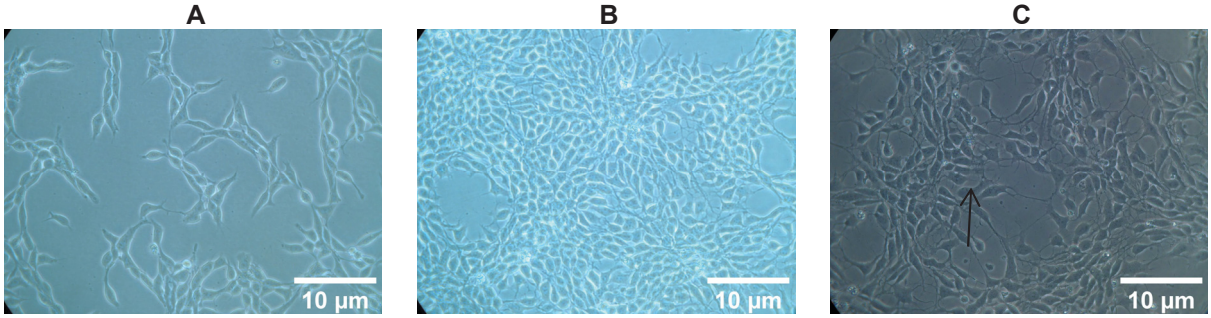

Undifferentiated LUHMES (400x) **D2 (400x)** **D4 (400x)**

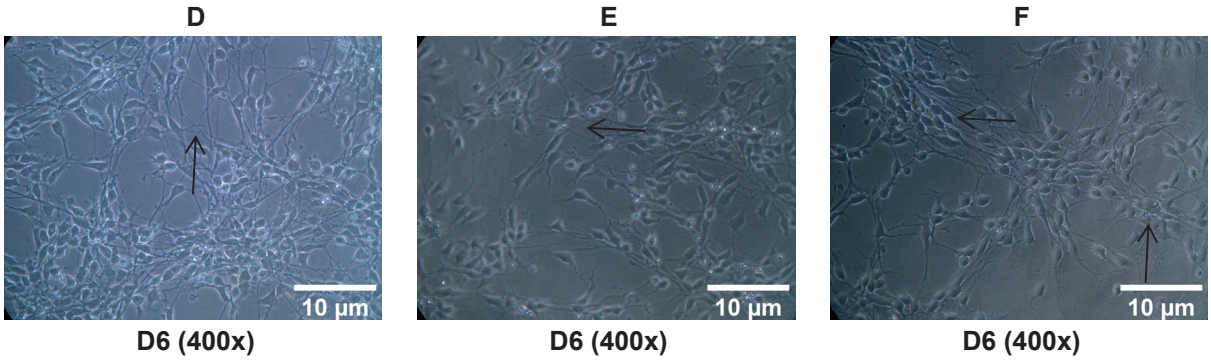

Fig.8: Differentiation of LUHMES cells. Undifferentiated LUHMES cells (A) and differentiating LUHMES cells on day 2 (B), day 4 (C), day 6 (D-F) of differentiation. The arrows point to a cell with neuronal morphology.

For further characterization of LUHMES cells, the cells were stained with neuronal (βIII-tubulin), cytoskeletal (phalloidin) and nuclear (Hoechst) markers. The phalloidin and βIII-tubulin staining showed branched and connected networks. The complete overlap of the βIII-tubulin and phalloidin staining visualized the interconnected neuronal networks further indicating that LUHMES cultures are pure neuronal cultures (Fig.9).

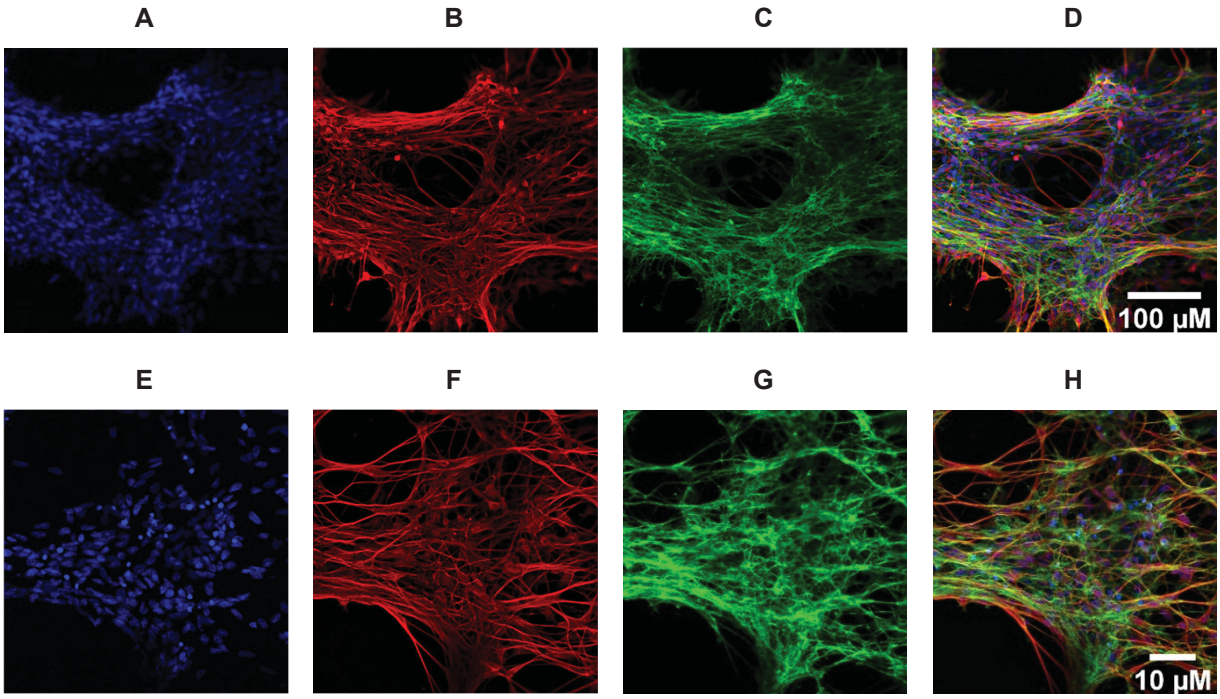

Fig.9: Confocal microscopy images of differentiated LUHMES cells on day 6 of differentiation. The differentiated LUHMES cells were stained with Hoechst (blue; A, E), phalloidin (red; B, F) and βIII-tubulin (green; C, G). Merge of the three stainings (D, H).

mRNA expression analyses

For molecular characterization of the neuronal differentiation of LUHMES cells, RNA was isolated from LUHMES cells on day 0 (undifferentiated cells), 4 and 6 of differentiation. The expression of neuronal (ENO2) and dopaminergic (DAT and TH) markers was analyzed using qRT-PCR. Compared to undifferentiated cells, the expression of the neuronal marker (ENO2) increased 47.19 ± 12.79-fold and 131.96 ± 29.48-fold on days 4 and 6 of differentiation, respectively. However, no statistically significant changes in the expression of ENO2 after 4 days of differentiation were detectable. The expression of the dopaminergic marker DAT increased 12.53 ± 2.90-fold and 16.85 ± 0.58-fold on day 4 and 6 of differentiation compared to undifferentiated cells, respectively. Moreover, TH was not present in undifferentiated LUHMES cells, clearly detectable on day 4 and increased 42.98 ± 7.68-fold on day 6 compared to day 4 of differentiation (Fig.10).

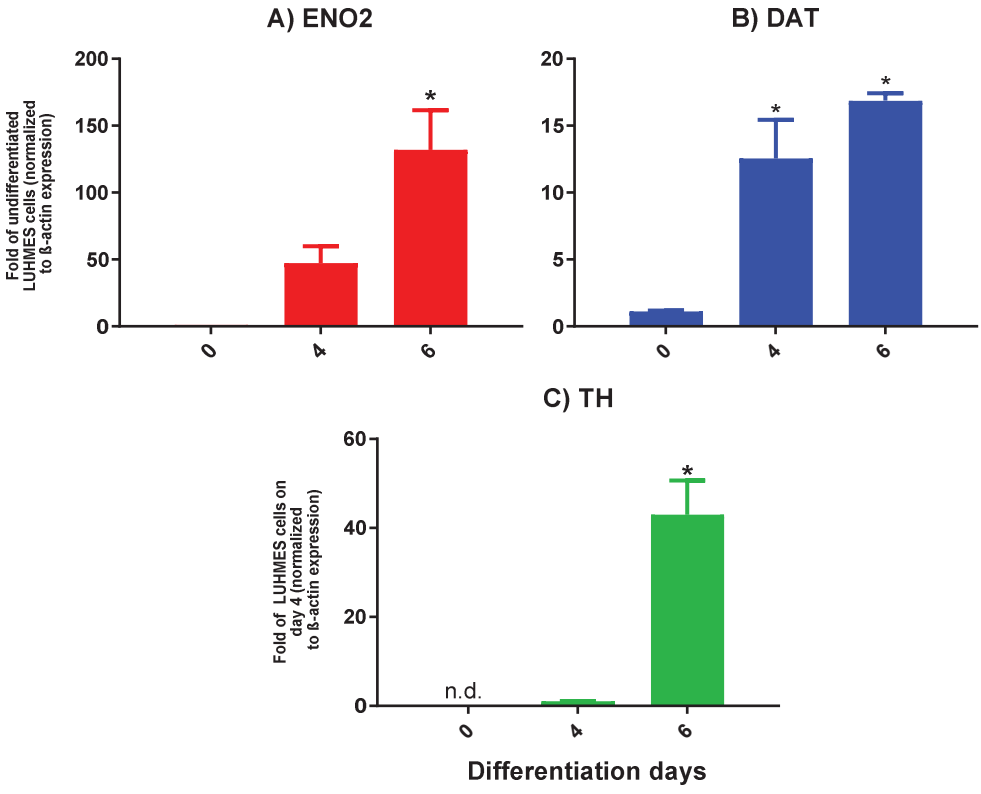

Fig.10: qRT-PCR analyses of neuronal differentiation of LUHMES cells. LUHMES cells were differentiated for 6 days. The mRNA expression profiles of neuronal (A; ENO2) and dopaminergic (B; DAT, C; TH) makers on day 0 (undifferentiated cells), 4 and 6 of differentiation were analyzed using qRT-PCR. Data are shown as fold of expression of day 4 and 6 compared to day 0 (normalized to ß-actin expression), as means ± SEM of three independent experiments with three technical replicates each. * indicates a significant difference ($p<0.05$) compared to undifferentiated cells or to cells on day 4 for TH calculated with one-way ANOVA followed by Dunnett's post hoc test. DAT: dopamine transporter, ENO2: neuron-specific enolase 2, n. d.: not detected, TH: tyrosine hydroxylase.

For screening compounds in a higher throughput format, testing in 96-well plates is necessary. Therefore, the next step was to establish cultivation of LUHMES cells in 96-well plates. Therefore, cells were seeded at a density of 40-60 x 10^3 cells/well in 96-well plates. After a thorough examination of the individual wells, inconsistencies between the wells were noticed. In particular, cells detachment, cell aggregations and morphological changes indicating cell death could be observed (Fig.11B+D).

A possible reason for these inconsistencies might be an inadequate coating protocol of the 96-well plates. Thus, the protocol was optimized and the concentration of fibronectin was increased from 1 to 1.5 µg/ml. Afterwards, the cells grew homogenously.

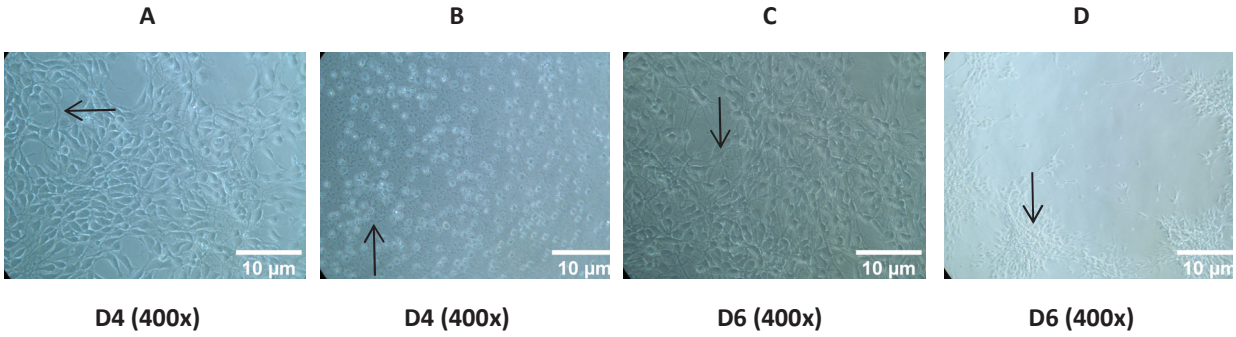

Fig.11: The obstacles of LUHMES cell differentiation in 96-well plates. LUHMES cells on day 4 of the differentiation with arrowheads pointing at a cell with neuronal morphology (A) and small rounded cells indicating cell death (B). LUHMES cells on day 6 of differentiation with arrowheads pointing at a cell with neuronal morphology (C) and aggregation (D).

Inconsistencies in the neuronal differentiation of hiPSCs, the time-consuming differentiation protocol and the limited amount of material gained after differentiation made this protocol unsuitable for compound testing in a medium-throughput set-up. The switch to dopaminergic neurons generated from LUHMES cells achieved promising results. The differentiation of LUHMES cells was reproducible and time efficient. Additionally, LUHMES cells grew homogenously in 96-well plates which facilitates the screening of compounds in a medium-throughput format.

3.2 Set up of a testing battery based on early KEs of the AOPs for PMD

EFSA recommended using the AOP concept for reassessing the hypothesis that some pesticides may cause PMD. Two AOPs were suggested. The first AOP describes the effect of the CI inhibitors, while the second one demonstrates the toxicity of the compounds affecting redox cycling. AOP1 starts with the binding of CI inhibitors to CI (MIE1) resulting in the inhibition of CI (KE1). The MIE of AOP2 is the alteration of redox cycling which starts with the release of electrons from the ETC. Both MIE result in mitochondrial dysfunction (KE2 of AOP1 and KE1 of AOP2). Impairment of the protein degradation (KE3 of AOP1 and KE2 of AOP2) occurs secondary to mitochondrial dysfunction and leads to degeneration of dopaminergic neurons (KE4 of AOP1 and KE3 of AOP2) and PMD (AO; Ockleford *et al.*, 2017).

To set up a testing battery based on the early KEs as described above, several cell biological assays were combined that are able to measure individual KEs. For the set-up of those assays, model compounds were used that are known to affect the described KEs of the AOPs. Rotenone is a potent CI inhibitor and was heavily investigated for its MoA over the last decades (Talpade *et al.*, 2008; Chen *et al.*, 2017). Furthermore, it was used for modelling PD in rodents mimicking the histopathological changes and locomotor impairment observed among the PD patients (Betarbet *et al.*, 2000; Cannon *et al.*, 2009; Salama *et al.*, 2012). Moreover, many epidemiological studies reported a higher risk of PD among individuals exposed to rotenone (Tanner *et al.*, 2011; Pouchieu *et al.*, 2018). For the first AOP, following the recommendation of EFSA, rotenone was used as the first model compound inhibiting CI (Ockleford *et al.*, 2017).

For the AOP2, paraquat was recommended by EFSA as a compound affecting the redox cycle. Paraquat acts as an electrons acceptor and reduces molecular oxygen. This results in the formation of superoxide anions that cause mitochondrial dysfunction due to oxidative damage, mitochondrial fragmentation and impaired ATP production (Bus and Gibson, 1984; Ockleford *et al.*, 2017). Paraquat was used over the last decades to induce PD in rodents (Liou *et al.*, 1996; Brooks *et al.*, 1999; McCormack *et al.*, 2002). Additionally, several epidemiological studies observed a higher risk of PD among individuals exposed to paraquat (Tanner *et al.*, 2011; Pouchieu *et al.*, 2018).

3.2.1 Assessment of mitochondrial activity based on metabolic activity

Mitochondrial dysfunction is one major shared KE (KE2 of the AOP1 and KE1 of AOP2) in the pathogenesis of PMD. To assessed a compound effect on mitochondrial dysfunction, the CTB assay was set up. This assay measured the NAD-dependent reduction of resazurin into its fluorescent form, resorufin. Reduction of resazurin takes place in the mitochondria and can also occur in the cytoplasm, as was reviewed by Rampersad, (2012). In this assay, rotenone, as a potent CI inhibitor, was used as a positive compound besides being the model compound for AOP1.

Treating LUHMES cells with different concentrations of rotenone (0 - 50 µM) over 6, 24 and 48 hours reduced cell viability in a concentration and time-dependent manner. The lowest concentration that significantly affected cell viability after 24 and 48 hours is 0.4 µM. It decreased the cell viability to 81.71 ± 3.67% and 64.36 ± 7.05% of control after 24 and 48 hours, respectively. The cell viability was reduced to 57.45 ± 1.39% of control at the highest concentration (50 µM) after 6 hours (Fig.12).

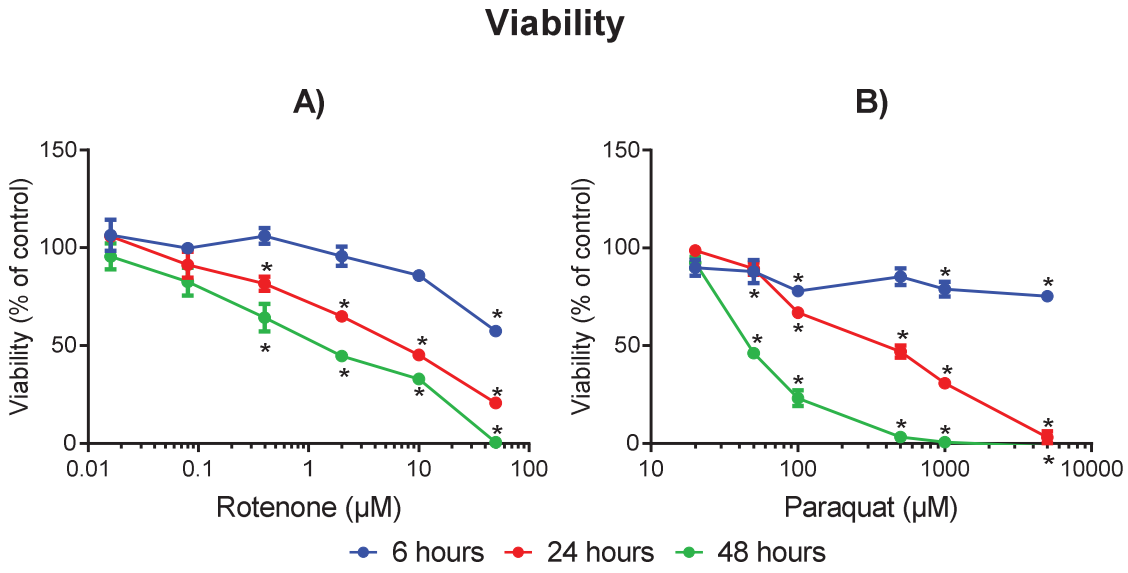

Fig.12: Effects of rotenone and paraquat on the viability of differentiated LUHMES cells. Differentiated LUHMES cells were exposed to a) rotenone (0-50 µM) and b) paraquat (0-5 mM) for 6, 24 and 48 hours. Viability based on the metabolic activity was assessed by the CTB assay. Data are shown as percentage of the solvent (0.1% DMSO) or media control, as means ± SEM of three independent experiments with three technical replicates each. * indicates a significant difference ($p<0.05$) from the respective media and solvent control based on one-way ANOVA, followed by Dunnett's post hoc test. CTB assay: Cell Titer Blue assay.

Addition of paraquat in serial dilutions (0 - 5 mM) to LUHMES cells over 6, 24 and 48 hours decreased the cell viability in a concentration and time-dependent manner after 24 and 48 hours. After 24 and 48 hours, 50 µM is the lowest concentration that significantly reduced cell viability to 89.43 ± 3.08% and 46.41 ± 2.12% of control, respectively. After 6 hours, 100 µM is the lowest concentration reducing cell viability to 77.96 ± 2.43% of control. The degree of reduction of cell viability between 24 and 48 hours is more pronounced in paraquat compared to rotenone (Fig.12).

For a better comparison of the potencies of the model compounds, IC_{50} values were calculated for the three tested time points. Rotenone is more potent than paraquat with IC_{50} values of 6.09 µM and 1.38 µM for rotenone versus 368.2 µM and 50.7 µM for paraquat after 24 and 48 hours, respectively (Table 17).

Table 17: IC_{50} values for the effects of rotenone and paraquat on cell viability (CTB assay)

Compounds	Exposure	*IC_{50} (95% CI)*
Rotenone	6 hours	n. e.
	24 hours	6.09 *(4.35 - 8.51)*
	48 hours	1.38 *(0.84 - 2.25)*
Paraquat	6 hours	n. e.
	24 hours	368.2 *(291.3 - 465.4)*
	48 hours	50.70 *(46.21 - 55.63)*

95% CI: 95% confidence interval, n. e.: no effect

3.2.2 Assessment of mitochondrial activity based on ATP levels

An additional readout for mitochondrial dysfunction is crucial as the CTB assay is not specific to the ETC (Rampersad, 2012), as described in section 3.2.1. The ATP level is a more specific readout for the mitochondrial function as ATP is mainly produced in the mitochondria at the level of the ETC. CI is the main site for entry of electrons from NADH. These electrons are carried to complex III (CIII) and subsequently been transported to complex IV (CIV) creating a H^+ gradient across the mitochondrial membrane. This gradient stimulates complex V (CV) to produce ATP molecules, as reviewed by Zhao *et al.*, (2019). Therefore, an assay that directly measured the cell viability based on ATP level, the CTG assay, was set up. Rotenone was used as a

positive control for inhibiting the synthesis of ATP, as a potent inhibitor of CI (Talpade *et al.*, 2008).

Different concentrations of rotenone (0-50 µM) were applied to LUHMES cells on day 6 of differentiation for 6, 24 and 48 hours. Rotenone decreased cell viability (CTG assay) in a concentration-dependent manner after 24 and 48 hours. 0.4 µM and 0.08 µM are the lowest concentrations reducing the cell viability (CTG assay) to 72.43 ± 3.62% and 80.64 ± 2.12% of control after 24 and 48 hours, respectively. The highest concentration of rotenone (50 µM) significantly reduced the ATP levels after 6 hours to 68.13 ± 3.18% of control (Fig.13).

Paraquat in serial dilutions of 0 to 5 mM was applied to LUHMES cells on day 6 of differentiation for 6, 24 and 48 hours. Paraquat reduced cell viability (CTG assay) after 24 and 48 hours in a concentration and time-dependent manner. 100 µM is the lowest concentration that significantly reduced ATP to 74.29 ± 6.06% of control after 24 hours, while 50 µM is the lowest concentration that significantly decreased cell viability (CTG assay) after 48 hours to 50.22 ± 12.93% of the control. The highest concentration of paraquat reduced ATP after 6 hours to 63.42 ± 10.30% of control. The degree of the decline in cell viability (CTG assay) between 24 and 48 hours is more marked for paraquat compared to rotenone (Fig.13).

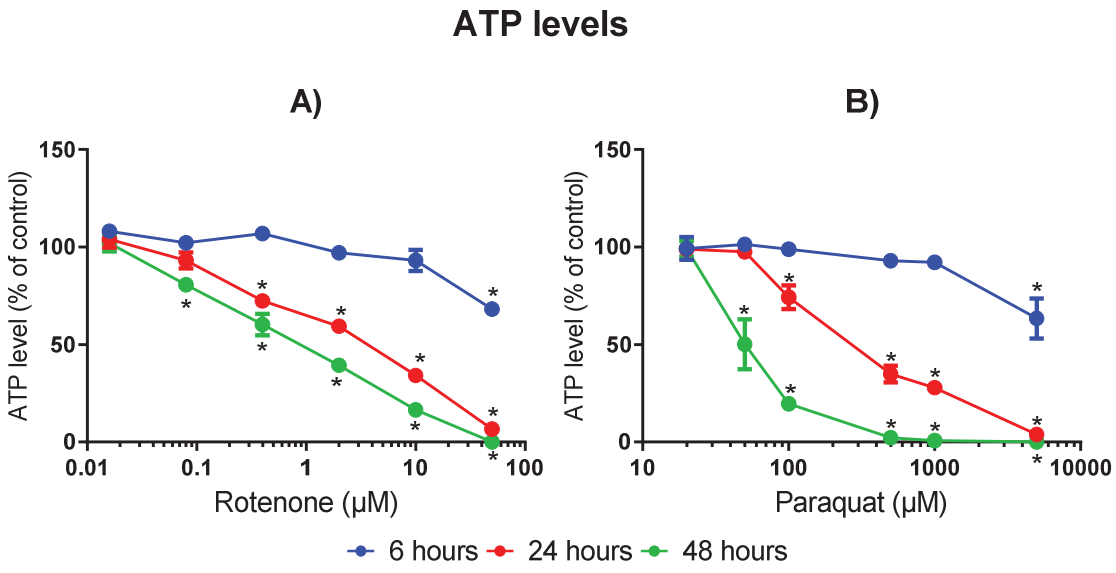

Fig.13: Effects of rotenone and paraquat on the ATP levels of differentiated LUHMES cells. Differentiated LUHMES cells were exposed to a) rotenone (0-50 µM) and b) paraquat (0-5 mM) for 6, 24 and 48 hours. Viability based on ATP levels were quantified by CTG assay. Data are shown as a percentage of the solvent (0.1% DMSO) or media control, as means ± SEM of three independent experiments with three technical replicates each. * indicates a significant difference ($p<0.05$) from the respective media and solvent control based on one-way ANOVA, followed by Dunnett's post hoc test. CTG assay: Cell Titer-Glo assay.

For evaluating the potencies of the model compounds, IC_{50} values were calculated. Rotenone is more potent than paraquat, with IC_{50} values of 2.94 µM and 0.87 µM for rotenone compared to 334.50 µM and 53.08 µM for paraquat after 24 and 48 hours, respectively. These results are in agreement with the results obtained from the CTB assay with overlapping 95% confidence intervals for cell viability based on the metabolic activity and ATP level, as demonstrated by IC_{50} values in Table 17 and 18.

Table 18: IC_{50} values for the effects of rotenone and paraquat on cell viability (CTG assay)

Compounds	Exposure	IC_{50} *(95% CI)*
Rotenone	6 hours	n. e.
	24 hours	2.94 *(2.10 – 4.11)*
	48 hours	0.87 *(0.63 – 1.21)*
Paraquat	6 hours	n. e.
	24 hours	334.50 *(267.0 – 419.20)*
	48 hours	53.08 *(45.75 – 61.57)*

95% CI: 95% confidence interval, n. e.: no effect

3.2.3 Proteasomal activity based on the activity of chymotrypsin subunit of proteasome 20S

The impairment of the protein degradation is the third KE in AOP1 and the second KE in AOP2 of PMD. The chymotrypsin-like activity subunit of UPP is responsible for the degradation of ubiquitinated proteins. Impaired activity of this subunit was observed in SN of PD patients (McNaught and Jenner 2001; McNaught et al. 2003). This degradation process is ATP dependent, as previously reviewed (Lecker, Goldberg and Mitch, 2006; Leestemaker and Ovaa, 2017). For investigating the KE3 of AOP1 and KE2 of AOP2, Proteasome-Glo™ Chymotrypsin-Like Cell-Based Assay was used to assess the activity of the chymotrypsin subunit of proteasome 20S.

LUHMES cells were exposed on day 6 of differentiation to rotenone (0-50 µM) and paraquat (0-5 mM) for 6, 24 and 48 hours. After 6 hours of exposure, the highest concentration of rotenone (50µM) inhibited the proteasomal activity to 64.03 ± 3.72% of control. Rotenone caused a concentration and time-dependent reduction of the proteasomal activity after 24 and 48 hours of application. 2 µM and 0.08 µM were the

lowest concentrations that reduced the proteasomal activity to 65.45 ± 3.92% and 86.07 ± 0.69% of control after 24 and 48 hours, respectively. For Paraquat, there was no effect after 6 hours and only the highest concentration (5 mM) inhibited the proteasomal activity after 24 hours to 19.59 ± 6.88% of control. After 48 hours, paraquat inhibited the proteasomal activity in a concentration-dependent manner with 50 µM being the lowest concentration that significantly decreased the proteasomal activity to 56.88 ± 6.65% of control (Fig.14).

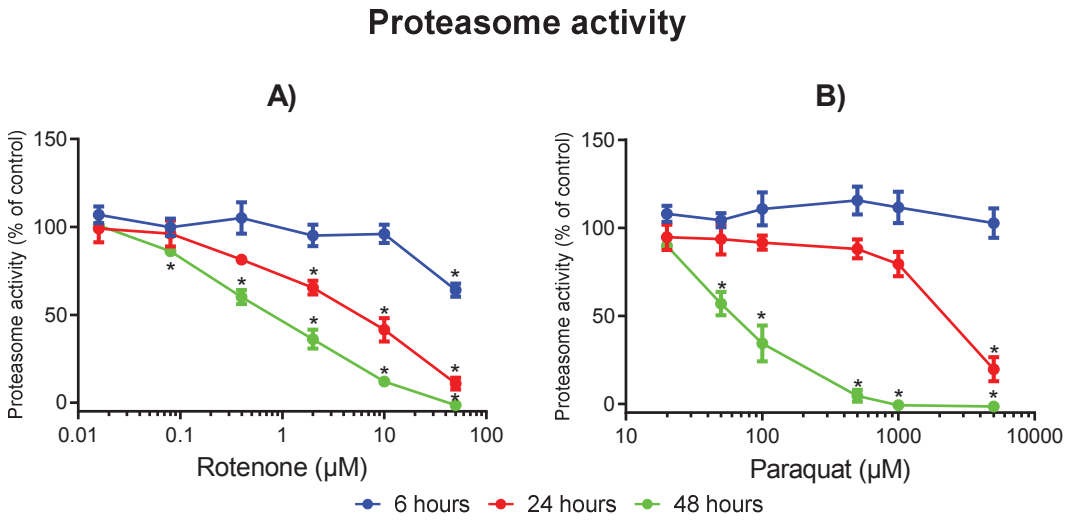

Fig.14: Effects of rotenone and paraquat on the activity of 20S proteasome of differentiated LUHMES cells. Differentiated LUHMES cells were exposed to a) rotenone (0-50 µM) and b) paraquat (0-5 mM) for 6, 24 and 48 hours. The proteasomal activity was assessed with the Proteasome-Glo™ Chymotrypsin-Like Cell-Based assay. Data are shown as a percentage of solvent (0.1% DMSO) or media control, as means ± SEM of three independent experiments with three technical replicates each. * indicates a significant difference ($p<0.05$) from the respective media and solvent control based on one-way ANOVA, followed by Dunnett's post hoc test.

For comparing the effects of the model compounds between the three tested endpoints, IC_{50} values were calculated. IC_{50} concentrations were not reached after 6 hours for both model compounds on cell viability and proteasomal activity. After 48 hours, IC_{50} values are 1.38, 0.87 and 0.80 µM for rotenone and 50.7, 53.08 and 63.99 µM for paraquat, on the cell viability (CTB and CTG assays) and proteasomal activity, respectively. IC_{50} values of the model compounds on the proteasomal activity match with these values on the cell viability assessed by CTB and CTG with overlapping 95% confidence intervals, with the exception of the effect of paraquat on the proteasomal activity after 24 hours (Tables 17-19).

Table 19: IC_{50} values for the effects of rotenone and paraquat on proteasomal activity

Compounds	Exposure	*IC_{50} (95% CI)*
Rotenone	6 hours	n. e.
	24 hours	4.79 *(3.16 - 7.26)*
	48 hours	0.80 *(0.63 - 1.03)*
Paraquat	6 hours	n. e.
	24 hours	2132 *(1505 - 3019)*
	48 hours	63.99 *(53.43 - 76.63)*

95% CI: 95% confidence interval, n. e.: no effect

The proteasomal activity strongly depends on the production of ATP (Lecker, Goldberg and Mitch, 2006; Leestemaker and Ovaa, 2017). On the other side, inhibition of proteasomal activity causes mitochondrial dysfunction (Ko *et al.*, 2020). Based on the overlapping IC_{50} values, it is therefore not clear if the reduction of proteasomal activity is a consequence of an impaired mitochondrial function or vice versa. To analyse if the different causal relationships can be distinguished, different concentrations of epoxomicin (0-50 µM), as a potent inhibitor of the proteasome 20S and an assay specific positive compound, were applied to LUHMES cells on day 6 for 6, 24 and 48 hours. Epoxomicin inhibited the proteasomal activity in a concentration-dependent manner, which was observed as early as 6 hours of exposure. This epoxomicin induced-inhibition of proteasome 20S occurred in a time-dependent manner when comparing the 6 hours with both 24 and 48 hours, but not between 24 and 48 hours. 5.56, 0.21, 1.85 µM of epoxomicin were the lowest concentrations that significantly reduced the proteasomal activity to 23.16 ± 7.50%, 81.53 ± 6.16% and 44.43 ± 14.74% of control after 6, 24 and 48 hours, respectively (Fig.15).

The cell viability (CTB and CTG assays) was assessed. Epoxomicin reduced cell viability after 24 and 48 hours in a concentrations-dependent manner and not after 6 hours. 5.56 µM is the lowest concentration that significantly decreased cell viability to 82.30 ± 0.86% and 38.14 ± 33.01% of control in CTB assay and to 67.98 ± 12.33% and 38.39 ± 23.43% of control in CTG assay after 24 and 48 hours, respectively (Fig.15).

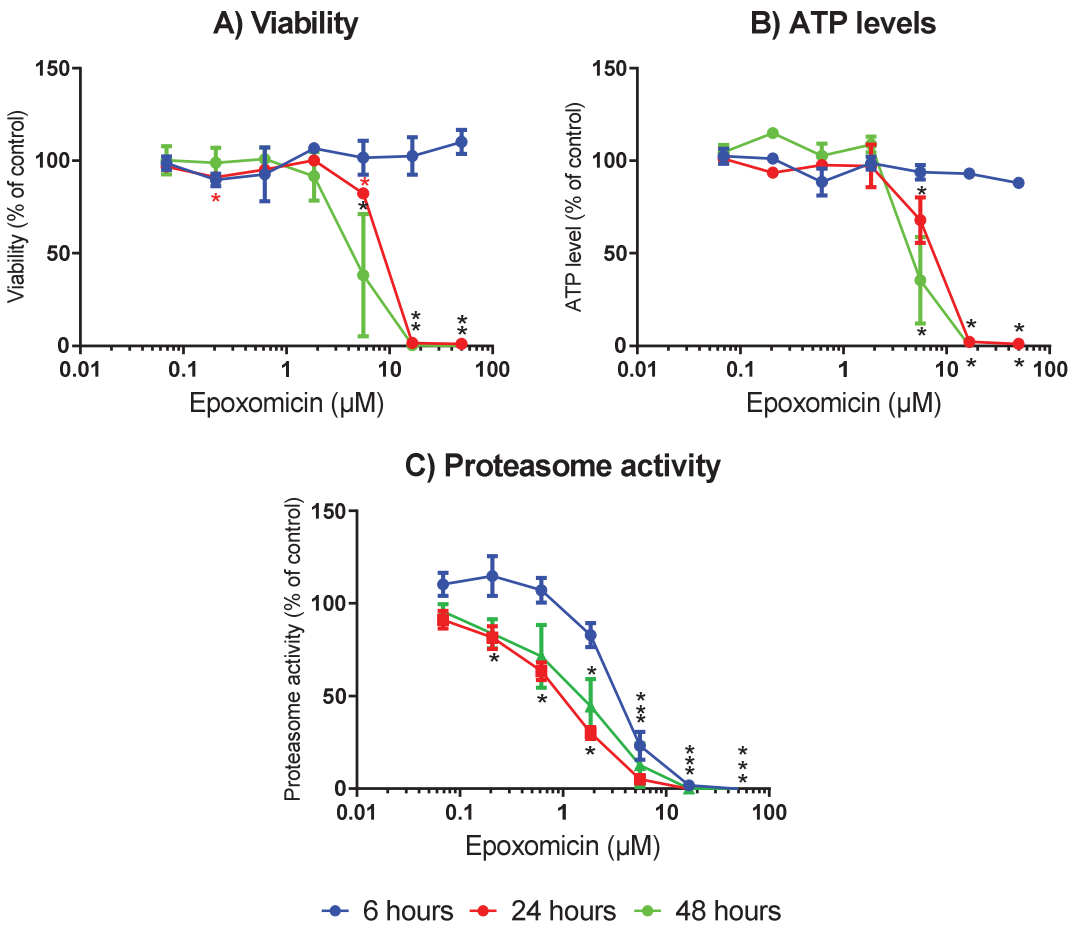

Fig.15: Effects of epoxomicin on differentiated LUHMES cells. Differentiated LUHMES cells were exposed to epoxomicin (0-50 µM) for 6, 24 and 48 hours. Afterwards, a) viability based on metabolic activity, b) viability based on ATP level and c) proteasomal activity were assessed by CTB, CTG and proteasomal activity assays, respectively. Data are shown as a percentage of solvent control (0.1% DMSO), as means ± SEM of three independent experiments with three technical replicates each. * indicates a significant difference ($p<0.05$) from the respective solvent control based on one-way ANOVA, followed by Dunnett's post hoc test. CTB assay: Cell Titer Blue assay, CTG assay: Cell Titer-Glo assay.

For determining and comparing the effects of the epoxomicin on cell viability (CTB and CTG assays) and proteasomal activity, IC_{50} values were calculated within the three tested endpoints. After 6 hours of exposure, an IC_{50} value on the proteasomal activity is 3.49 µM, while IC_{50} concentrations on cell viability are not reached. After 24 and 48 hours, IC_{50} values are 0.87 and 1.31 µM on the proteasomal activity, versus 7.49 and 4.63 µM on cell viability (CTB assay) and 6.72 and 5.36 µM on cell viability (CTG assay), respectively (Table 20).

Table 20: IC_{50} values for the effects of epoxomicin on viability and proteasomal activity

Endpoint	Exposure	IC_{50} *(95% CI)*
Cell viability (CTB assay)	6 hours	n. e.
	24 hours	7.49 *(6.14 - 9.14)*
	48 hours	4.63 *(3.11 - 6.90)*
Cell viability (CTG assay)	6 hours	n. e.
	24 hours	6.72 *(5.35 - 8.45)*
	48 hours	~ 5.36 *(very wide)*
Proteasomal activity	6 hours	3.49 (2.69 - *4.54)*
	24 hours	0.87 *(0.72 - 1.04)*
	48 hours	1.31 *(0.83 - 2.05)*

95% CI: 95% confidence interval, n. e.: no effect

These results demonstrate that the epoxomicin dependent-inhibition of the activity of 20S proteasome occurs before impairing the energetic function of the mitochondria (Table 20; Fig.15). On the other side, inhibition of the proteasomal function by the model compounds seems to be mediated by an effect on mitochondrial function (Tables 17-19; Fig.12-14). This demonstrates that the test battery is able to distinguish MoA that act primarily on the proteasome from MoA that involves proteasome dysfunction due to mitochondrial dysfunction.

3.2.4 Assessment of cytotoxicity based on the membrane integrity

The fourth KE in AOP1 and the third KE in AOP2 are the degeneration of dopaminergic neurons. Thereby two forms of cell death, apoptosis or necrosis can lead to neuronal degeneration. In this testing battery, two assays were set up of which one measures necrotic and the other one detects apoptotic cell death to be able to differentiate between the two forms of cell death. The CytoTox-ONE™ Homogeneous Membrane Integrity Assay measures the release of LDH into the media as an indirect indicator for necrotic cell death. In this assay, complete lysing of the cells with Triton X-100 causes the maximal LDH release and serves as an endpoint specific positive control. Different concentrations of rotenone (0-50 µM) were added to LUHMES cells on day 6 of differentiation for 6, 24 and 48 hours. Rotenone (50 µM) causes a significant LDH release to 19.04 ± 2.66%, 33.16 ± 0.66%

and 55.61 ± 3.57% of the lysis control, after 6, 24 and 48 hours, respectively (Fig.16).

Application of paraquat (0-5 mM) for 6 hours did not induce LDH release, while the highest concentration of paraquat (5 mM) caused a significantly LDH release after 24 hours to 21.78 ± 2.67% of the lysis control. Paraquat induced a concentration-dependent release of LDH after 48 hours, by which 500 µM is the lowest concentration that released LDH to 37.25 ± 4.96% of the lysis control (Fig.16).

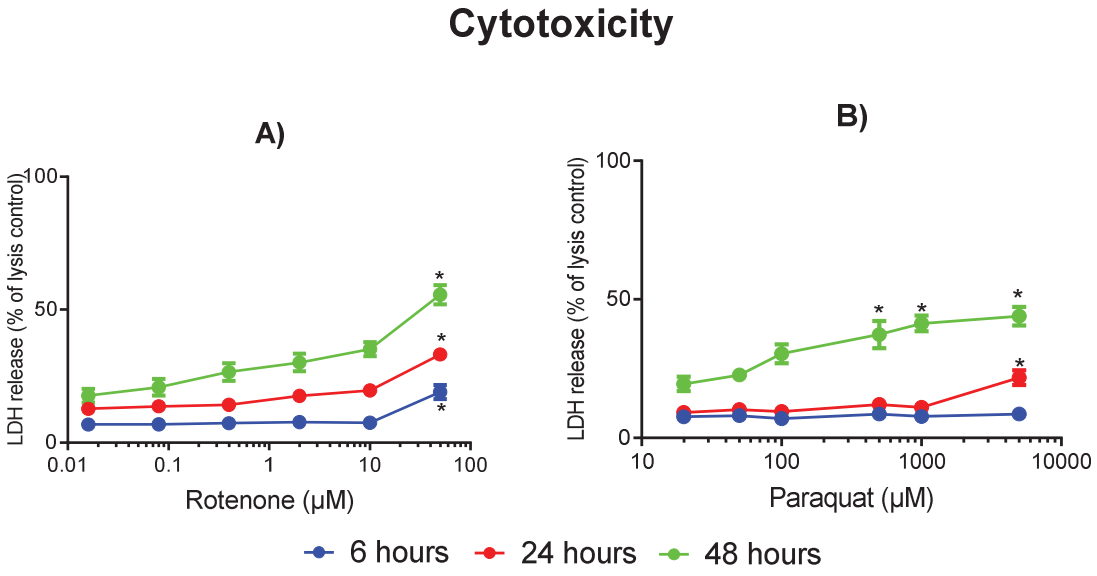

Fig.16: Cytotoxicity of rotenone and paraquat on differentiated LUHMES cells. Differentiated LUHMES cells were exposed to a) rotenone (0-50 µM) and b) paraquat (0-5 mM) for 6, 24 and 48 hours. The cytotoxicity was assessed with the CytoTox-ONE assay. Data are shown as a percentage of lysis control (complete cell lysis with Triton X-100; 0.43%), as means ± SEM of three independent experiments with three technical replicates each. * indicates a significant difference ($p<0.05$) from the respective media and solvent control based on one-way ANOVA, followed by Dunnett's post hoc test. LDH: lactate dehydrogenase.

3.2.5 Assessment of apoptosis based on activation of caspase 3/7

For assessing apoptosis, as the second type of cellular death (KE4 of AOP1 and KE3 of AOP2), activation of caspase 3/7 as a marker for apoptosis was assessed by Caspase-Glo® 3/7 Assay. The other function of mitochondria besides energy production is controlling the apoptosis. Mitochondria control the intrinsic apoptotic pathway ended by activation of the caspase 3/7, as reviewed by Wang and Youle, (2009). This is used as another readout for evaluating mitochondrial dysfunction.

In order to assess apoptosis by the model compounds, the Caspase-Glo® 3/7 Assay was used. Different concentrations of rotenone (0-50 µM) and paraquat (0-5 mM)

were added to LUHMES cells on day 6 for 6 and 24 hours. Rotenone activated caspase 3 and 7 after 6 hours and 24 hours. The lowest concentrations that induced apoptosis were 0.4 µM after 6 hours and 2 µM after 24 hours to 172.46 ± 6.13 and 226.96 ± 32.58% of control, respectively. The maximal effect was observed at 10 µM with activations to 317.27 ± 39.57% and 243.08 ± 33.36% of the control after 6 and 24 hours, respectively. Paraquat did not induce activation of caspase 3 and 7 after 6 or 24 hours (Fig.17).

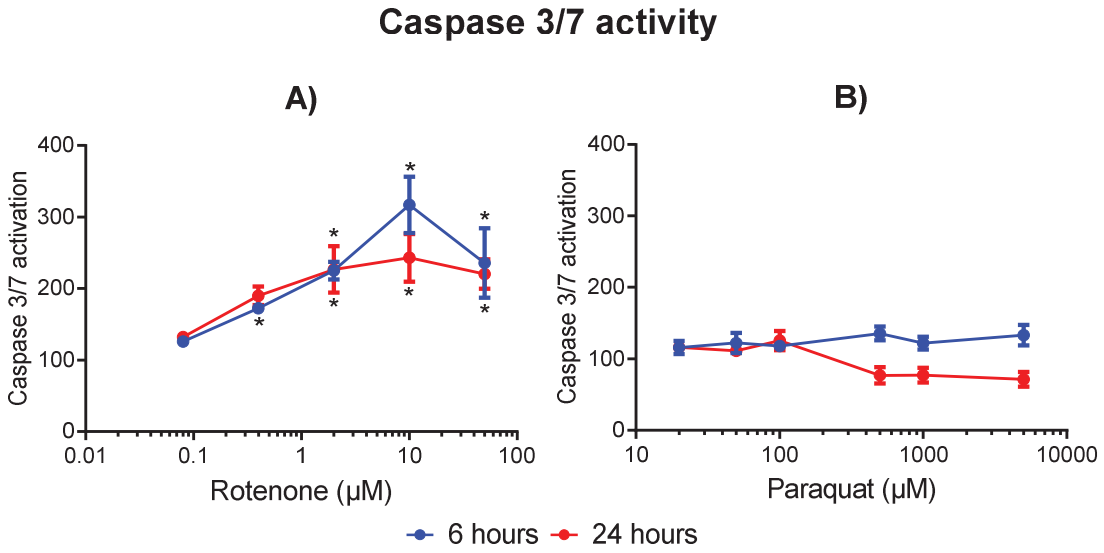

Fig.17: Apoptotic effects of rotenone and paraquat on differentiated LUHMES cells. Differentiated LUHMES cells were exposed to a) rotenone (0-50 µM) and b) paraquat (0-5 mM) for 6 and 24 hours. The apoptosis was evaluated with the caspase-3/-7 assay. Data are shown as percentage of solvent (0.1% DMSO) or media control, as means ± SEM of three independent experiments with three technical replicates each. * indicates a significant difference ($p<0.05$) from the respective media and solvent control based on one-way ANOVA, followed by Dunnett's post hoc test.

Staurosporine was used as a positive compound for activating the caspase 3 and 7, as it induces apoptosis through activation of the caspase-dependent pathway (Jantas-Skotniczna *et al.*, 2006). The effects of Staurosporine (0-10 µM) was compared with the effects of the model compounds. Staurosporine was applied to differentiated LUHMES cells on day 6 for 6 and 24 hours. It induced early activation of the caspase 3 and 7 after 6 hours in a concentration-dependent manner. This activation was reduced after 24 hours. The cytotoxicity of staurosporine and its effects on the cell viability (CTB assay) over 6, 24 and 48 hours of the application were tested. Staurosporine did not reduce the cell viability (CTB assay) or release LDH after 6 hours. The cell viability was reduced and LDH was released after 24 and 48 hours in a concentration-dependent manner (Fig.18).

So, the apoptosis was observed early after 6 hours of exposure to staurosporine and rotenone. At this time point, the energetic function of mitochondria was not affected. Later, after 24 and 48 hours, rotenone and staurosporine impaired energy production, so the necrosis was the dominant mechanism of cell death.

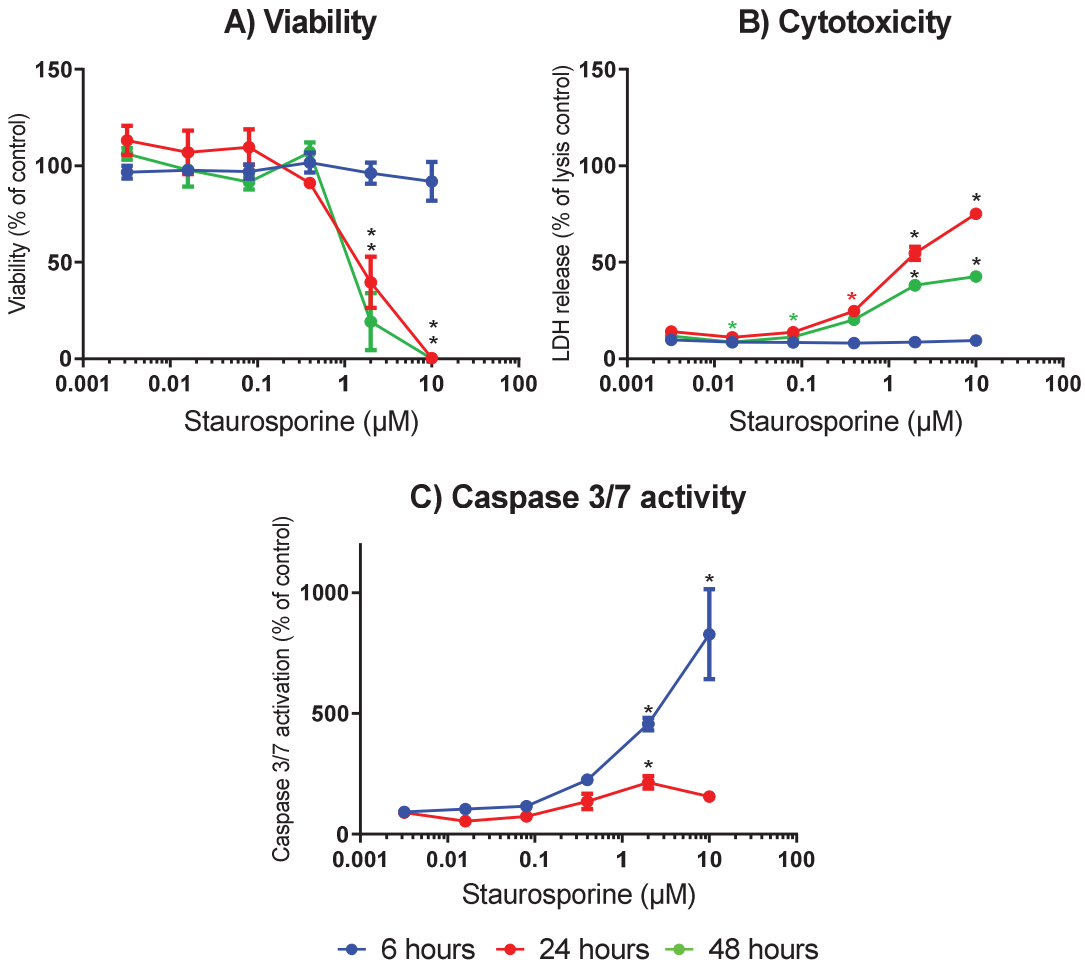

Fig.18: Effects of staurosporine on cell viability and cytotoxicity in differentiated LUHMES cells. Differentiated LUHMES cells were exposed to staurosporine (0-10 µM) for 6, 24 and 48 hours. and a) viability based on the metabolic activity, b) cytotoxicity and c) apoptosis were assessed by CTB, CytoTox-ONE and caspase 3/7 assays, respectively. Data are shown as a percentage of lysis control (complete cell lysis with Triton X-100; 0.43%) for the CytoTox-ONE Assay and percentage of the solvent control (0.05% DMSO) for the CTB assay, as means ± SEM of three independent experiments with three technical replicates each. * indicates a significant difference ($p<0.05$) from the respective solvent control based on one-way ANOVA, followed by Dunnett's post hoc test. CTB assay: Cell Titer Blue assay, LDH: lactate dehydrogenase.

3.2.6 Effects of negative compounds on early key events leading to PMD

To determine the specificity of the test battery, two negative compounds, saccharin and diethylene glycol were tested. The compounds were selected based on their previous use as negative compounds in an *in vitro* developmental neurotoxicity

testing (Aschner *et al.*, 2017). Saccharin is an artificial sweetener that is widely used in the food and pharmacy industry. Exposure to this artificial sweetener is not associated with PMD (Pinheiro *et al.*, 2005). Diethylene glycol is a sugar derivative used in the food industry. For this compound, there also exists no association to PMD (Mortensen *et al.*, 2017).

Treatment of the differentiated LUHMES cells with saccharin (0 - 1 mM) and diethylene glycol (0 - 1 mM) for 6, 24 and 48 hours did not affect any of the endpoints assessed in the battery (Fig.19 and 20). Therefore, both negative compounds have been identified as negatives across the battery.

3.3 Chemical testing

3.3.1 Effect of organophosphate pesticides on early KEs leading to PMD

Organophosphate pesticides are used worldwide for controlling pests (Elersek and Filipic, 2011) although there is evidence that exposure to some organophosphate pesticides increases the risk for PD (Allen and Levy, 2013; Narayan *et al.*, 2017). Here the effect of chlorpyrifos, parathion, malathion and dichlorvos on early KEs during PMD development were analyzed.

Chlorpyrifos is one of the commonly used organophosphate pesticides and previous studies demonstrated that chlorpyrifos may increase the risk of PD (Narayan *et al.*, 2017; Deveci and Karapehlivan, 2018; Ali *et al.*, 2019). Application of different concentrations of chlorpyrifos (0 - 250 µM) to LUHMES cells on day 6 of differentiation for 6, 24 and 48 hours reduced cell viability (assessed by CTB and CTG assays) and proteasomal activity and released LDH in a concentration-dependent manner after 24 and 48 hours. Caspase 3/7 was activated after 6 and 24 hours. After 24 and 48 hours, 27.8 µM is the lowest concentration that significantly reduced the cell viability (CTB assay) to 71.83 ± 4.90% and 55.60 ± 7.42% of control and proteasomal activity to 78.97 ± 2.91% and 67.79 ± 5.92% of control. The cell viability (CTG assay) was decreased to 80.71 ± 6.42% and 72.65 ± 12.44% of control, respectively. However, the change in cell viability assessed by CTG assay was not statistically significant (Fig.21).

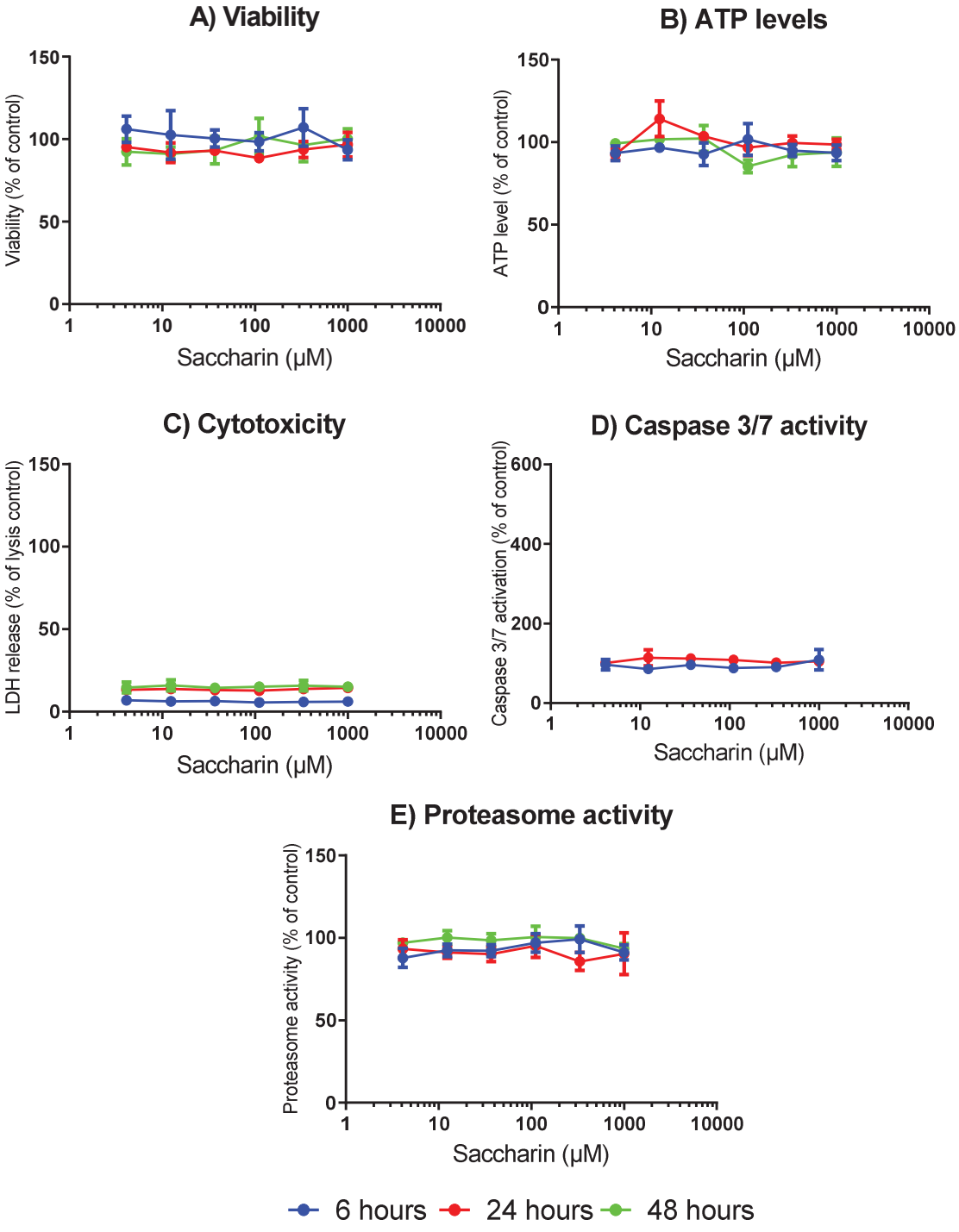

Fig.19: Effects of saccharin on differentiated LUHMES cells. Differentiated LUHMES cells were exposed to saccharin (0-1 mM) for 6, 24 and 48 hours. Afterwards, a) viability based on metabolic activity, b) viability based on ATP level, c) cytotoxicity, d) apoptosis, and e) proteasomal activity were assessed by CTB, CTG, CytoTox-ONE, caspase 3/7 activity and proteasomal activity assays, respectively. Data are shown as a percentage of lysis control (complete cell lysis with Triton X-100; 0.43%) for the CytoTox-ONE Assay and percentage of the media control for the other assays, as means ± SEM of three independent experiments with three technical replicates each. A one-way ANOVA, followed by Dunnett's post hoc test revealed no significant differences between media control and treatment. CTB assay: Cell Titer Blue assay, CTG assay: Cell Titer-Glo assay, LDH: lactate dehydrogenase.

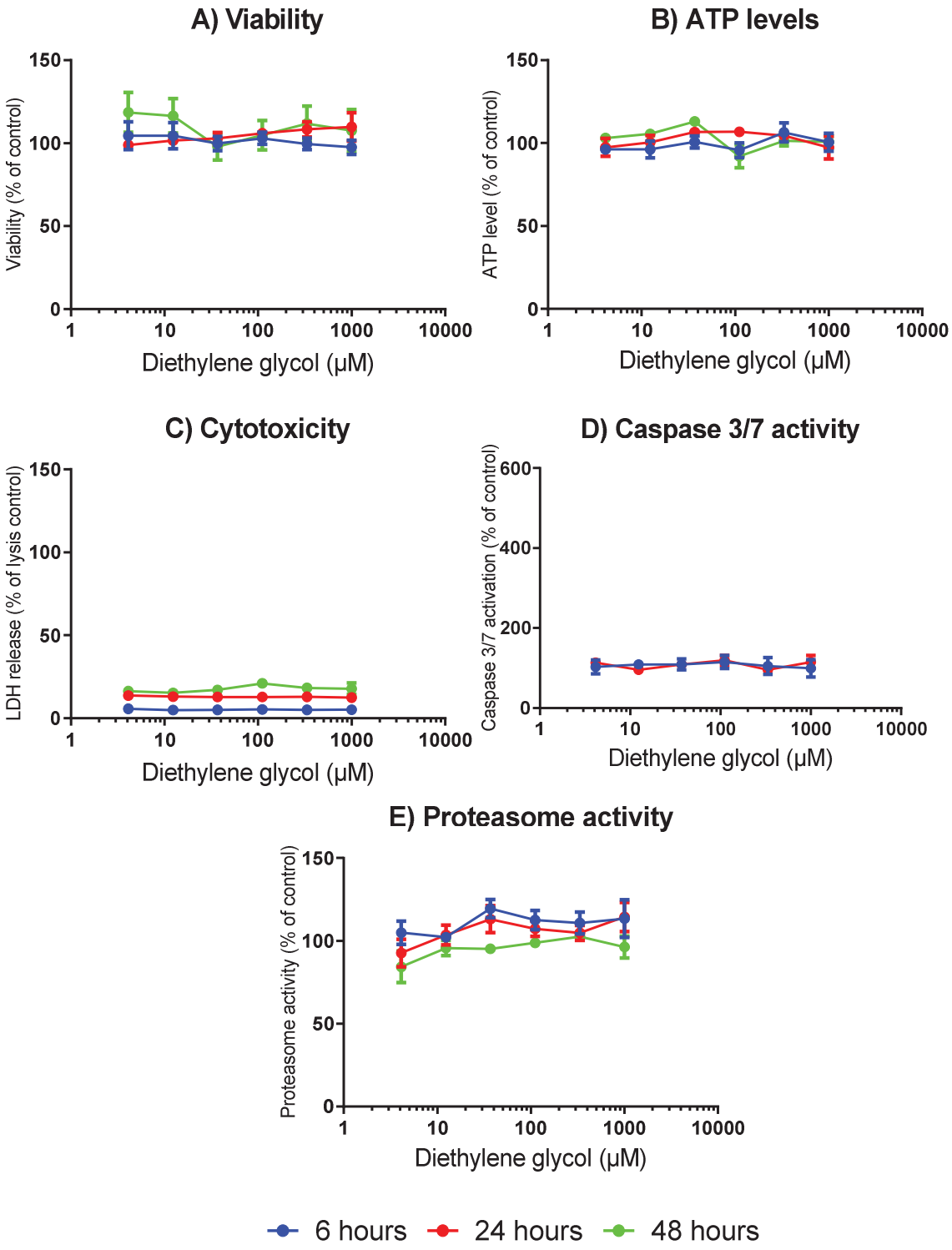

Fig.20: Effects of diethylene glycol on differentiated LUHMES cells. Differentiated LUHMES cells were exposed to diethylene glycol (0-1 mM) for 6, 24 and 48 hours. Afterwards, a) viability based on metabolic activity, b) viability based on ATP level, c) cytotoxicity, d) apoptosis, and e) proteasomal activity were assessed by CTB, CTG, caspase 3/7 activity and proteasomal activity assays, respectively. Data are shown as a percentage of lysis control (complete cell lysis with Triton X-100; 0.43%) for the CytoTox-ONE Assay and percentage of the media control for the other assays, as means ± SEM of three independent experiments with three technical replicates each. A one-way ANOVA, followed by Dunnett's post hoc test revealed no significant differences between media control and treatment. CTB assay: Cell Titer Blue assay, CTG assay: Cell Titer-Glo assay, LDH: lactate dehydrogenase.

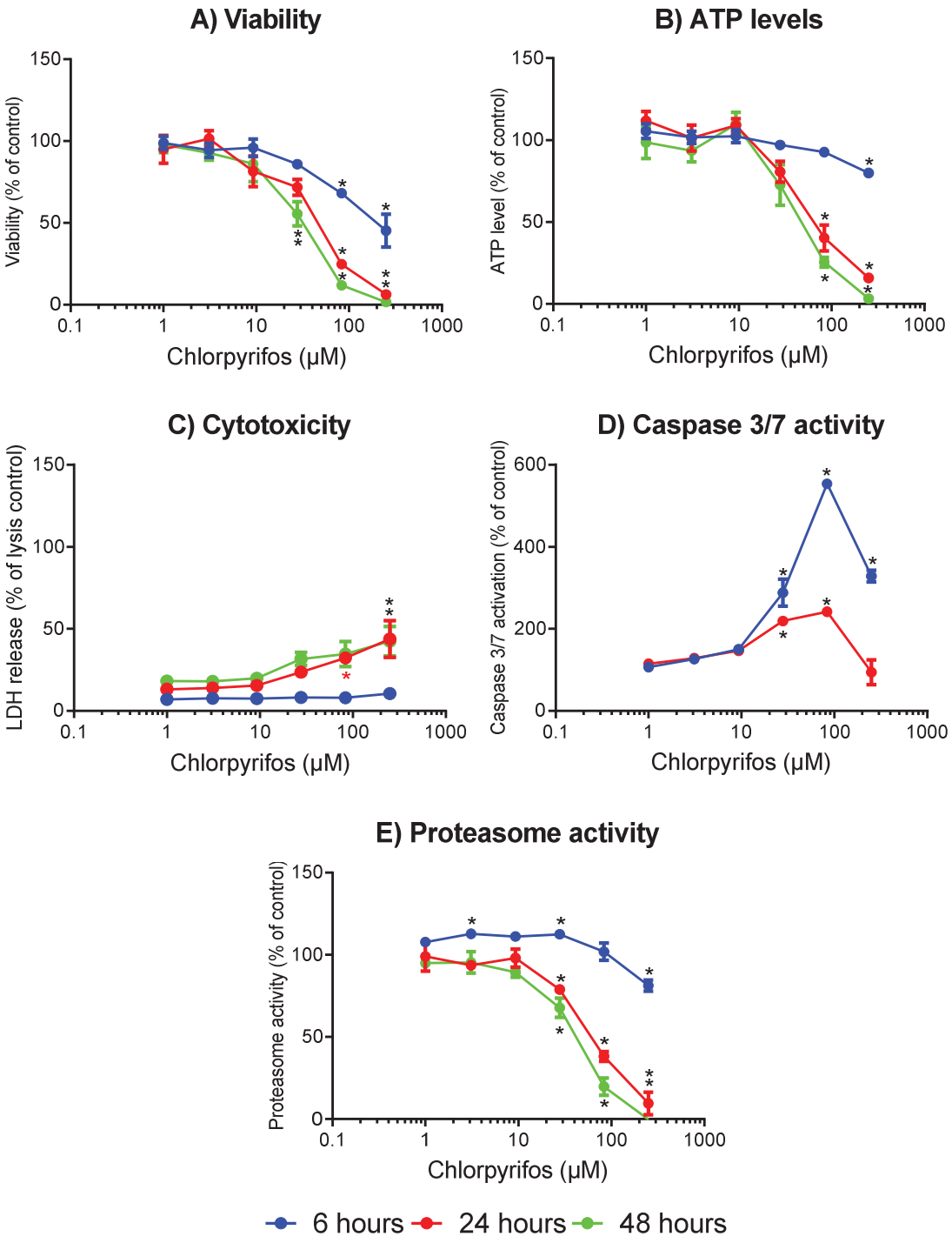

Fig.21: Effects of chlorpyrifos on differentiated LUHMES cells. Differentiated LUHMES cells were exposed to chlorpyrifos (0-250 µM) for 6, 24 and 48 hours. After exposure, a) viability based on metabolic activity, b) viability based on ATP level, c) cytotoxicity, d) apoptosis, and e) proteasomal activity were assessed by CTB, CTG, CytoTox-ONE, caspase 3/7 activity and proteasomal activity assays, respectively. Data are shown as a percentage of lysis control (complete cell lysis with Triton X-100; 0.43%) for the CytoTox-ONE assay and percentage of the solvent control (0.07% DMSO) for the other assays, as means ± SEM of three independent experiments with three technical replicates each. * indicates a significant difference ($p<0.05$) from the respective solvent control based on a one-way ANOVA, followed by Dunnett's post hoc test. CTB assay: Cell Titer Blue assay, CTG assay: Cell Titer-Glo assay, LDH: lactate dehydrogenase.

To compare the effects of chlorpyrifos on cell viability (CTB and CTG assays) and proteasomal activity, IC_{50} values were calculated for the three tested time points. After 6 hours of exposure, the IC_{50} value for cell viability (CTB assay) is 205.1 µM, while IC_{50} values for the cell viability (CTG assay) and proteasomal activity are not reached. After 24 and 48 hours, IC_{50} values are 47.28, 70.18 and 62.49 µM, and 32.22, 48.21 and 39.54 µM on cell viability assessed by CTB and CTG assays and the proteasomal activity, respectively. After 24 and 48 hours, IC_{50} values of chlorpyrifos on the mitochondrial activity are in a similar range with values for proteasomal activity with overlapping 95% confidence intervals (Table 21).

Table 21: IC_{50} values for the effects of chlorpyrifos on viability and proteasomal activity

Endpoint	Exposure	*IC_{50} (95% CI)*
Cell viability (CTB assay)	6 hours	205.1 *(136.2 - 308.8)*
	24 hours	47.28 *(34.30 - 65.16)*
	48 hours	32.22 *(24.80 - 41.86)*
Cell viability (CTG assay)	6 hours	n. e.
	24 hours	70.18 *(52.58 - 93.67)*
	48 hours	48.21 *(35.89 - 64.76)*
Proteasomal activity	6 hours	n. e.
	24 hours	62.49 *(50.65 - 77.11)*
	48 hours	39.54 *(33.15 - 47.15)*

95% CI: 95% confidence interval, n. e.: no effect

Similar to the effects of chlorpyrifos on mitochondrial activity, 27.8 µM was the lowest concentration that activated caspase 3/7 to 288.03 ± 33.46% and 219.20 ± 10.07% of control after 6 and 24 hours, respectively. The caspase 3/7 activation was higher after 6 hours compared to 24 hours in the highest concentrations (27.8 – 250 µM). After 6 hours, chlorpyrifos did not induce LDH release. However, LDH release was induced after 24 hours at 83.3 µM to 32.30 ± 1.14% of the lysis control. The highest concentration of chlorpyrifos (250 µM) induced LDH release to 43.86 ± 11.12% and 42.42 ± 9.01% of the lysis control, after 24 and 48 hours, respectively (Fig.21).

Parathion is another organophosphate potentially increases the risk for PD (Basha, *et al.*, 2001; Allen and Levy, 2013; Narayan *et al.*, 2017). Serial dilutions of parathion (0 - 500 µM) were added to LUHMES cells on day 6 of differentiation for 6, 24 and 48 hours. Parathion decreased cell viability (assessed by CTB and CTG assays) and proteasomal activity and induced LDH release in a concentration-dependent manner after 24 and 48 hours. Parathion also activated caspase 3/7 after 6 and 24 hours. After 24 hours, 256 µM is the lowest concentration that decreased the cell viability (CTB and CTG assays) to 77.98 ± 9.65% and 70.23 ± 7.31% of the control, respectively. At this concentration, the proteasomal activity was reduced to 66.57 ± 5.03% of control (Fig.22).

After 6 hours, IC_{50} values for cell viability (CTB and CTG assays) and proteasomal activity are not reached. After 24 and 48 hours of exposure, IC_{50} values are 299.4 and 347 µM for cell viability (CTB assay), 341.5 and 343.6 µM for cell viability (CTG assay) and 313.9 and 380.7 µM for proteasomal activity, respectively. Similar IC_{50} values with overlapping 95% confidence intervals indicates that the effect on cell viability assessed by CTB and CTG assays cannot be distinguished from the effect on proteasomal activity (Table 22).

Similar to parathion-dependent effects on the mitochondrial activity, 256 µM is the lowest concentration that activated caspase 3/7 to 267.46 ± 25.02% and 180.84 ± 22.26% of control after 6 and 24 hours, respectively. The caspase 3/7 activation was higher after 6 hours compared to 24 hours. Parathion did not induce LDH release after 6 hours. After 24 and 48 hours, 320 µM is the lowest concentration that significantly released LDH to 26.74 ± 2.63% and 40.52 ± 3.81% of lysis control after 24 and 48 hours, respectively (Fig.22).

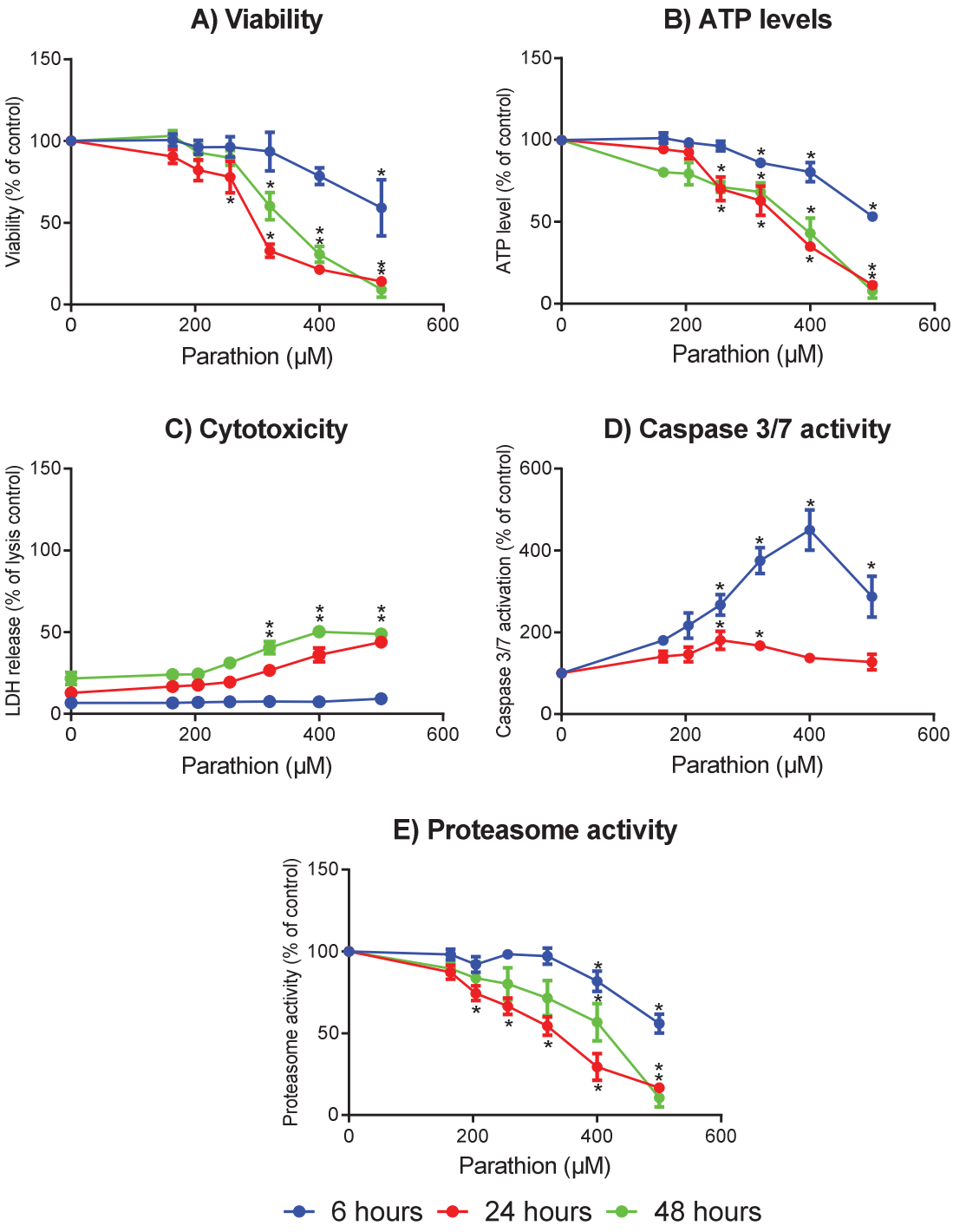

Fig.22: Effects of parathion on differentiated LUHMES cells. Differentiated LUHMES cells were exposed to parathion (0-500 µM) for 6, 24 and 48 hours. Afterwards, a) viability based on metabolic activity, b) viability based on ATP level, c) cytotoxicity, d) apoptosis, and e) proteasomal activity were assessed by CTB, CTG, CytoTox-ONE, caspase 3/7 activity and proteasomal activity assays, respectively. Data are shown as a percentage of lysis control (complete cell lysis with Triton X-100; 0.43%) for the CytoTox-ONE assay and percentage of the solvent control for (0.15% DMSO) the other assays, as means ± SEM of three independent experiments with three technical replicates each. * indicates a significant difference ($p<0.05$) from the respective solvent control based on one-way ANOVA, followed by Dunnett's post hoc test. CTB assay: Cell Titer Blue assay, CTG assay: Cell Titer-Glo assay, LDH: lactate dehydrogenase.

Table 22: IC_{50} values for the effects of parathion on viability and proteasomal activity

Endpoint	Exposure	*IC_{50} (95% CI)*
Cell viability (CTB assay)	6 hours	n. e.
	24 hours	299.4 *(278.8 – 321.4)*
	48 hours	347 *(330.5 – 364.3)*
Cell viability (CTG assay)	6 hours	n. e.
	24 hours	341.5 *(320.5 – 363.9)*
	48 hours	343.6 *(307.4 - 384.1)*
Proteasomal activity	6 hours	n. e.
	24 hours	313.9 *(291.6 – 337.8)*
	48 hours	380.7 *(336.3 - 430.8)*

95% CI: 95% confidence interval, n. e.: no effect

Malathion is an organophosphate pesticide which has a medical use. It is used for treating pediculosis and scabies (Idriss and Levitt, 2009). Previous studies demonstrated a potential association between exposure to malathion and an increased risk for PD (Allen and Levy, 2013; Narayan *et al.*, 2017; Mohammadzadeh *et al.*, 2018). Different concentrations of malathion (0 - 500 µM) were added to LUHMES cells on day 6 of differentiation for 6, 24 and 48 hours. Malathion decreased the cell viability and proteasomal activity, and increased LDH release in a concentration-dependent manner after 24 and 48 hours of exposure. Malathion did not activate caspase 3/7 after 6 or 24 hours. After 24 hours, 222.22 µM of malathion was the lowest concentration that decreased cell viability (CTB assay) and proteasomal activity to 21.11 ± 13.09% and 13.35 ± 6.33% of control, respectively. Cell viability was reduced to 3.47 ± 2.12% of control in CTG assay after 24 hours at this concentration (Fig.23).

After 6 hours, IC_{50} values for cell viability and proteasomal activity are 470.8 and 462.1 µM, while the IC_{50} value for the cell viability assessed by CTG assay is not reached. IC_{50} values are 216.1 and 94.94 µM for cell viability (CTB assay), 129.4 and 138 µM for cell viability (CTG assay), and 182.3 and 93.3 µM for proteasomal activity after 24 and 48 hours, respectively. IC_{50} values of malathion on the cell viability assessed by CTB and CTG assays after 24 and 48 hours are in a similar range as

values for proteasomal activity with overlapping 95% confidence intervals demonstrating that effect on cell viability cannot be distinguished from the effect on proteasomal activity (Table 23).

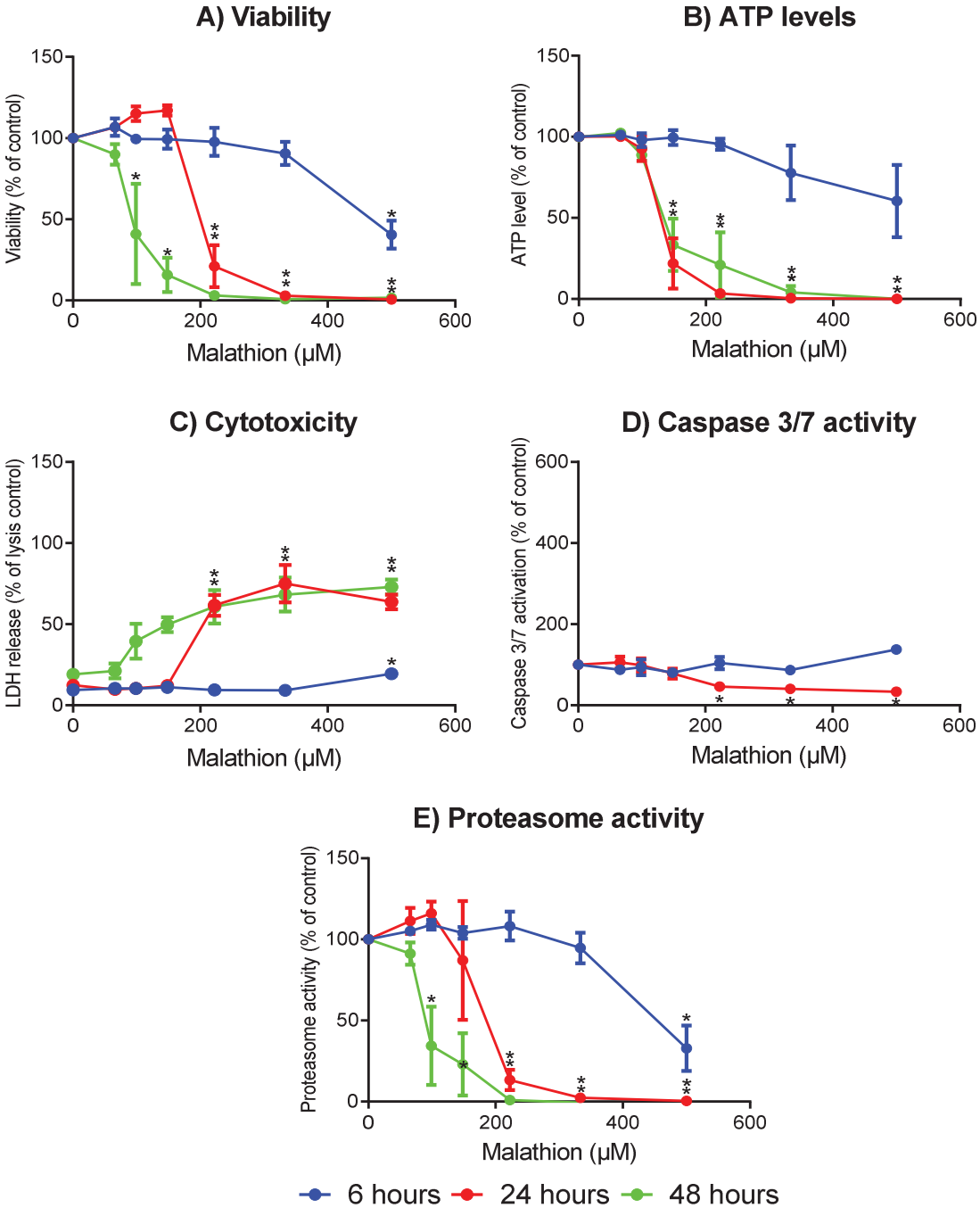

Fig.23: Effects of malathion on differentiated LUHMES cells. Differentiated LUHMES cells were exposed to malathion (0-500 µM) for 6, 24 and 48 hours. Afterwards, a) viability based on metabolic activity, b) viability based on ATP level, c) cytotoxicity, d) apoptosis, and e) proteasomal activity were assessed by CTB, CTG, CytoTox-ONE, caspase 3/7 activity and proteasomal activity assays, respectively. Data are shown as a percentage of lysis control (complete cell lysis with Triton X-100; 0.43%) for the CytoTox-ONE assay and percentage of the solvent control (0.17% DMSO) for the other assays, as means ± SEM of three independent experiments with three technical replicates each. * indicates a significant difference ($p<0.05$) from the respective solvent control based on one-way

ANOVA, followed by Dunnett's post hoc test. CTB assay: Cell Titer Blue assay, CTG assay: Cell Titer-Glo assay, LDH: lactate dehydrogenase.

Malathion did not activate the caspase 3/7 after 6 or 24 hours of application. The highest concentration of malathion (500 µM) caused a significant LDH release to 19.46 ± 3.08% of the lysis control after 6 hours. Similar to the effect of malathion on the cell viability (CTB assay), 222.22 µM is the lowest concentration that induced a significant LDH release to 61.59 ± 6.58% of the lysis control after 24 hours (Fig.23).

Table 23: IC_{50} values for the effects of malathion on viability and proteasomal activity

Endpoint	Exposure	*IC_{50} (95% CI)*
Cell viability (CTB assay)	6 hours	470.8 *(435.3 - 509.3)*
	24 hours	~216.1 *(very wide)*
	48 hours	94.94 *(79.42 - 113.5)*
Cell viability (CTG assay)	6 hours	n. e.
	24 hours	129.4 *(118.5 - 141.3)*
	48 hours	138 *(118.3 - 160.9)*
Proteasomal activity	6 hours	462.1 (417.5 - 511.5)
	24 hours	182.3 *(148.1 - 224.3)*
	48 hours	93.3 *(77.42 - 112.4)*

95% CI: 95% confidence interval, n. e.: no effect

Dichlorvos is one of the organophosphate pesticides, which may increase the risk of PD (Binukumar *et al.*, 2010; Wani *et al.*, 2017). Different concentrations of dichlorvos (0-500 µM) were added to LUHMES cells on 6 days of differentiation for 6, 24 and 48 hours. Dichlorvos did not affect cell viability (assessed by CTB and CTG assays) or proteasomal activity after 6 hours. However, it reduced cell viability (CTB and CTG assays) and proteasomal activity after 24 and 48 hours in a concentration- and time-dependent manner.

After 24 hours, 125 µM is the lowest concentration that decreased cell viability to 79.27 ± 3.12% of control in CTB assay and to 78.12 ± 2.12% of control in CTG assay. The proteasomal activity was decreased after 24 hours by this concentration to 69.38 ± 14.40% of control. However, the change in proteasomal activity was not statistically significant. After 48 hours, 125 µM decreased cell viability (assessed by

CTB and CTG assays) and proteasomal activity to 23.45 ± 1.98%, 15.29 ± 1.47% and 14.19 ± 0.86% of control, respectively (Fig.24).

IC_{50} values of dichlorvos on cell viability (CTB and CTG assays) and proteasomal activity were calculated for the three tested time points. After 6 hours of exposure, IC_{50} values for cell viability (CTB and CTG assays) and proteasomal activity are not reached. IC_{50} values are 228, 205 and 173.5 µM after 24 hours and 95.08, 66.15 and 76.03 µM after 48 for cell viability assessed by CTB and CTG assays, and proteasomal activity, respectively. IC_{50} values of dichlorvos on cell viability are in a similar range as values for proteasomal activity with overlapping 95% confidence intervals after 24 and 48 hours. This indicates that the effect of dichlorvos on cell viability are not distinguished from the effect on proteasomal activity (Table 24).

Table 24: IC_{50} values for the effects of dichlorvos on viability and proteasomal activity

Endpoint	Exposure	IC_{50} *(95% CI)*
Cell viability (CTB assay)	6 hours	n. e.
	24 hours	228 *(196.2 - 264.8)*
	48 hours	95.08 *(87.97 - 102.8)*
Cell viability (CTG assay)	6 hours	n. e.
	24 hours	205 *(176.9 - 237.7)*
	48 hours	66.15 *(57.93 - 75.55)*
Proteasomal activity	6 hours	n. e.
	24 hours	173.5 *(129.9 - 231.6)*
	48 hours	76.03 *(71.73 - 80.59)*

95% CI: 95% confidence interval, n. e.: no effect

Dichlorvos did not induce activation of caspase 3/7 after 6 or 24 hours, while 125 µM is the lowest concentrations that significantly released LDH 53.09 ± 6.71% of lysis control after 48 hours. The maximal LDH release was observed with the highest concentration of dichlorvos (500 µM) to 32.19 ± 5.29% and 63.09 ± 4.40% of lysis control, after 24 and 48 hours, respectively (Fig.24).

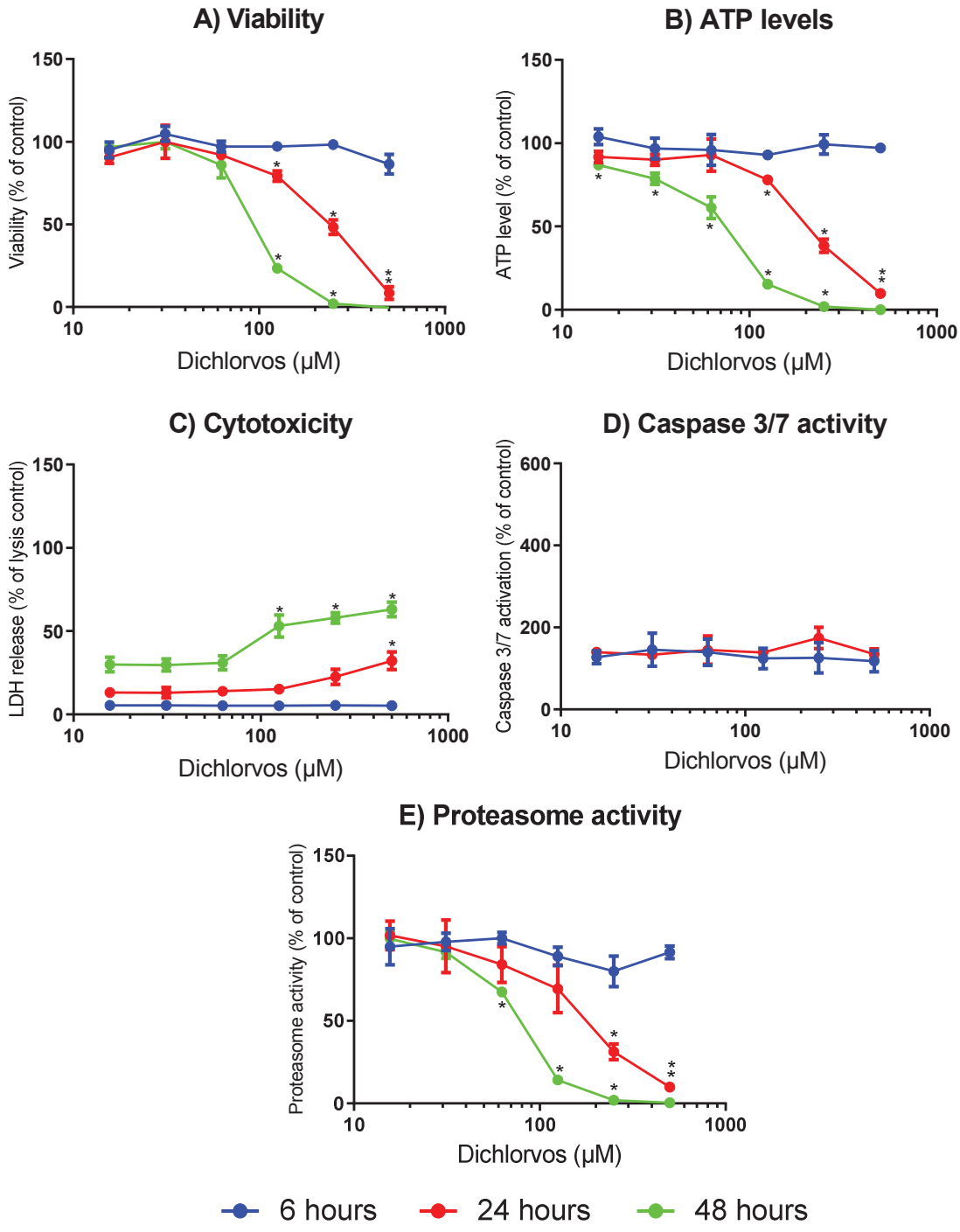

Fig.24: Effects of dichlorvos on differentiated LUHMES cells. Differentiated LUHMES cells were exposed to dichlorvos (0-500 µM) for 6, 24 and 48 hours. Afterwards, a) viability based on metabolic activity, b) viability based on ATP level, c) cytotoxicity, d) apoptosis, and e) proteasomal activity were assessed by CTB, CTG, CytoTox-ONE, caspase 3/7 activity and proteasomal activity assays, respectively. Data are shown as a percentage of lysis control (complete cell lysis with Triton X-100; 0.43%) for the CytoTox-ONE assay and percentage of the solvent control (0.17% DMSO) for the other assays, as means ± SEM of three independent experiments with three technical replicates each. * indicates a significant difference ($p<0.05$) from the respective solvent control based on one-way ANOVA, followed by Dunnett's post hoc test. CTB assay: Cell Titer Blue assay, CTG assay: Cell Titer-Glo assay, LDH: lactate dehydrogenase.

3.3.2 Effects of the metabolites of the organophosphate pesticides on early KEs leading to PMD

Chlorpyrifos oxon, paraoxon and malaoxon are the oxon metabolites of chlorpyrifos, parathion and malathion, respectively. There are several studies demonstrated that the oxon metabolites are more potent than the parent pesticides (Sparling and Fellers, 2007; Aker *et al.*, 2008). Therefore, there is concern that the oxon might be associated with an increased risk for PD. Here, the effects of chlorpyrifos oxon, paraoxon and malaoxon on early KEs during PMD development were analyzed.

Organophosphate pesticides are converted to their oxon metabolites mainly in the liver, but also in the brain to a lower extent. Cytochrome p450 2B subfamily (CYP2B) enzymes that are expressed in astrocytes are responsible for forming the oxon from the parent pesticides (Eaton *et al.*, 2008; Miksys and Tyndale, 2013). LUHMES cells are pure neuronal cell line and subsequently have a limited ability to metabolize the organophosphate pesticides (Tong *et al.*, 2017). Therefore, this neuronal cell line needs to be exposed to the metabolites separately in order to study, whether the metabolites also affect the KEs leading to PMD pathogenesis.

Serial dilutions of chlorpyrifos oxon (0 - 200 µM) were applied to LUHMES cells on day 6 for 6, 24 and 48 hours. Chlorpyrifos oxon reduced cell viability (assessed by CTB and CTG assays) and proteasomal activity concomitant with LDH release after 24 and 48 hours. It activated caspase 3/7 after 6 and 24 hours of application. After 24 and 48 hours, 22.22 µM is the lowest concentration that significantly decreased the cell viability to 76.84 ± 5.78% and 76.95 ± 5.96% of control in the CTB assay and to 75.96 ± 7.10% and 77.50 ± 2.22% of control in the CTG assay. The proteasomal activity was not significantly changed by 22.22 µM after 24 hours, however, it was reduced to 93.87 ± 3.82% of control (non-statistically significant) after 48 hours (Fig.25).

IC_{50} values were used to compare the potency of chlorpyrifos oxon with its parent pesticide. After 6 hours, the IC_{50} concentrations on cell viability (CTB and CTG assays) and proteasomal activity for chlorpyrifos oxon are not reached. IC50 values for chlorpyrifos oxon are 102.2 and 74.27 µM on cell viability (CTB assay), 91.96 and 61.73 µM (CTG assay) and 118.5 and 91.86 µM on proteasomal activity, while these values for chlorpyrifos are 47.28 and 32.22 µM on cell viability (CTB assay), 70.18 and 48.21 µM (CTG assay) and 62.49 and 39.54 µM on proteasomal activity after 24

and 48 hours, respectively. The lower IC_{50} values for chlorpyrifos indicate that a stronger inhibition of cell viability and proteasomal activity compared to the oxon (Tables 21 and 25).

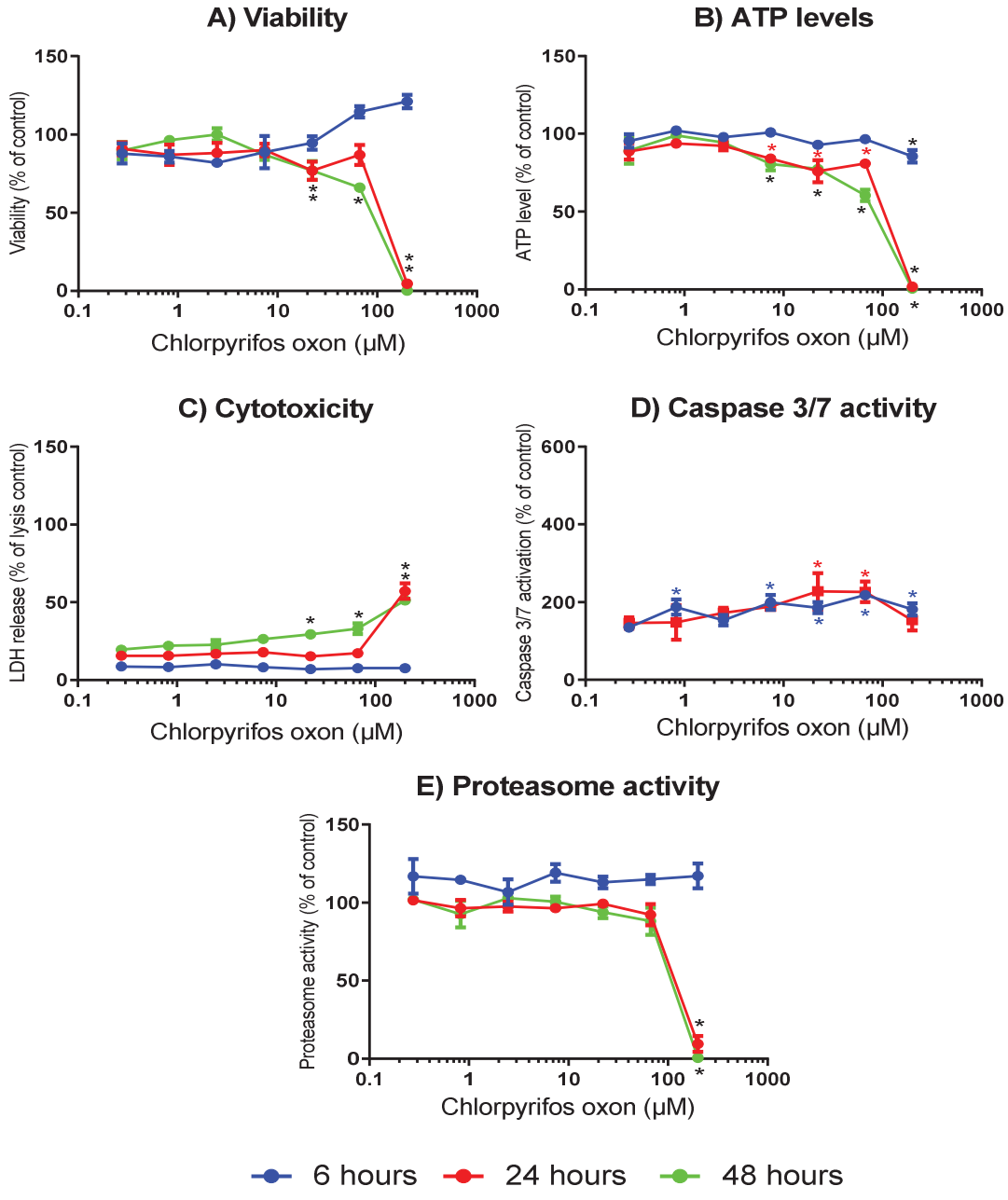

Fig.25: Effects of chlorpyrifos oxon on differentiated LUHMES cells. Differentiated LUHMES cells were exposed to chlorpyrifos oxon (0-200 µM) for 6, 24 and 48 hours. Afterwards, a) viability based on metabolic activity, b) viability based on ATP level, c) cytotoxicity, d) apoptosis, and e) proteasomal activity were assessed by CTB, CTG, CytoTox-ONE, caspase 3/7 activity and proteasomal activity assays, respectively. Data are shown as a percentage of lysis control (complete cell lysis with Triton X-100; 0.43%) for the CytoTox-ONE assay and percentage of the solvent control (0.1% DMSO) for the other assays, as means ± SEM of three independent experiments with three technical replicates each. * indicates a significant difference ($p<0.05$) from the respective control based on one-way ANOVA, followed by Dunnett's post hoc test. CTB assay: Cell Titer Blue assay, CTG assay: Cell Titer-Glo assay, LDH: lactate dehydrogenase.

0.83 µM of chlorpyrifos oxon is the lowest concentration to activate caspase 3/7 to 187.27 ± 19.40% of control after 6 hours. The maximum activation after 6 hours (at 66.67 µM) was 218.48 ± 5.68%. In comparison, the parent pesticide caused an activation at a higher concentration (83.3 µM) to a maximum activation of 553.52 ± 10.93% of control. For both compounds, the effects were not accompanied by LDH release after 6 hours. After 24 hours, the effects between chlorpyrifos oxon and the parent pesticide are more comparable with the earliest induction of caspase activation at 22.22 µM of oxon and 27.8 µM of chlorpyrifos to 227.57 ± 47.27% and 219.20 ± 10.07% of control, respectively. In both cases, the caspase activation is reduced at the highest concentration accompanied by induction in LDH release. The data indicate that chlorpyrifos more potently affects the early KEs during PMD as measured in this battery than its oxon metabolite (Fig.21 and 25).

Table 25: IC_{50} values for the effects of chlorpyrifos oxon on viability and proteasomal activity

Endpoint	Exposure	*IC_{50} (95% CI)*
Cell viability (CTB assay)	6 hours	n. e.
	24 hours	102.2 *(68.92 - 151.5)*
	48 hours	74.27 *(56.69 - 97.30)*
Cell viability (CTG assay)	6 hours	n. e.
	24 hours	91.96 *(61.65 - 137.2)*
	48 hours	61.73 *(44.42 - 85.78)*
Proteasomal activity	6 hours	n. e.
	24 hours	118.5 *(100.3 - 139.9)*
	48 hours	91.86 *(49.04 - 172.1)*

95% CI: 95% confidence interval, n. e.: no effect

Different concentrations of paraoxon (0 - 500 µM) were added to LUHMES cells on day 6 for 6, 24 and 48 hours. After 24 and 48 hours, the highest concentrations of paraoxon reduced cell viability (assessed by CTB and CTG assays), however, paraoxon did significantly impair the proteasomal activity. Paraoxon activated caspase 3/7 after 6 hours and mainly after 24 hours, while LDH release was observed with the highest concentration of paraoxon after 48 hours. After 24 and 48 hours, 500 µM is the lowest concentration that significantly decreased the cell viability to 77.54 ± 4.50% and 67.53 ± 4,89% of control in CTB assay, respectively.

This concentration decreased cell viability to 78.31± 2.50% and 37.07 ± 13.30% of control in CTG assay after 24 and 48 hours, respectively. 500 µM did not decrease the proteasomal activity after 24 hours, however, it reduced the proteasomal activity after 48 hours to 72.14 ± 16.49% of control but this reduction was non-statistically significant (Fig.26).

IC_{50} values on the cell viability (CTB and CTG assays) and proteasomal activity for paraoxon are not reached after 6 or 24 hours. After 48 hours, IC_{50} values for the cell viability assessed by CTB assay are 347 and 395 µM and by CTG assay are 343.6 and 403.7 µM for parathion and paraoxon, respectively, while an IC_{50} concentration for paraoxon on the proteasomal activity was not reached. After 48 hours, IC_{50} values for parathion and paraoxon on cell viability assessed by CTB assay are in the similar range with value for cell viability assessed by CTG assay with overlapping 95% confidence intervals (Tables 22 and 26).

Table 26: IC_{50} values for the effects of paraoxon on viability and proteasomal activity

Endpoint	Exposure	*IC_{50} (95% CI)*
Cell viability (CTB assay)	6 hours	n. e.
	24 hours	n. e.
	48 hours	395 *(274.8 - 567.9)*
Cell viability (CTG assay)	6 hours	n. e.
	24 hours	n. e.
	48 hours	403.7 *(279.3 - 583.4)*
Proteasomal activity	6 hours	n. e.
	24 hours	n. e.
	48 hours	n. e.

95% CI: 95% confidence interval, n. e.: no effect

After 6 hours, 148.15 µM of paraoxon activated caspase 3/7 to 212.93 ± 29.12% of control, while the activation induced by other concentrations was not statistically significant. Compared to the parent pesticide, the maximal activation of caspase 3/7 occurred early (6 hours) at 400 µM of parathion to 450.20 ± 49.52% of control. After 6 and 24 hours, paraoxon did not induce LDH release, while parathion induced LDH release after 24 hours. These data indicate stronger apoptotic and necrotic effects of parathion compared to paraoxon (Fig. 22 and 26).

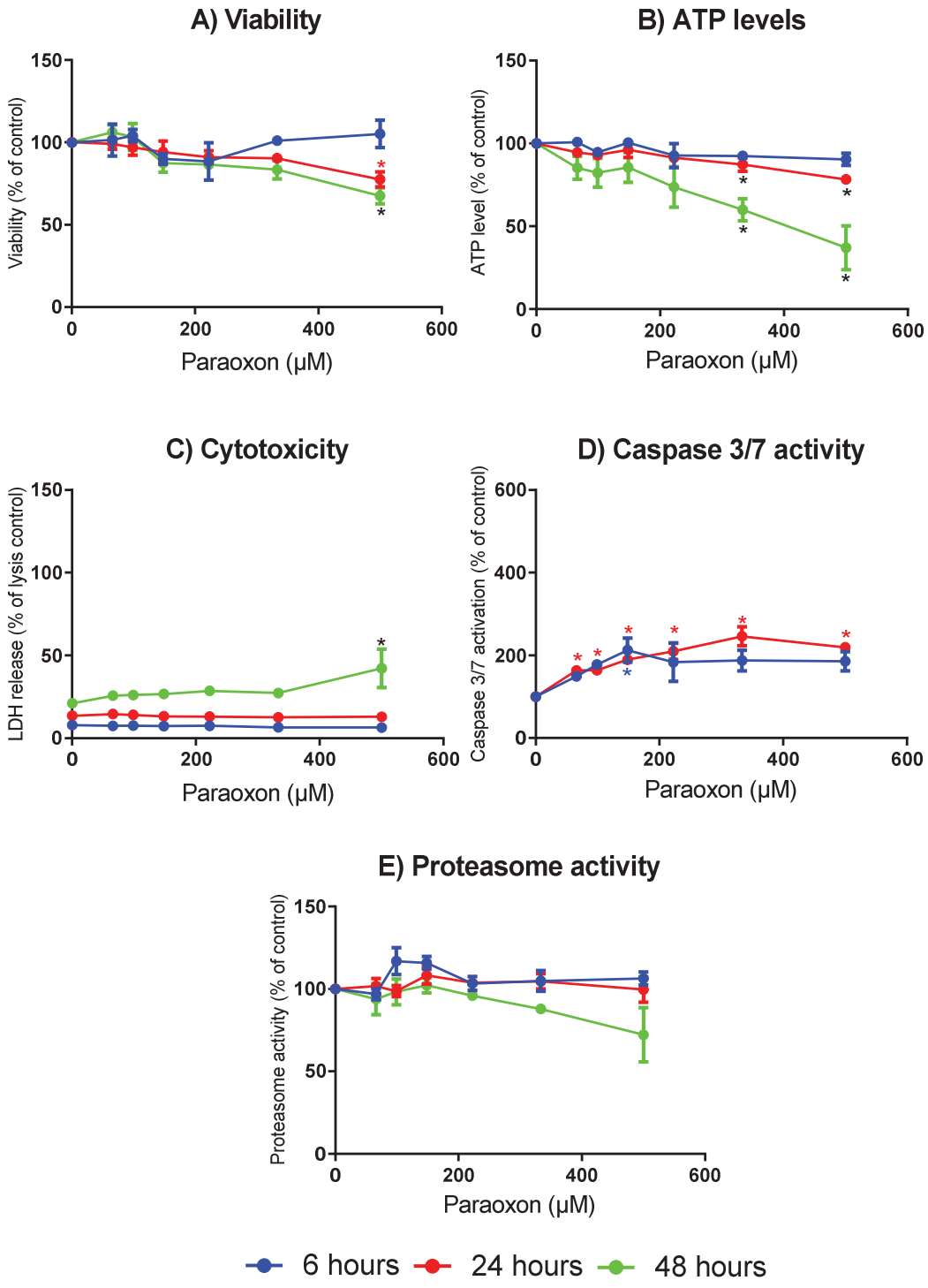

Fig.26: Effects of paraoxon on differentiated LUHMES cells. Differentiated LUHMES cells were exposed to paraoxon (0-500 µM) for 6, 24 and 48 hours. Afterwards, a) viability based on metabolic activity, b) viability based on ATP level, c) cytotoxicity, d) apoptosis, and e) proteasomal activity were assessed by CTB, CTG, CytoTox-ONE, caspase 3/7 activity and proteasomal activity assays, respectively. Data are shown as a percentage of lysis control (complete cell lysis with Triton X-100; 0.43%) for the CytoTox-ONE assay and percentage of the solvent control (0.17% DMSO) for the other assays, as means ± SEM of three independent experiments with three technical replicates each. * indicates a significant difference ($p<0.05$) from the respective control based on one-way ANOVA, followed by Dunnett's post hoc test. CTB assay: Cell Titer Blue assay, CTG assay: Cell Titer-Glo assay, LDH: lactate dehydrogenase.

Serial dilutions of malaoxon (0 - 500 µM) were added to LUHMES cells on day 6 of differentiation for 6, 24 and 48 hours. Application of malaoxon for 24 and 48 hours reduced the cell viability (CTB and CTG assays) and proteasomal activity and induced LDH release in a concentration-dependent manner. Malaoxon activated caspase 3/7 after 6 hours of application. After 24 hours, 333.33 µM is the lowest concentration to reduce cell viability to 61.78 ± 17.37% of control in CTG assay and proteasomal activity to 64.37 ± 12.71% of control. This concentration decreased cell viability to 37.55 ± 2.89% of control in CTB assay after 24 hours of application. 333.33 µM reduced cell viability (CTB and CTG assays) and proteasomal activity after 48 hours to 16.95 ± 6.62%, 27.01 ± 12.35% and 54.97 ± 19.58% of control, respectively. However, the change in proteasomal activity was not statistically significant (Fig.27).

The activity profiles of malathion and malaoxon in the test battery were assessed. After 24 and 48 hours, IC_{50} values are 216.1 and 94.94 µM for malathion and 286.2 and 171 µM for malaoxon on cell viability (CTB assay), while these values are 129.4 and 138 µM for malathion and 345.2 and 260.5 µM for malaoxon on cell viability (CTG assay), respectively. IC_{50} values on the proteasomal activity are 182.3 and 93.3 µM for malathion and 348.5 and 296.1 µM for malaoxon after 24 and 48 hours, respectively. The IC_{50} values of malathion are lower than that of malaoxon on cell viability and proteasomal activity within the tested time points after 24 and 48 hours (Tables 23 and 27).

Interestingly, malaoxon is not similar to malathion and activated caspase 3/7 after 6 hours of application. 148.15 µM of malaoxon is the lowest concentration that activated caspase 3/7 to 167.65 ± 1.92% of control, while 222.22 µM maximally activated caspase 3/7 to 200.51 ± 24.72% of control. Malaoxon did not induce LDH release after 6 hours. After 24 hours, 222.22 µM is the lowest concentration to release LDH to 32.34 ± 2.55% of lysis control. Compared to the parent pesticide, 222.22 µM of malathion is the lowest concentration that induced LDH release to 61.59 ± 6.58% of lysis control after 24 hours. This indicates that malathion induced more necrotic cell death than malaoxon (Fig. 23 and 27).

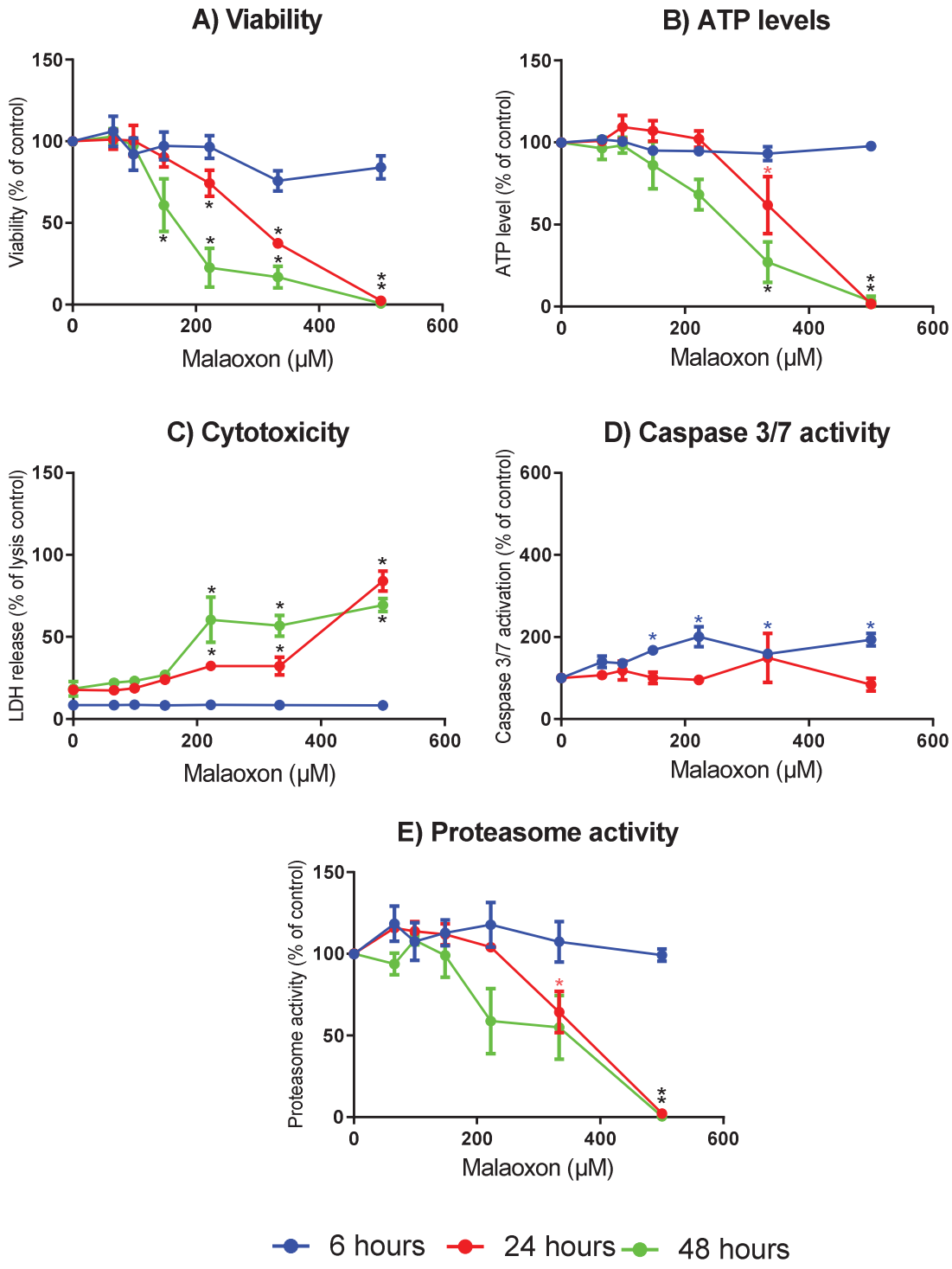

Fig. 27: Effects of malaoxon on differentiated LUHMES cells. Differentiated LUHMES cells were exposed to malaoxon (0-500 µM) for 6, 24 and 48 hours. Afterwards, a) viability based on metabolic activity, b) viability based on ATP level, c) cytotoxicity, d) apoptosis, and e) proteasomal activity were assessed by CTB, CTG, CytoTox-ONE, caspase 3/7 activity and proteasomal activity assays, respectively. Data are shown as a percentage of lysis control (complete cell lysis with Triton X-100; 0.43%) for the CytoTox-ONE assay and percentage of the solvent control (0.17% DMSO) for the other assays, as means ± SEM of three independent experiments with three technical replicates each. * indicates a significant difference ($p<0.05$) from the respective control based on one-way ANOVA, followed by Dunnett's post hoc test. CTB assay: Cell Titer Blue assay, CTG assay: Cell Titer-Glo assay, LDH: lactate dehydrogenase.

Table 27: IC_{50} values for the effects of malaoxon on viability and proteasomal activity

Endpoint	Exposure	*IC_{50} (95% CI)*
Cell viability (CTB assay)	6 hours	n. e.
	24 hours	286.2 *(261.0 - 313.9)*
	48 hours	171 *(148.9 - 196.3)*
Cell viability (CTG assay)	6 hours	n. e.
	24 hours	345.2 *(291.3 - 409.1)*
	48 hours	260.5 *(227.2 - 298.6)*
Proteasomal activity	6 hours	n. e.
	24 hours	348.5 *(290.0 - 418.8)*
	48 hours	296.1 *(234.5 - 373.9)*

95% CI: 95% confidence interval, n. e.: no effect

Altogether the activity profile of chlorpyrifos and parathion in the test battery is similar to that of the model compound rotenone. Similar to rotenone, the effects on mitochondrial activity and proteasomal activity could not be distinguished and in both cases show a clear time dependence between 6 and 24 hours, as well as 6 and 48 hours with only small differences between 24 and 48 hours. Furthermore, the activity profile concerning both cell death assays is comparable with an early induction of apoptosis followed by necrosis with increasing time and concentration (Fig.12-14, 16, 17, 21 and 22). The activity profile of malathion and dichlorvos in the test battery is similar to that of the model compound paraquat. Indeed, the effects of malathion, dichlorvos and paraquat on the mitochondrial and proteasomal activities are not distinguishable. However, there was less overlap between proteasomal activity and mitochondrial activity after 24 hours of exposure to paraquat. Additionally, their effects have a clear time dependence between the three tested time points 6, 24 and 48 hours. Concerning cell death, they did not induce apoptosis after 6 or 24 hours. Later, they induced necrosis with increasing time and concentration (Fig.12-14, 16, 17, 23 and 24). Chlorpyrifos and parathion are more potent than their oxon metabolites. The parent pesticides induced more inhibition of the mitochondria and proteasome compared to their oxon metabolites. Though, the effects of parathion and paraoxon on cell viability were comparable after 48 hours. Chlorpyrifos and parathion induced more apoptosis than oxons after 6 hours. The comparison of the

effects of malathion with malaoxon reproduced the same results as a comparison of other parent pesticides with their metabolites. Malathion is more potent than malaoxon. Consistently, malathion decreased the cell viability (CTB and CTG assays) and proteasomal activities more than malaoxon. Malathion induced more necrosis than its metabolite, however, malaoxon but not malathion induced apoptosis after 6 hours (Fig.21-23, 25-27).

Based on the chemical testing, it can be summarized that all organophosphates and their metabolites affect early KEs of the AOPs on PMD as measured in this battery but that they show a different profile concerning time of the effects as well as the induction of cell death. Notably, LUHMES cells seem to be a suitable model for early KEs testing. However, the specificity of the compounds to affect dopaminergic neurons with a higher potency than non-dopaminergic neurons needs further experiments using different cell systems.

3.4 Metabolome analyses

3.4.1 Neuronal differentiation significantly alters the metabolic fingerprint of LUHMES cells

Within eight days of differentiation, a gradual decline in the concentrations of amino acids alanine (Ala), aspartate (Asp), glutamate (Glu), and glutamine (Gln) was detected. Furthermore, a significant decrease in the antioxidant glutathione (GSH) was observed. This is consistent with the observed Gln and Glu reduction, since, upon internalization, Gln is metabolized to Glu which is one of the three building blocks of the tripeptide GSH. Neuronal differentiation of LUHMES cells further decreased the concentrations of TCA cycle intermediates succinate (Suc) and citrate (Cit). In addition, these observations can be attributed to the impaired Glu metabolism, since Glu is a precursor of the TCA cycle intermediate alpha-ketoglutarate (αKG). Therefore, the impaired influx into the TCA cycle due to the significantly decreased Glu levels could explain the reduction in Suc and Cit. Apart from alterations in metabolites involved in bioenergetic processes, neuronal differentiation significantly decreased the levels of phosphocholine (PC) and total choline (tCho). Furthermore, significant increases in creatine concentrations were observed (Fig.28).

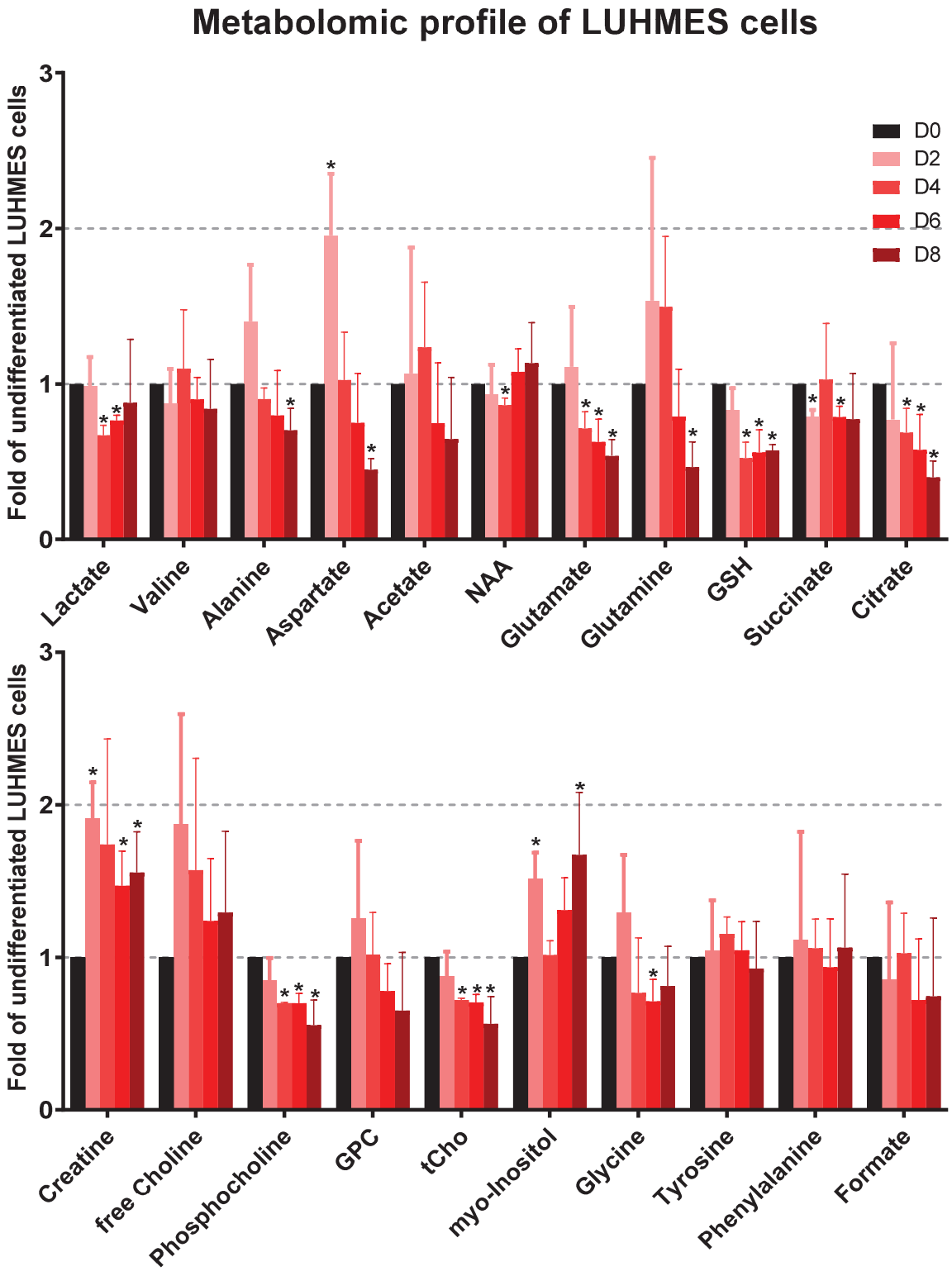

Fig.28: Metabolomic profile of differentiating LUHMES cells. The water-soluble metabolome of LUHMES cells was assessed on day 0, 2, 4, 6 and 8 of differentiation with HR ^{1}H-NMR spectroscopy. Data is shown as fold-change of the undifferentiated LUHMES cells on day 0, as means ± SDs of three independent experiments. * indicates a significant difference compared to undifferentiated LUHMES based on one-sided t-tests ($p<0.05$). GPC: glycerophosphocholine, GSH: glutathione, NAA: naphthaleneacetic acid, tCho: total choline.

3.4.2 Exposure to paraquat induces metabolic changes similar to rotenone

In order to assess the metabolic consequences of mitochondrial inhibition, on day six of differentiation, LUHMES cells were incubated for 48 hours with IC_{50} concentration of rotenone (1.5 µM). Subsequently, mitochondrial inhibition resulted in a significant accumulation of the amino acids valine (Val), Ala, tyrosine (Tyr), phenylalanine (Phe), and glycine (Gly). Additionally, elevated levels of TCA cycle precursors (Gln, Glu) and TCA cycle intermediates (Suc and Cit) were observed. Reduced levels of the TCA cycle product Asp and increased level of lactate (Lac) upon rotenone exposure indicate a shift of the energy metabolism towards aerobic glycolysis (Warburg effect) due to the rotenone-induced mitochondrial dysfunction. Furthermore, increased levels of tCho and PC were observed (Fig.29).

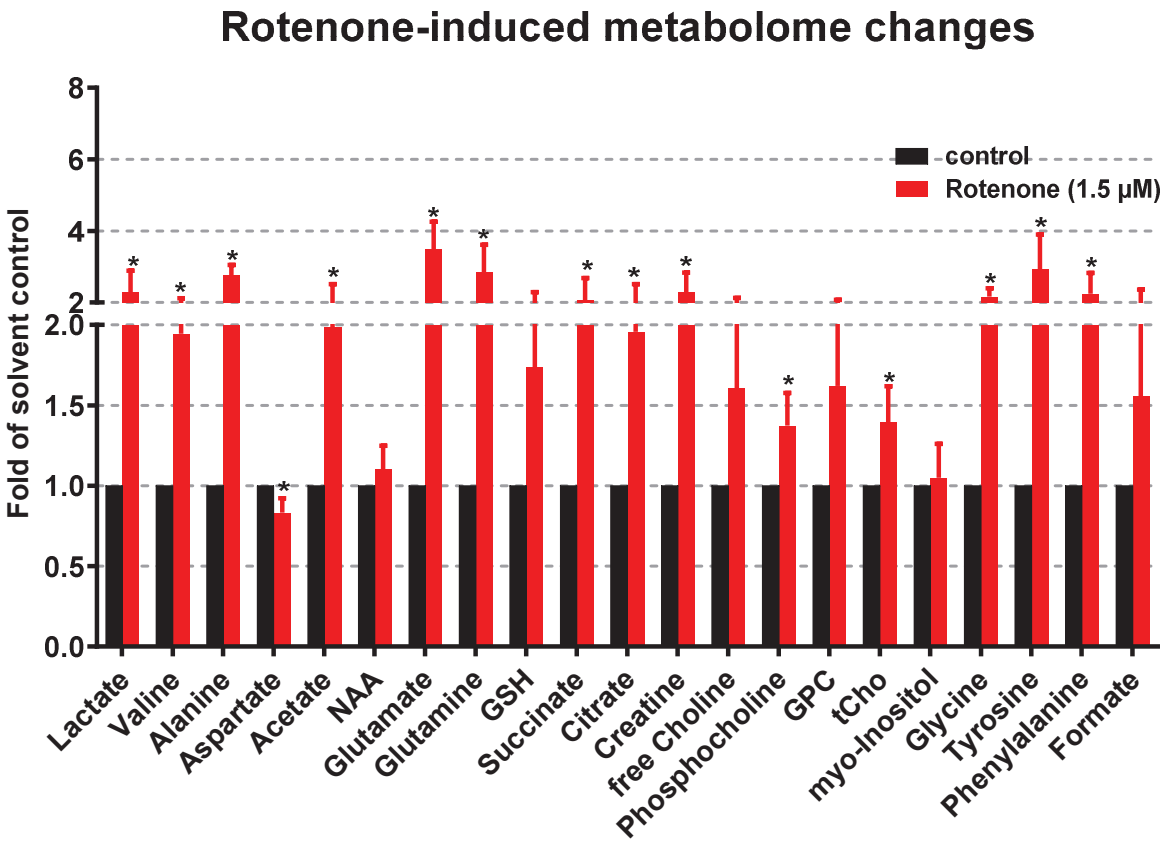

Fig.29: Effects of rotenone exposure on the metabolome of differentiated LUHMES cells. Differentiated LUHMES cells were exposed to rotenone (1.5 µM) for 48 hours. The rotenone-induced effects on the water-soluble metabolome were evaluated with HR ^{1}H-NMR spectroscopy. The data is presented as fold-change of the respective solvent controls, as means ± SDs of three independent experiments. * indicates a significant difference compared to the solvent control based on one-sided t-tests ($p<0.05$). GPC: glycerophosphocholine, GSH: glutathione, NAA: naphthaleneacetic acid, tCho: total choline.

As a redox cycler, paraquat is known to cause mitochondrial dysfunction (Ockleford *et al.*, 2017). In order to assess whether paraquat causes similar metabolic changes as observed upon 1.5 µM rotenone exposure, LUHMES cells on day six of differentiation were exposed for 48 hours to 50 µM paraquat (IC_{50} concentration). In contrast to rotenone, paraquat significantly reduced the levels of several amino acids (Val and Ala). However, similar to the observations upon rotenone treatment, paraquat increased levels of the TCA cycle precursors (Gln and Glu) and TCA cycle intermediates (Suc and Cit). Altered tCho and PC levels were not observed but an increase in glycerophosphocholine (GPC) was detected upon paraquat treatment (Fig.30).

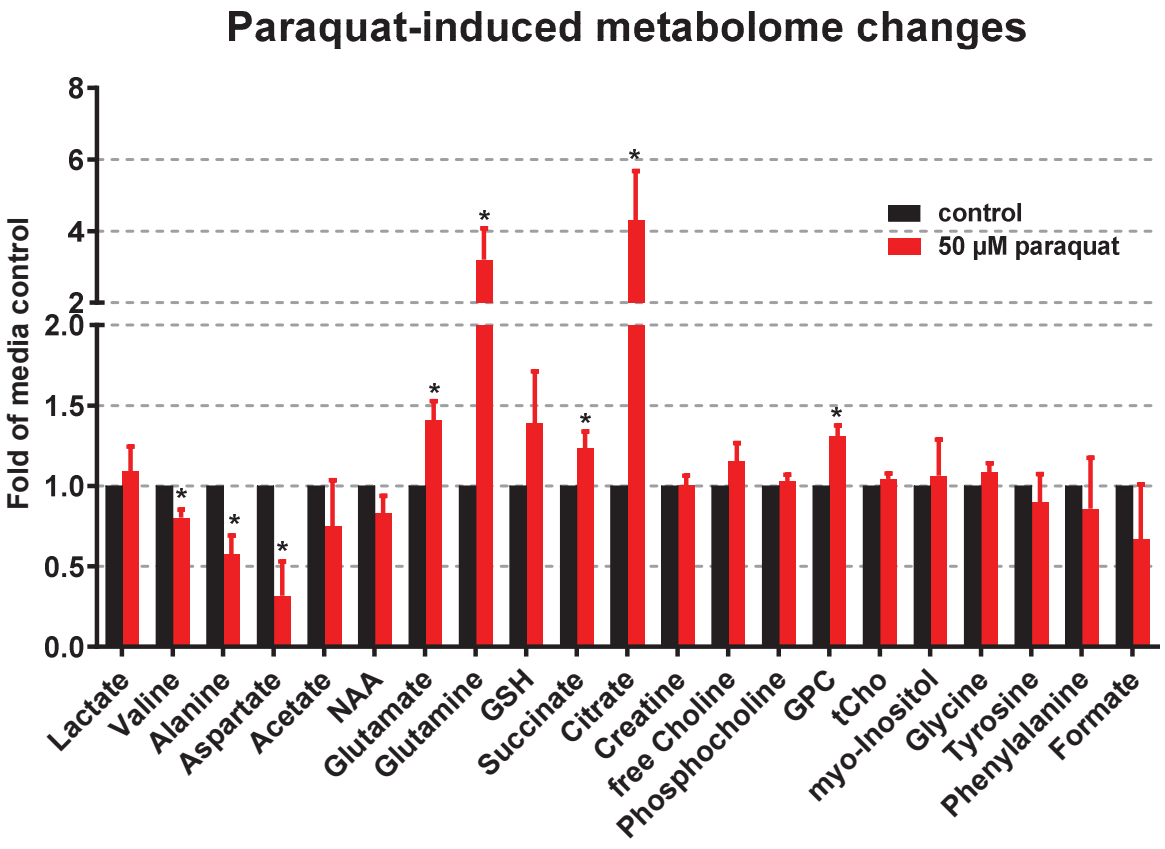

Fig.30: Effects of paraquat exposure on the metabolome of differentiated LUHMES cells. Differentiated LUHMES cells were exposed to paraquat (50 µM) for 48 hours. The paraquat-induced effects on the water-soluble metabolome were evaluated by HR ^{1}H-NMR spectroscopy. The data is presented as fold-change of the respective media controls, as means ± SDs of three independent experiments. * indicates a significant difference compared to the media control based on one-sided t-tests ($p<0.05$). GPC: glycerophosphocholine, GSH: glutathione, NAA: naphthaleneacetic acid, tCho: total choline.

In conclusion, paraquat and rotenone have similar effects on the TCA cycle of LUHMES cells. These data are in accordance with the results from the CTB and CTG

assays. Both compounds significantly impaired the flow through the ETC as observed by decreased cell viability. The impaired ETC can be the cause for the accumulation of TCA cycle precursors and intermediates, as was previously observed with impairment of the ETC (Chen *et al.*, 2018).

3.4.3 Metabolic consequences of exposure to organophosphate pesticides

Finally, LUHMES cells differentiated for six days were exposed to IC_{50} concentrations of the organophosphate pesticides chlorpyrifos and parathion for 48 hours. In contrast to paraquat, both compounds showed minor effects on the metabolome however, some similarities to rotenone exposure were detected. Similar to targeted mitochondrial inhibition, exposure to 35 µM chlorpyrifos significantly increased the levels of Ala, Phe, Gln, and the TCA cycle intermediate Cit. Furthermore, GSH levels were increased while myo-Inositol (Myo) levels were decreased (Fig.31).

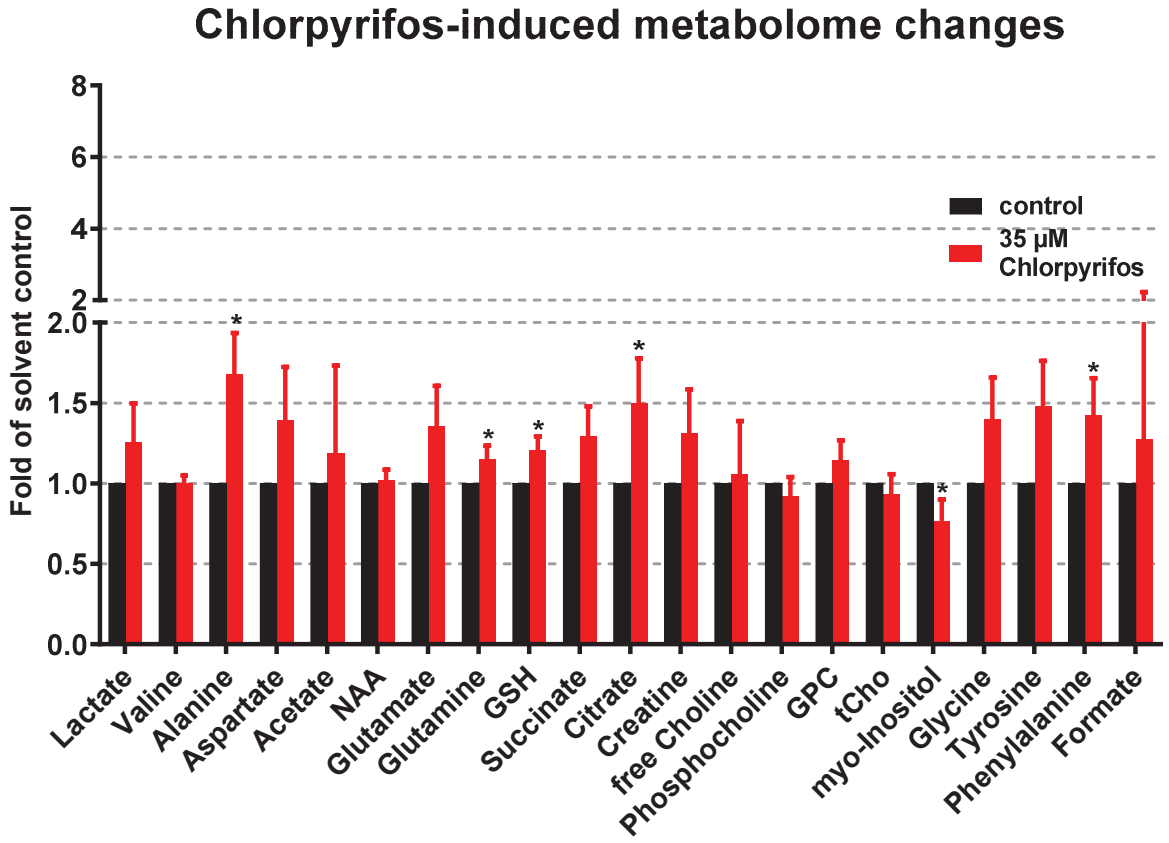

Fig.31: Effects of chlorpyrifos on the metabolome of differentiated LUHMES cells. Differentiated LUHMES cells were exposed to chlorpyrifos (50 µM) for 48 hours. The chlorpyrifos-induced effects on the water-soluble metabolome were evaluated by HR ^{1}H-NMR spectroscopy. Data is presented as fold-change of the respective solvent controls, as means ± SDs of three independent experiments. * indicates a significant difference compared to the solvent control based on one-sided t-tests ($p<0.05$). GPC: glycerophosphocholine, GSH: glutathione, NAA: naphthaleneacetic acid, tCho: total choline.

Also, exposure to 350 µM parathion caused similar metabolic effects as observed in rotenone-treated LUHMES cells, since increased concentration of the amino acid Ala, the TCA precursors Glu and Gln, and choline metabolites tCho and PC were detected (Fig.32). All in all, exposure to the organophosphates caused only minor metabolic changes compared to the model compounds.

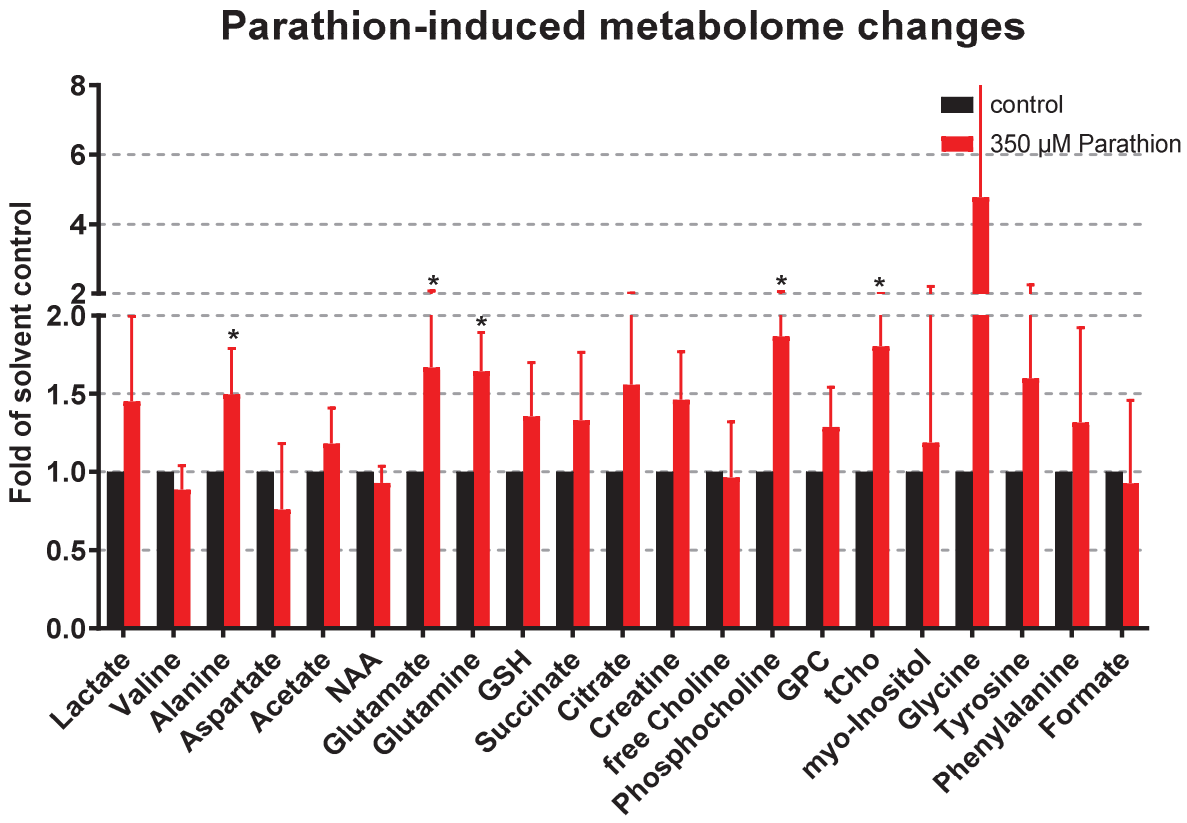

Fig.32: Effects of parathion on the metabolome of differentiated LUHMES cells. Differentiated LUHMES cells were exposed to chlorpyrifos (50 µM) for 48 hours. The parathion-induced effects on the water-soluble metabolome were evaluated by HR ^{1}H-NMR spectroscopy. Data is presented as fold-change of the respective solvent controls, as means ± SDs of three independent experiments. * indicates a significant difference compared to the solvent control based on one-sided t-tests ($p<0.05$). GPC: glycerophosphocholine, GSH: glutathione, NAA: naphthaleneacetic acid, tCho: total choline.

4 Discussion

The aim of this thesis was to establish a human-based, AOP-informed and MoA-based *in vitro* test battery to assess the potential hazard of pesticides contributing to the pathogenesis of PMD. Human iPSC and LUHMES based cell systems differentiated to dopaminergic neurons were used to set up a test battery based on the AOPs published by Ockleford *et al.,* (2017). Moreover, model compounds were used to establish cell-based *in vitro* assays dependent on the KEs of the proposed AOPs. Additionally, the effects of some commonly used pesticides and their oxon metabolites were assessed in the test battery. Finally, the metabolic consequences of the model compounds and some organophosphate pesticides were investigated.

4.1 Human iPSC and LUHMES cell differentiation into dopaminergic neurons

Neuronal differentiation of hiPSCs was conducted to obtain dopaminergic neurons, according to a protocol adapted from a previous study by Zhang *et a*l., (2014a) . The generation of dopaminergic neurons is a crucial goal in order to identify whether pesticide compounds under investigation in the present study affect the dopaminergic system and consequently may cause a degeneration of dopaminergic neurons in SN leading to PMD (Alexander, 2004). Although the differentiation of hiPSCs produced dopaminergic neurons as reflected by the increased TH and GIRK expression, a lack of reproducibility and inconsistencies between the differentiations were observed. Another disadvantage was that only a limited amount of material was gained after differentiation protocol that takes longer than 25 days. These disadvantages indicate that the differentiation of dopaminergic neurons based on hiPSCs with this protocol is not suited to generate dopaminergic neurons for medium-throughput compound screening. Therefore, a test system based on LUHMES cells was set up in a suitable format to be used for compound screening. These cells are a well-established test system of dopaminergic neurons as reflected by early expression of DAT and dopamine receptor D_2 after 2 days, while the TH expression increased first at 6 days of differentiation (Scholz *et al.*, 2011). Also, Pöltl *et al.*, (2012) reported that the expression of TH on the protein level was not detected in undifferentiated cells but increases over 6 days of differentiation. This work does not provide a full characterization as the test system is well described in the literature (Scholz *et al.*, 2011). In the present work, the neuronal identity was verified by the increase of the neuronal (ENO2) and dopaminergic (TH and DAT) markers expression. Furthermore,

the immunofluorescence staining indicates that differentiated LUHMES cells are pure neurons.

4.2 Set-up of a testing battery based on early KEs of the AOPs for PMD

To set up a test battery based on early KEs in the AOPs on the pathogenesis of PMD, the two model compounds, rotenone and paraquat, were used. Both compounds were extensively studied, have been well described MoAs and solid evidence associates human exposure to a high risk for PD. This association is based on epidemiological findings (Tanner *et al.*, 2011; Ntzani *et al.,* 2013) as well as *in vivo* and *in vitro* experiments (Brooks et al., 1999; Betarbet et al., 2000; Cannon et al., 2009; Chen et al., 2017). For these reasons, EFSA selected both compounds as representative model compounds for the two developed AOPs (Ockleford *et al.*, 2017). Thereby, rotenone models the MIE of CI inhibitors which bind to CI resulting in its inhibition followed by mitochondrial dysfunction (AOP1), whereas paraquat represents the MIE of compounds affecting the redox cycling ended by mitochondrial dysfunction (AOP2). After that, both of the AOPs converge on the KE mitochondrial dysfunction and continue via degeneration of dopaminergic neurons of the NSP to the AO PMD. For setting up the test battery, the effects of rotenone and paraquat on the early KEs of both AOPs were investigated.

Rotenone and paraquat reduced cell viability and proteasomal activity in a concentrations-dependent manner. In the present experiments, 0.4 µM decreased the cell viability measured by CTB and CTG assays to between 60 and 80% of control after 24 and 48 hours. These findings are in agreement with other studies, which showed that 0.5 µM of rotenone reduced the cell viability and ATP level of LUHMES cells from 20 to 50% of control after 24 and 48 hours (Pöltl *et al.*, 2012; Krug *et al.*, 2014). Similar to the present findings, Dolga *et al.*, (2014) and Krug *et al.*, (2014) demonstrated only small time dependence between 24 and 48 hours after rotenone exposure. However, the effects of paraquat on the LUHMES cells in the present experiments required high concentrations (around 368 and 51 µM) in order to significantly reduce cell viability to 50% of control with a clear time dependence between 24 and 48 hours, respectively. These findings are in agreement with the previous study by Hirayama *et al.*, (2018) using SH-SY5Y cells. The authors showed that 1 mM and 300 µM reduced the cell viability to around 50% of control after 24 and 48 hours, respectively.

According to the calculated IC_{50} from the present experiment, rotenone is more potent than paraquat on cell viability. This finding is in line with the previous study by Tong *et al.*, (2017) who showed that the IC_{50} values after 24 hours rotenone and paraquat exposure to LUHMES cells in an ATP assay were 1.5 µM and >100 µM, respectively. The difference in potency was also observed in SK-N-MC cells with IC_{50} values for rotenone and paraquat on the cell viability of 22.5 nM and 121.8 µM, respectively, after 48 hours of exposure (Ramachandiran *et al.*, 2007). The lower degree of potency of paraquat compared to rotenone could be attributed to the fact that rotenone is highly lipophilic in contrast to paraquat, which allows it to easily cross the cell membrane resulting in a better availability (Talpade *et al.*, 2008).

The effects of the model compounds on proteasomal activity cannot be distinguished from cell viability (CTB, CTG) in the battery. Coherently to the concomitant effects of the model compounds observed in the current work, similar inhibitory effects of rotenone on cell viability and proteasomal activity were reported in LUHMES cells by Delp *et al.*, (2019) as well as in SH-SY5Y cells after 24 hours by Sun *et al.*, (2019) and 96 hours by Shamoto-Nagai *et al.*, (2003). Similar to the results of the present work, paraquat induced a comparable degree of inhibition in mitochondrial and proteasomal activities after its application to SH-SY5Y cells for 3 and 6 hours (Ding and Keller, 2001). In contrast to my findings, paraquat (500 µM) reduced the proteasomal activity more than the cell viability of SH-SY5Y cells after 48 hours of exposure (Yang and Tiffany-Castiglioni, 2007). However, the authors assessed the activity of 26S and not 20S proteasome using ATP in the assay buffer.

The concomitant effects of model compounds on mitochondria and proteasome are explained by the KER in the two AOPs. The KER between the two KEs is ranked as moderate to strong (Terron *et al.*, 2018) and the possible explanation is that the degradation of the misfolded proteins is an active process that depends on ATP. Therefore the rotenone- and paraquat-dependent inhibition of mitochondrial function and ATP production results in the inhibition of the proteasomal activity and an accumulation of misfolded proteins (Farout *et al.*, 2006; Chou *et al.*, 2010). It is important to determine whether the inhibitory effects of model compounds on 20S proteasome is due to the primary effects on the proteasome or the secondary effects on mitochondria. In the pathogenesis of PMD, the proteasomal activity is secondary to the mitochondrial dysfunction, as shown in the AOPs (Ockleford *et al.*, 2017).

Since the inhibition of proteasomal function also affects the viability (Ko *et al.*, 2020), it has to be clarified if the effect seen here is really specific or a secondary effect. Therefore, the specificity of the proteasomal assay was assessed using epoxomicin as a selective proteasome inhibitor. Indeed, the exposure to epoxomicin showed that the inhibition of the activity of 20 S proteasome in differentiated LUHMES cells occurred before the disturbance of the mitochondrial function. Similarly, Höglinger *et al.*, (2003) showed that epoxomicin induced earlier reduction of proteasomal activity before impairing the cells survival of the mesencephalic culture of Wistar rat embryos. Thus, the test battery is able to distinguish MoA that act primarily on the proteasome from MoA that involves proteasome dysfunction as a secondary effect of mitochondrial dysfunction.

In the present experiments, rotenone induced early apoptosis as reflected with caspase 3/7 activation and late necrosis. These effects were similar to staurosporine, however, the degree of activation of caspase 3/7 deceased with the high concentration of rotenone in contrast to a concentration-dependent caspase 3/7 activation induced by staurosporine after 6 hours. This finding could be explained by the fact that apoptosis is an active process that depends on cell energy (Leist *et al.*, 1997). The highest concentration of rotenone but not staurosporine that impaired the mitochondria and therefore cellular energy production after 6 hours resulted in a reduction in the caspase 3/7 activation. In agreement with the present findings, Sundquist *et al.*, (2006) reported that the concentrations and duration of exposure to apoptotic inducers affect the cellular response. The authors added that the apoptosis can be reduced or even replaced by necrosis at high concentrations or extending the time of exposure to apoptotic inducers and this notion is consistent with the observation for rotenone in the current work. In the current thesis, paraquat did not induce caspase 3/7 activation. Coherently, Hirayama *et al.*, (2018) stated that paraquat did not activate caspase 3/7 but caused later necrosis in SH-SY5Y. However, Klintworth *et al.*, (2007) showed that rotenone induced apoptosis of SH-SY5Y cells but not PC12 cells while paraquat induced apoptosis in PC12 cells and not SH-SY5Y cells. The possible explanation for this discrepancy in the apoptotic effects of the model compounds is the different ability to activate c-Jun N-terminal protein kinase depending on cell lines. Indeed, rotenone and paraquat activated this kinase in SH-SY5Y and PC12 cells, respectively.

In order to assess the KE “neuronal degeneration”, the two pathways of cells death were investigated using caspase 3/7 activation as a marker of apoptosis and LDH leakage as an indirect indicator for necrosis. Importantly, mitochondrial dysfunction may lead to neuronal cell death because the neurons have limited compensation to upregulate the glycolysis during ATP reduction (Almeida, *et al.*, 2004; Herrero-Mendez *et al.*, 2009). The WOE of KER between mitochondrial dysfunction and degeneration of dopaminergic neurons is ranked strong (Terron *et al.*, 2018) because dopaminergic neurons in NSP are more dependent on ATP than other neuronal subtypes. This may be related to their long, highly branching and unmyelinated axons with many synapses (Bolam and Pissadaki, 2012). Although necrotic and apoptotic cell death is assessed in this battery, it is not clear if this cell death is specific for dopaminergic neurons or if the dopaminergic neurons are more sensitives than other neuronal cultures. Therefore, the specificity of the cell death endpoints needs to be assessed in order to determine if the assessment of cell death represents the dopaminergic neuron specific KE “neuronal degeneration”. Similar is, of course, true for the other early KEs assessed in this test battery.

Rotenone is a general CI inhibitor, while paraquat is a redox cycler which induces oxidative stress. Both of them do not selectively initiate an adverse event in dopaminergic neurons (Corasaniti *et al.*, 1998; Ullrich and Humpel, 2009) nor do they selectively accumulate in dopaminergic neurons (Schmidt and Alam, 2006; Talpade *et al.*, 2008). However, dopaminergic neurons are more susceptible to mitochondrial dysfunction (Bolam and Pissadaki, 2012). Consistently, Pamies *et al.*, (2018) reported that dopaminergic neurons (TH positive) were more vulnerable to the effects of rotenone after 24 hours compared to other neurons (microtubule-associated protein 2 positive) of a human brain spheroid model. Furthermore, Gao *et al.*, (2002) reported that rotenone selectively degenerated the dopaminergic neurons in a mixed culture of rat neurons and glial cells. Moreover, Ren *et al.*, (2005) reported that rotenone selectively interfered with dopaminergic neurons of rat embryonic midbrain neuronal cultures. The authors added that this selectivity is attributed to depolymerization of microtubules which impairs the transport of dopaminergic vesicles ended by the accumulation of dopamine in the soma. This event leads to the leakage of dopamine from the vesicle, consequently increasing the concentrations of cytoplasmic dopamine. Autooxidation of dopamine generated ROS together with mitochondrial dysfunction induced by rotenone making the dopaminergic neurons

more vulnerable to rotenone. Di Monte, (2003) suggested that the accumulation of dopamine with the redox cycling by paraquat which ended by mitochondrial dysfunction could add an explanation to the vulnerability of dopaminergic neurons to paraquat. Based on the data presented in this work, it is not clear if the effects of the model compounds are specific for dopaminergic neurons. However, the test battery set-up here is able to assess early KEs of PMD and can be used to identify compounds that show a similar activity profile similar to that of the two well-established model compounds. For a further understanding of the specificity of the test battery, the effects of the model compounds in this battery need to be directly compared to effects in test systems where dopaminergic neurons are absent or underrepresented.

4.3 Chemical testing

The aim of the third part of this thesis was to assess the effects of some commonly-used organophosphate pesticides in the established testing battery. Organophosphate pesticides are commonly used worldwide and play a pivotal role in crop production (Elersek and Filipic, 2011; Sharma *et al.*, 2019). Emerging epidemiological (Allen and Levy, 2013; Narayan *et al.*, 2017), *in vivo* (Binukumar *et al.*, 2010; Acker *et al.*, 2011; Deveci and Karapehlivan, 2018) and *in vitro* (Park *et al.*, 2013; Wani *et al.*, 2017) evidence support the notion that some of these pesticides are associated with an increased risk of PD.

The results from testing the organophosphate pesticides in the current work categorized them into two groups according to the similarity of their activity profile to that of the two model compounds. The activity profile of chlorpyrifos and parathion is similar to that of rotenone. Their effects on the mitochondrial activity could not be distinguished from that on the proteasome with a clear time-dependence between 6 and 24 hours as well as 6 and 48 hours but with only small differences between 24 and 48 hours. In the cell death assays, similar to rotenone, they show an early induction of apoptosis followed by necrosis with increasing time and concentrations. Consistent to the results of the current work, the application of chlorpyrifos on SN56 cells, murine cholinergic neurons, caused a comparable degree of reduction in cell viability and proteasomal activity after 24 hours (Moyano *et al.*, 2019). Indeed, 500 µM of chlorpyrifos induced a parallel degree of reduction of proteasomal activity and ATP level in SH-SY5Y cells after 24 hours of application (Chen *et al.*, 2017). Up to

date, the data regarding the effects of other organophosphate pesticides on UPP is scarce. For example, Rhodes et al. (2013) demonstrated that parathion did not inhibit 26S proteasome of SK-N-MC cells after 24 hours, however, only low concentration of parathion was used (10 µM). High IC_{50} values for parathion on cell viability and proteasomal activity were observed in the current work after 24 hours of 300 to 340 µM parathion exposure. In support of the present work, Wang *et al.*, (2019) showed that IC_{50} value for parathion on cell viability of NB41A3 cells, a mouse neuroblastoma cell line, is even higher (660 µM) after 24 hours. The similarity of chlorpyrifos and parathion effects with that of rotenone could be explained by the fact that all of them inhibit the mitochondrial ETC. Indeed, Salama *et al.*, (2014) suggested the inhibition of CI as a possible mechanism of chlorpyrifos-induced neurotoxicity. Furthermore, Turton *et al.*, (2020) showed that inhibition of cell viability of SH-SY5Y cells by chlorpyrifos and parathion is mediated by inhibition of mitochondrial CII and CIII. The inhibition of the ECT as MoA for chlorpyrifos and parathion is supported by showing that incubation with coenzyme Q10, as an electron shuttle, antagonized their effects on cell viability. Also, Moreno and Madeira, (1990) reported that parathion inhibited mitochondrial CIV. On the other side, the activity profile of malathion and dichlorvos was similar to that of paraquat. Here, the effects on the mitochondrial activity are also not distinguishable from that on the proteasomal activity with a time-dependent decrease between all three timepoints. Regarding the cell death, both compounds, similar to paraquat, did not induce apoptosis, however, they caused necrosis at later time points and at high concentrations. Similar to the result of the current work, Venkatesan *et al.,* (2017) showed that even a higher concentration of malathion (1 mM) was required to reduce cell viability of N2a cells to around 75% of control and to release LDH without caspase 3/7 activation. Taken together, the present findings suggest that necrosis is the manner of malathion-induced cell death and the LUHMES cells appear to be more sensitive compared to other cells used to test pesticides affecting the KEs. Redox cycling is the MIE of paraquat which results in ROS formation and subsequently mitochondrial dysfunction. Similarly, malathion induces oxidative stress in rat hepatocyte followed by cytotoxicity. This effect could be antagonized by N-acetyl cysteine (Mostafalou *et al.*, 2012). Furthermore, Mohammadzadeh *et al.*, (2018) demonstrated that malathion elevated malondialdehyde and reduced glutathione in the CS of Wistar rat. Similarly, Binukumar *et al.,* (2011) observed that dichlorvos induced oxidative stress in CS and

SN of brain of rats. Collectively, these findings suggest that both pesticides may share some similarity with the MoA of paraquat. In conclusion, the distinction based on the activity profiles for the tested organophosphate pesticides to that of the model compounds are supported by published data (Binukumar BK *et al.*, 2011; Mostafalou *et al.*, 2012; Salama *et al.*, 2014; Ockleford *et al.*, 2017; Turton *et al.*, 2020).

It is well established that metabolizing organophosphate pesticides to their oxon metabolites alters their potencies (Sparling and Fellers, 2007; Aker *et al.*, 2008). Since LUHMES cells do not have metabolizing capacities (Eaton *et al.*, 2008; Miksys and Tyndale, 2013; Tong *et al.*, 2017), the oxon metabolites of pesticides under investigation were tested separately. The results of the current work indicated that the pesticides are more potent than their oxon metabolites on mitochondrial and proteasomal activities. Consistently, Qiao *et al*., (2001) showed that chlorpyrifos oxon is less toxic than chlorpyrifos on inhibiting protein synthesis of both PC12 and C6 glioma cells. Furthermore, Gao *et al.,* (2017) showed a minor difference between chlorpyrifos and its oxon on cell viability of rat embryonic cortical cultures. The authors demonstrated that 1 µM of chlorpyrifos oxon reduced cell viability to around 95% of control while chlorpyrifos did not. Estevan *et al.* (2014) reported that the IC_{50} values of chlorpyrifos on cell viability were lower on D3 mouse embryonic stem cells and higher on 3T3 mouse fibroblast than for its oxon. For parathion, it was shown that the parent compound induced oxidative stress and cytotoxicity, while paraoxon did not. One possible explanation for this difference is the short half-life and high reactivity of paraoxon (IARC Working Group on the Evaluation of Carcinogenic Risk to Humans, 2017). On the other hand, Wang *et al.*, (2019) showed that paraoxon more potently inhibits cell viability in NB41A3 cells after 24 hours. The discrepancies in sensitivity of organophosphate pesticides compared to their oxon metabolites could be explained by different susceptibilities of the various cell lines. However, the molecular mechanisms behind the different cellular susceptibilities are not clear. For malaoxon, for example, it was shown that the inflammatory process is one of the major MoA (IARC Working Group on the Evaluation of Carcinogenic Risk to Humans, 2017). This would explain why cell line that does not represent an inflammatory response, such as LUHMES cells are less vulnerable to malaoxon.

4.4 LUHMES cell metabolomics

Using high-resolution ^{1}H-NMR spectroscopy, distinct metabolic changes were associated with neuronal differentiation, exposure to the PD model compounds paraquat and rotenone, and exposure to organophosphate pesticides, chlorpyrifos and parathion, in LUHMES cells.

The metabolic profile of LUHMES cells undergoing neuronal differentiation

Neuronal differentiation decreased the glycolytic and TCA cycle activity of LUHMES cells, indicating that reduced proliferation decreases the energetic and biosynthetic demands of the cells. This was detected by a significant decline in Lac, TCA cycle-dependent amino acids (Ala and Asp), and TCA intermediates (Suc and Cit) upon differentiation. This switch can be initiated by decreased glucose uptake and the decline in Glu, which is a precursor of the TCA cycle intermediate αKG (Fig.33). This phenomenon was confirmed by Martins and Sood, (2016), since they also reported decreased glycolytic activity in differentiating LUHMES cells. Furthermore, decreased Glu and consequently reduced Ala were detected during the differentiation of human striatal neural stem cells (Chung *et al.*, 2013). Additionally, differentiated LUHMES cells exhibited decreased GSH levels indicating a reduced antioxidant capacity which can make the cells more susceptible to oxidative stress (Martins and Sood, 2016). Since ROS are in particular generated as side products in the ETC (Raha and Robinson, 2000), the reduced energy metabolism of differentiating LUHMES cells decreases the need for ROS clearance (Martins and Sood, 2016). Glu is one of the three building blocks of the tripeptide GSH, therefore the GSH content could be regulated by decreased metabolism of Gln and Glu. Choline metabolism is crucial for membrane remodeling in differentiating cells (Zeisel, 2006). In accordance with that, significant changes in choline metabolites were observed, highlighting that profound structural changes are involved in the differentiation of LUHMES cells. In line with my results, Martins and Sood, 2016 also observed accumulation of choline and reduced PC levels in differentiating LUHMES cells and Chung *et al.,* 2013 detected reduced PC + GPC contents of the differentiated human striatal neural stem cells.

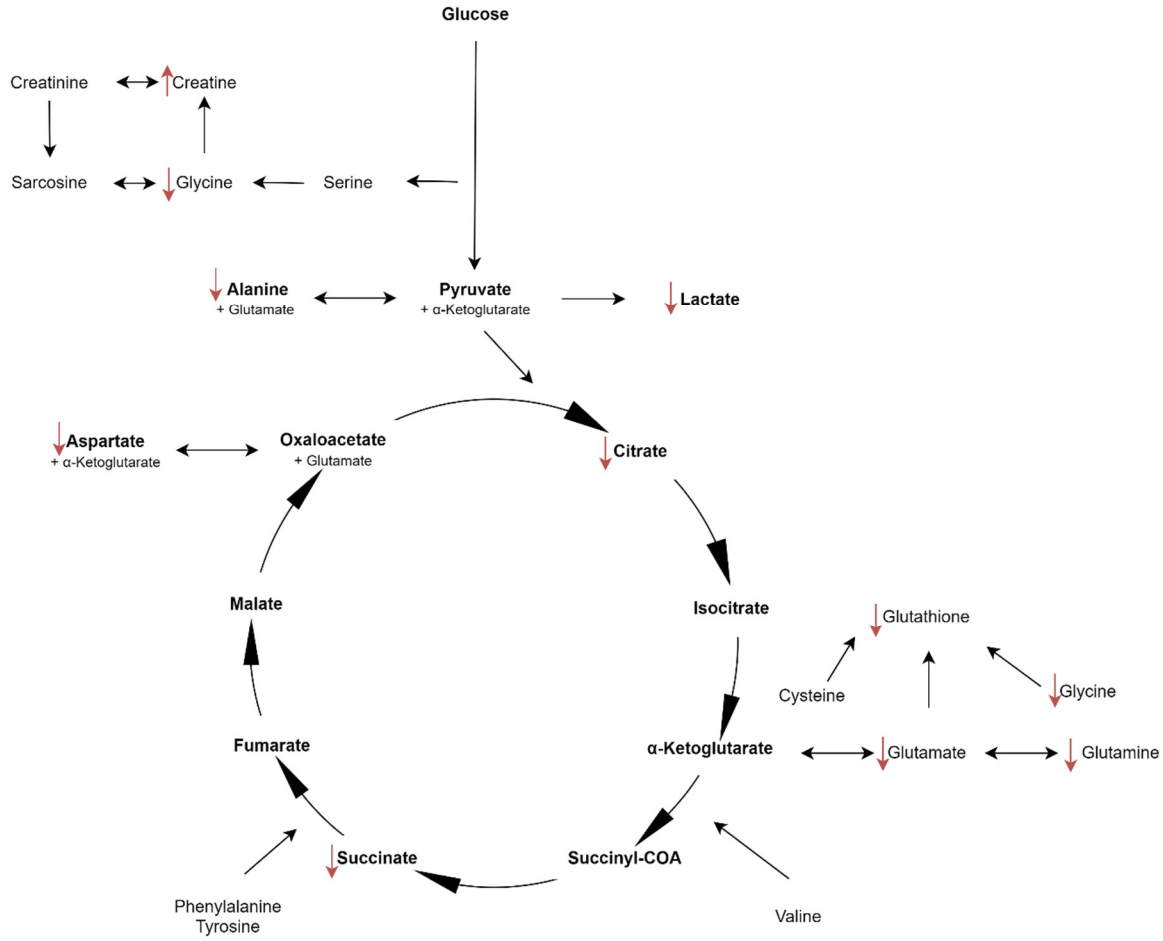

Fig.33: Schematic summary of metabolic changes during differentiation of LUHMES cells. This figure was adapted from Sui *et al.*, (2012)

Exposure to the model compounds paraquat and rotenone efficiently interferes with LUHMES cells metabolism

Rotenone and paraquat exposure induced accumulation of TCA cycle precursors (Gln, Glu) and intermediates (Suc, Cit), indicating that the impaired flow through the ETC causes this accumulation due to the continuous uptake of precursors like glucose and Gln (Chen *et al.*, 2018). However, while rotenone significantly increased the concentrations of several TCA cycle-dependent amino acids (Val, Ala), paraquat did not. This highlights that, besides sharing some metabolic phenotypes, the model compounds have distinct targets in LUHMES cell metabolism (Fig.34).

Previous research showed that the toxicity of rotenone in LUHMES cells is, at least in part, mediated by inactivation of small-conductance calcium-activated potassium (SK) channels. SK channel activity effectively prevents neuronal excitotoxicity due to

glutamate-receptor mediated deregulation of intracellular Ca^{2+} (Dolga *et al.*, 2011). In accordance with that, SK channel activation rescued the phenotype of rotenone exposure both *in vitro* and *in vivo* (Dolga *et al.*, 2011, 2014). Since administration of 20 µM Glu induced similar neurotoxic effects on primary cortical neuron cultures than rotenone, its toxicity is presumably caused by glutamate receptor-mediated excitotoxicity. Therefore, the Glu accumulation observed upon exposure to the model compounds could have a contributing role in rotenone-induced toxicity.

In accordance with my results, 1-methyl-4-phenylpyridinium (MPP^+), a potent CI inhibitor, increased Lac, Cre, and GSH levels in LUHMES cells. Furthermore, the authors observed increased concentrations of phosphatidylcholine, resembling my results showing increased choline metabolite levels upon rotenone exposure. Contrary to my work, MPP^+ decreased Glu and Ala concentrations (Krug *et al.*, 2014).

Opposing my observations, Martins and Sood, (2016) reported that 10 µM paraquat exposure reduced Gln, Glu, and Suc but increased Cit after 24 hours in LUHMES cells. However, 100 µM paraquat had no effect on Glu and Gln, but decreased Suc and Cit. Given these inconsistent results, they are challenging to evaluate and to compare with my work. It is noteworthy to mention, that the chosen longer exposure time of 48 hours could affect the metabolic consequences. Furthermore, modelling of PD by genetic modification of LUHMES cells (loss of DJ-1) resulted in a reduction of Gln uptake, its contribution to the TCA cycle, and reduced production of the Gln-dependent amino acids Ala (Meiser *et al.*, 2016).

In conclusion, it becomes obvious that different approaches in modeling PD do not result in the same metabolic alterations probably due to different molecular targets or different timing. The approaches that were chosen, however, share the majority of metabolic consequences. Furthermore, my results emphasize that PD is associated with a variety of metabolic alterations causing diverse adverse effects in humans.

Exposure of LUHMES cells to organophosphate pesticides partly reflects the consequences observed after paraquat and rotenone exposure

Chlorpyrifos and parathion induced similar but less pronounced changes compared to rotenone exposure, increasing TCA-cycle precursors (Gln and Glu), the TCA cycle-intermediate Cit, and the TCA-dependent amino acid Ala (Fig.34).

Supporting my results, exposure of *danio rerio* to a non-toxic concentration of chlorpyrifos for five days elevated Gln, Glu and phenylalanine concentrations. However, in contrast to my result, chlorpyrifos decreased choline (Tufi, 2016). Kokushi *et al.,* 2015 demonstrated that exposure of *cyprinus carpio* to chlorpyrifos for 48 hours slightly decreased Gln, Ala, Val, and Lac levels, however, these changes were not statistically significant. Moreover, exposure of rats to chlorpyrifos for 90 days decreased Suc and tyrosine levels (Xu *et al.*, 2015). It is important to mention, that these studies assessed metabolite concentrations in whole organs or organisms, while we focused on intracellular effects in a specific cell population, i.e. differentiated LUHMES cells. Supporting my results, parathion elevates choline concentrations in human embryonic stem cells (Sekowski *et al.*, 2014).

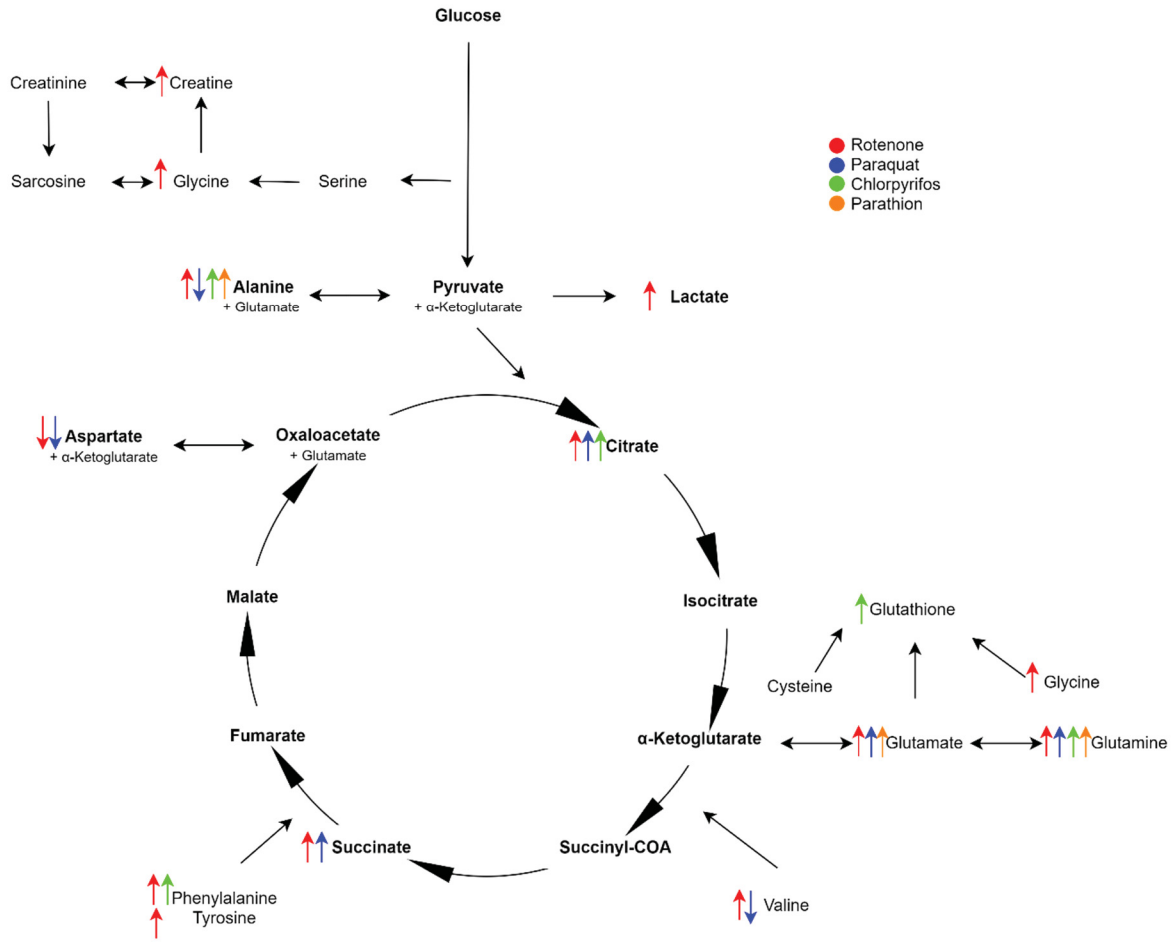

Fig.34: Schematic summary of metabolic consequences of pesticide exposures on differentiated LUHMES cells, adapted from Sui *et al.*, (2012). Red, blue, green and orange arrows indicate the metabolic effects of rotenone, paraquat, chlorpyrifos and parathion, respectively.

The weaker effects chlorpyrifos and parathion compared to rotenone may be attributed to the fact that, in contrast to the pesticides, rotenone is a potent CI inhibitor and thus has a more profound metabolic phenotype. In spite of using the IC_{50} concentrations of the pesticides, chlorpyrifos and parathion may, therefore, induce weaker metabolic effects compared to rotenone. Moreover, the observed metabolic effects of chlorpyrifos and parathion could be independent of the induction of PD-like alterations inside LUHMES cells, since the correlations between organophosphate exposure and PD are not yet profound. PD-unrelated effects within the cells could be the cause of the metabolic phenotypes.

4.5 Discussion on the usefulness of the LUHMES-based testing strategy for AOP-based compound evaluation

LUHMES cells are provided by two sources; the University of Konstanz (UKN), which were used for this thesis, and the American-Type-Culture-Collection (ATCC). Gutbier *et al.*, (2018) stated that these cells have different susceptibility to toxins. Additionally, the differentiated LUHMES cells from ATCC have lower levels of TH expression resulting in a lower dopamine concentration compared to the cells from the UKN. For this reason, the cells provided by UKN are better for the application in a test battery that represents the effects on a dopaminergic test system.

Tong *et al.*, (2017) stated that differentiated LUHMES cells have the highest expression of TH after day 7 of differentiation compared to SH-SY5Y and neural stem cells. The authors concluded that LUHMES cells have convenient characteristics to be used for high-throughput compound screening because they have a rapid neuronal differentiation and high level of expression of neuronal markers. Moreover, differentiated LUHMES cells are more susceptible to the majority of tested neurotoxicants compared to differentiated SH-SY5Y and neural stem cells.

Besides the expression of dopaminergic markers TH and DAT, LUHMES cells express the marker of dopaminergic neuronal subtypes in the SN (GIRK) indicating the suitability of using them as a cellular model to investigate the pathogenesis events of PD. TH is expressed lately in the LUHMES cells, however, the other markers of dopaminergic neurons (DAT and dopamine receptor D_2) are expressed early (Scholz *et al.*, 2011; Zhang *et al.*, 2014b). Therefore, determination of dopaminergic neuronal differentiation should be based on dopaminergic neuronal markers that are expressed at an earlier timepoint than TH (Scholz *et al.*, 2011).

One limitation of using LUHMES cells is the short culture time, which ranges from two to three days after differentiation. This does not allow to assess the effects of prolonged compound exposure. Additionally, LUHMES cells are pure neuronal cultures without glial cells (Tong *et al.*, 2017). However glia-dependent neuroinflammation is one of the KE of AOPs (Ockleford *et al.*, 2017) which is not represented by the system used in this work. Both limitations can be circumvented by growing LUHMES in 3D in the presence of human astrocytes and microglia. This allows maintaining the LUHMES cells for longer periods and investigating neuroinflammation (Brüll *et al.*, 2020).

4.6 Conclusion and outlook

In this work, a human *in vitro* testing battery based on LUHMES cells to assess the effects of chemicals on early KEs during the pathogenesis of PMD was established. This battery represents the KEs mitochondrial dysfunction, inhibition of proteasomal activity and neuronal cell death. The battery was set up using two well-established model compounds that represent both MIEs in the AOPs for PMD namely binding to CI and affecting redox cycling. The activity profiles of cell-based assays across the battery allowed the separation of the two different MIEs.

Furthermore, the effects of the commonly used organophosphate pesticides chlorpyrifos, parathion, malathion and dichlorvos were assessed with the battery. Based on their activity profile, it was possible to differentiate between chlorpyrifos and parathion, which show activity profile similar to that of rotenone, and malathion, and dichlorvos, which shows an activity profile similar to that of paraquat. In addition, the major metabolites of the tested organophosphate pesticides were less potent than their parent pesticides.

Furthermore, the metabolic homeostasis of LUHMES cells, as a surrogate for dopaminergic neurons, appears to be highly sensitive to external stimuli and in particular to mitochondrial dysfunction. This clearly highlights the potential of implementing LUHMES cell metabolomics in the toxicological testing guidelines in the future. However, additional experiments are needed to clarify which metabolic alterations are specific for which pesticide and which are the distinct cellular consequences.

Taken together, this battery is suitable for an initial compound screening to identify chemicals that might potentially disrupt early KEs during the pathogenesis of PMD by

two MIEs, i.e. redox cycling-induced cell death or death involving CI inhibition. While the first does not involve caspase 3/7-induced apoptosis, the latter is represented by induction of caspase activities.

In the future, it needs to be investigated if the early KEs assessed in this battery are affected with higher sensitivity in LUHMES cells compared to non-dopaminergic neurons. Furthermore, it needs to be shown if the activity profile for pesticides that are not associated with PMD can be differentiated from that of the model compounds and the organophosphate pesticides tested in this thesis. Moreover, the kinetic considerations via an approach of "*in vitro in vivo* Extrapolation" (IVIVE) are needed for moving from hazard to risk (Croom *et al.*, 2015). In addition, testing of multiple sub-toxic or low-toxic (IC_{20}) concentrations of the model compounds and organophosphate pesticides are necessary to investigate the cellular and metabolic consequences in more detail. Targeted metabolomics and a combination of metabolomics and transcriptomics would provide a deeper understanding of metabolic changes associated with PD and organophosphates pesticides exposure.

5 Bibliography

Acker, C. I. *et al.* (2011) 'Repeated malathion exposure induces behavioral impairment and AChE activity inhibition in brains of rat pups', *Ecotoxicology and Environmental Safety*, 74(8), pp. 2310–2315. doi: 10.1016/j.ecoenv.2011.07.035.

Adem, A. *et al.* (1987) 'Muscarinic receptors in human SH-SY5Y neuroblastoma cell line: regulation by phorbol ester and retinoic acid-induced differentiation', *Developmental Brain Research*, 33(2), pp. 235–242. doi: 10.1016/0165-3806(87)90156-8.

Aker, W. G. *et al.* (2008) 'Comparing the relative toxicity of malathion and malaoxon in blue catfish *Ictalurus furcatus*', *Environmental Toxicology*. John Wiley & Sons, Ltd, 23(4), pp. 548–554. doi: 10.1002/tox.20371.

Alexander, G. E. (2004) 'Biology of Parkinson's disease: pathogenesis and pathophysiology of a multisystem neurodegenerative disorder.', *Dialogues in clinical neuroscience*. Les Laboratoires Servier, 6(3), pp. 259–80. Available at: http://www.ncbi.nlm.nih.gov/pubmed/22033559 (Accessed: 22 January 2020).

Ali, S. J. *et al.* (2019) 'Chlorpyrifos Exposure Induces Parkinsonian Symptoms and Associated Bone Loss in Adult Swiss Albino Mice', *Neurotoxicity Research*. Neurotoxicity Research, 36(4), pp. 700–711. doi: 10.1007/s12640-019-00092-0.

Allen, M. T. and Levy, L. S. (2013) 'Parkinson's disease and pesticide exposure – a new assessment', *Critical Reviews in Toxicology*, 43(6), pp. 515–534. doi: 10.3109/10408444.2013.798719.

Almeida, A., Moncada, S. and Bolaños, J. P. (2004) 'Nitric oxide switches on glycolysis through the AMP protein kinase and 6-phosphofructo-2-kinase pathway', *Nature Cell Biology*. Nature Publishing Group, 6(1), pp. 45–51. doi: 10.1038/ncb1080.

Ankley, G. T. *et al.* (2010) 'Adverse outcome pathways: A conceptual framework to support ecotoxicology research and risk assessment', *Environmental Toxicology and Chemistry*, 29(3), pp. 730–741. doi: 10.1002/etc.34.

Aschner, M. *et al.* (2017) 'Example Lists and Criteria for Their Selection and Use', 34(1), pp. 49–74. doi: 10.14573/altex.1604201.Reference.

Bal-Price, A. *et al.* (2018) 'Adverse Outcome Pathway on Inhibition of the mitochondrial complex I of nigro-striatal neurons leading to parkinsonian motor deficits', *OECD*

Series on Adverse Outcome Pathways No. 7, (7), pp. 0–184. doi: 10.1787/b46c3c00-en.

Ball, N. *et al.* (2019) 'Parkinson's Disease and the Environment', *Frontiers in Neurology*. Frontiers, 10, p. 218. doi: 10.3389/fneur.2019.00218.

Basha, P. M., Begum, S. and Nayeemunnisa (2001) 'Methyl parathion induced alterations in monoaminergic system of developing rat pups', *Indian Journal of Experimental Biology*, 39(3), pp. 276–279.

Bentea, E. *et al.* (2015) 'Nigral proteasome inhibition in mice leads to motor and non-motor deficits and increased expression of Ser129 phosphorylated Î±-synuclein', *Frontiers in Behavioral Neuroscience*. Frontiers, 9, p. 68. doi: 10.3389/fnbeh.2015.00068.

Betarbet, R. *et al.* (2000) 'Chronic systemic pesticide exposure reproduces features of Parkinson's disease', *Nature Neuroscience*. Nature Publishing Group, 3(12), pp. 1301–1306. doi: 10.1038/81834.

Binukumar, B. K. *et al.* (2010) 'Nigrostriatal neuronal death following chronic dichlorvos exposure: crosstalk between mitochondrial impairments, α synuclein aggregation, oxidative damage and behavioral changes.', *Molecular brain*, 3(1), p. 35. doi: 10.1186/1756-6606-3-35.

Binukumar BK *et al.* (2011) 'Protection of dichlorvos induced oxidative stress and nigrostriatal neuronal death by chronic Coenzyme Q10 pretreatment', *Toxicology and Applied Pharmacology*. Elsevier Inc., 256(1), pp. 73–82. doi: 10.1016/j.taap.2011.07.015.

Bolam, J. P. and Pissadaki, E. K. (2012) 'Living on the edge with too many mouths to feed: Why dopamine neurons die', *Movement Disorders*, 27(12), pp. 1478–1483. doi: 10.1002/mds.25135.

Bové, J. and Perier, C. (2012) 'Neurotoxin-based models of Parkinson's disease', *Neuroscience*. Elsevier Inc., 211, pp. 51–76. doi: 10.1016/j.neuroscience.2011.10.057.

Bovolenta, T. M. *et al.* (2017) 'Systematic Review and Critical Analysis of Cost Studies Associated with Parkinson's Disease', *Parkinson's Disease*, 2017(March 2016). doi: 10.1155/2017/3410946.

Brooks, A. . *et al.* (1999) 'Paraquat elicited neurobehavioral syndrome caused by

dopaminergic neuron loss', *Brain Research*. Elsevier, 823(1–2), pp. 1–10. doi: 10.1016/S0006-8993(98)01192-5.

Brüll, M. *et al.* (2020) 'Incorporation of stem cell-derived astrocytes into neuronal organoids to allow neuro-glial interactions in toxicological studies', *ALTEX*. doi: 10.14573/altex.1911111.

Bus, J. S. and Gibson, J. E. (1984) 'Paraquat: model for oxidant-initiated toxicity.', *Environmental Health Perspectives*. National Institute of Environmental Health Sciences, 55, p. 37. doi: 10.1289/EHP.845537.

Cannon, J. R. *et al.* (2009) 'A highly reproducible rotenone model of Parkinson's disease.', *Neurobiology of disease*. NIH Public Access, 34(2), pp. 279–90. doi: 10.1016/J.NBD.2009.01.016.

Chen, Q. *et al.* (2018) 'Rewiring of Glutamine Metabolism Is a Bioenergetic Adaptation of Human Cells with Mitochondrial DNA Mutations', *Cell Metabolism*. Cell Press, 27(5), pp. 1007-1025.e5. doi: 10.1016/J.CMET.2018.03.002.

Chen, T. *et al.* (2017) 'Effects of Commonly Used Pesticides in China on the Mitochondria and Ubiquitin-Proteasome System in Parkinson's Disease.', *International journal of molecular sciences*. Multidisciplinary Digital Publishing Institute (MDPI), 18(12). doi: 10.3390/ijms18122507.

Chou, A. P. *et al.* (2010) 'Mechanisms of rotenone-induced proteasome inhibition', *NeuroToxicology*, 31(4), pp. 367–372. doi: 10.1016/j.neuro.2010.04.006.

Chung, Y.-L. *et al.* (2013) 'Profiling metabolite changes in the neuronal differentiation of human striatal neural stem cells using 1H-magnetic resonance spectroscopy', *NeuroReport*, 24(18), pp. 1035–1040. doi: 10.1097/WNR.0000000000000056.

Clark, E. P. (1929) 'The occurrence of rotenone in the Peruvian fish poison "cube"', *Science*. American Association for the Advancement of Science, pp. 478–479. doi: 10.1126/science.70.1820.478-a.

Colman, A. (2013) 'Profile of John Gurdon and Shinya Yamanaka, 2012 Nobel laureates in medicine or physiology.', *Proceedings of the National Academy of Sciences of the United States of America*. National Academy of Sciences, 110(15), pp. 5740–1. doi: 10.1073/pnas.1221823110.

Corasaniti, M. T. et al. (1998) 'Paraquat: a useful tool for the in vivo study of

mechanisms of neuronal cell death', Pharmacol Toxicol. 1998/10/09, 83(1), pp. 1–7. doi: 10.1111/j.1600-0773.1998.tb01434.x.

Croom, E. L. *et al.* (2015) 'Improving in vitro to in vivo extrapolation by incorporating toxicokinetic measurements: A case study of lindane-induced neurotoxicity', *Toxicology and Applied Pharmacology*. Academic Press, 283(1), pp. 9–19. doi: 10.1016/J.TAAP.2014.11.006.

Davis, G. C. *et al.* (1979) 'Chronic Parkinsonism secondary to intravenous injection of meperidine analogues.', *Psychiatry research*. Elsevier, 1(3), pp. 249–54. doi: 10.1016/0165-1781(79)90006-4.

Delp, J. *et al.* (2019) 'Development of a neurotoxicity assay that is tuned to detect mitochondrial toxicants', *Archives of Toxicology*. Springer Berlin Heidelberg, 93(6), pp. 1585–1608. doi: 10.1007/s00204-019-02473-y.

Deveci, H. A. and Karapehlivan, M. (2018) 'Chlorpyrifos-induced parkinsonian model in mice: Behavior, histopathology and biochemistry', *Pesticide Biochemistry and Physiology*. Elsevier Inc, 144, pp. 36–41. doi: 10.1016/j.pestbp.2017.11.002.

Devi, L. *et al.* (2008) 'Mitochondrial import and accumulation of α-synuclein impair complex I in human dopaminergic neuronal cultures and Parkinson disease brain', *Journal of Biological Chemistry*, 283(14), pp. 9089–9100. doi: 10.1074/jbc.M710012200.

Di Monte, D. A. (2003) 'The environment and Parkinson's disease: Is the nigrostriatal system preferentially targeted by neurotoxins?', *Lancet Neurology*, 2(9), pp. 531–538. doi: 10.1016/S1474-4422(03)00501-5.

Ding, Q. and Keller, J. N. (2001) 'Proteasome inhibition in oxidative stress neurotoxicity: Implications for heat shock proteins', *Journal of Neurochemistry*, 77(4), pp. 1010–1017. doi: 10.1046/j.1471-4159.2001.00302.x.

Dolga, A. M. *et al.* (2011) 'KCa2 channels activation prevents [Ca2+]i deregulation and reduces neuronal death following glutamate toxicity and cerebral ischemia', *Cell Death and Disease*, 2(4), pp. 1–10. doi: 10.1038/cddis.2011.30.

Dolga, A. M. *et al.* (2014) 'Subcellular expression and neuroprotective effects of SK channels in human dopaminergic neurons', *Cell Death and Disease*, 5(1). doi: 10.1038/cddis.2013.530.

Doss, M. X. and Sachinidis, A. (2019) 'Current Challenges of iPSC-Based Disease Modeling and Therapeutic Implications', *Cells*, 8(5), p. 403. doi: 10.3390/cells8050403.

Dowding, C. H., Shenton, C. L. and Salek, S. S. (2006) 'A review of the health-related quality of life and economic impact of Parkinson's disease', *Drugs and Aging*, 23(9), pp. 693–721. doi: 10.2165/00002512-200623090-00001.

Eaton, D. L. *et al.* (2008) 'Critical Reviews in Toxicology Review of the Toxicology of Chlorpyrifos With an Emphasis on Human Exposure and Neurodevelopment Review of the Toxicology of Chlorpyrifos With an Emphasis on Human Exposure and Neurodevelopment Rolf Schulte-Hermann', 8444. doi: 10.1080/10408440802272158.

Elersek, T. and Filipic, M. (2011) 'Organophosphorous Pesticides - Mechanisms of Their Toxicity', in *Pesticides - The Impacts of Pesticides Exposure*. doi: 10.5772/14020.

Estevan, C. *et al.* (2014) 'Organophosphorus pesticide chlorpyrifos and its metabolites alter the expression of biomarker genes of differentiation in D3 mouse embryonic stem cells in a comparable way to other model neurodevelopmental toxicants', *Chemical Research in Toxicology*, 27(9), pp. 1487–1495. doi: 10.1021/tx500051k.

Farout, L. *et al.* (2006) 'Inactivation of the proteasome by 4-hydroxy-2-nonenal is site specific and dependant on 20S proteasome subtypes', *Archives of Biochemistry and Biophysics*. Academic Press, 453(1), pp. 135–142. doi: 10.1016/J.ABB.2006.02.003.

Fernández-Santiago, R. *et al.* (2015) 'Aberrant epigenome in iPSC-derived dopaminergic neurons from Parkinson's disease patients.', *EMBO molecular medicine*. Wiley-Blackwell, 7(12), pp. 1529–46. doi: 10.15252/emmm.201505439.

Fritsche, E. *et al.* (2018) 'Current Availability of Stem Cell-Based In Vitro Methods for Developmental Neurotoxicity (DNT) Testing', *Toxicological Sciences*. Oxford Academic, 165(1), pp. 21–30. doi: 10.1093/toxsci/kfy178.

Gao, H. M. *et al.* (2002) 'Distinct role for microglia in rotenone-induced degeneration of dopaminergic neurons', *J Neurosci*. 2002/02/05, 22(3), pp. 782–790. doi: 10.1523/jneurosci.22-03-00782.2002.

Gao, J. *et al.* (2017) 'Chlorpyrifos and chlorpyrifos oxon impair the transport of membrane bound organelles in rat cortical axons.', *Neurotoxicology*. NIH Public Access, 62, pp. 111–123. doi: 10.1016/j.neuro.2017.06.003.

Gunnarsson, L.-G. and Bodin, L. (2017) ‘Parkinson’s disease and occupational exposures: a systematic literature review and meta-analyses.’, *Scandinavian journal of work, environment & health*. Nordic Association of Occupational Safety and Health (NOROSH), 43(3), pp. 197–209. doi: 10.5271/sjweh.3641.

Gutbier, S. *et al.* (2018) ‘Major changes of cell function and toxicant sensitivity in cultured cells undergoing mild, quasi-natural genetic drift’, *Archives of Toxicology*. Springer, 92(12), pp. 3487–3503. doi: 10.1007/s00204-018-2326-5.

Hartfield, E. M. *et al.* (2014) ‘Physiological Characterisation of Human iPS-Derived Dopaminergic Neurons’, *PLoS ONE*. Edited by P. Lewis. Public Library of Science, 9(2), p. e87388. doi: 10.1371/journal.pone.0087388.

Herrero-Mendez, A. *et al.* (2009) ‘The bioenergetic and antioxidant status of neurons is controlled by continuous degradation of a key glycolytic enzyme by APC/C–Cdh1’, *Nature Cell Biology*. Nature Publishing Group, 11(6), pp. 747–752. doi: 10.1038/ncb1881.

Hirayama, N. *et al.* (2018) ‘Necrosis in human neuronal cells exposed to paraquat’, *Journal of Toxicological Sciences*, pp. 193–202. doi: 10.2131/jts.43.193.

Hirtz, D. *et al.* (2007) ‘How common are the "common" neurologic disorders?’, *Neurology*. American Academy of Neurology, 68(5), pp. 326–37. doi: 10.1212/01.wnl.0000252807.38124.a3.

Höglinger, G. U. *et al.* (2003) ‘Dysfunction of mitochondrial complex I and the proteasome: Interactions between two biochemical deficits in a cellular model of Parkinson’s disease’, *Journal of Neurochemistry*, 86(5), pp. 1297–1307. doi: 10.1046/j.1471-4159.2003.01952.x.

IARC Working Group on the Evaluation of Carcinogenic Risk to Humans (2017) *Some Organophosphate Insecticides and Herbicides*. 112th edn. Lyon (FR): International Agency for Research on Cancer. Available at: https://www.ncbi.nlm.nih.gov/books/NBK436760/ (Accessed: 20 April 2020).

Idriss, S. and Levitt, J. (2009) ‘Malathion for head lice and scabies: Treatment and safety considerations’, *Journal of Drugs in Dermatology*, 8(8), pp. 715–720.

Jantas-Skotniczna, D., Kajta, M. and Lasoń, W. (2006) ‘Memantine attenuates staurosporine-induced activation of caspase-3 and LDH release in mouse primary

neuronal cultures', *Brain Research*. Elsevier, 1069(1), pp. 145–153. doi: 10.1016/J.BRAINRES.2005.11.055.

Khedr, E. M. *et al.* (2012) 'Epidemiological study and clinical profile of Parkinson's disease in the Assiut Governorate, Egypt: a community-based study.', *Neuroepidemiology*. Karger Publishers, 38(3), pp. 154–63. doi: 10.1159/000335701.

Klein, C. and Westenberger, A. (2012) 'Genetics of Parkinson's disease.', *Cold Spring Harbor perspectives in medicine*. Cold Spring Harbor Laboratory Press, 2(1), p. a008888. doi: 10.1101/cshperspect.a008888.

Kleinstreuer, N. C. *et al.* (2016) 'Adverse outcome pathways: From research to regulation scientific workshop report', *Regulatory Toxicology and Pharmacology*. Elsevier Ltd, 76, pp. 39–50. doi: 10.1016/j.yrtph.2016.01.007.

Klintworth, H. *et al.* (2007) 'Activation of c-Jun N-terminal protein kinase is a common mechanism underlying paraquat- and rotenone-induced dopaminergic cell apoptosis', *Toxicological Sciences*, 97(1), pp. 149–162. doi: 10.1093/toxsci/kfm029.

Ko, K. R. *et al.* (2020) 'SH-SY5Y and LUHMES cells display differential sensitivity to MPP+, tunicamycin, and epoxomicin in 2D and 3D cell culture', *Biotechnology Progress*, 36(2). doi: 10.1002/btpr.2942.

Kokushi, E. *et al.* (2015) 'Effects of chlorpyrifos on the metabolome of the freshwater carp, Cyprinus Carpio', *Environmental Toxicology*, 30(3), pp. 253–260. doi: 10.1002/tox.21903.

Kovalevich, J. and Langford, D. (2013) 'Considerations for the use of SH-SY5Y neuroblastoma cells in neurobiology.', *Methods in molecular biology (Clifton, N.J.)*. NIH Public Access, 1078, pp. 9–21. doi: 10.1007/978-1-62703-640-5_2.

Kowal, S. L. *et al.* (2013) 'The current and projected economic burden of Parkinson's disease in the United States', *Movement Disorders*, 28(3), pp. 311–318. doi: 10.1002/mds.25292.

Krug, A. K. *et al.* (2014) 'Transcriptional and metabolic adaptation of human neurons to the mitochondrial toxicant MPP +', *Cell Death and Disease*, 5(5), pp. 1–15. doi: 10.1038/cddis.2014.166.

Lazarou, M. *et al.* (2009) 'Assembly of mitochondrial complex I and defects in disease', *Biochimica et Biophysica Acta (BBA) - Molecular Cell Research*. Elsevier, 1793(1), pp.

78–88. doi: 10.1016/J.BBAMCR.2008.04.015.

Lecker, S. H., Goldberg, A. L. and Mitch, W. E. (2006) 'Protein degradation by the ubiquitin-proteasome pathway in normal and disease states', *Journal of the American Society of Nephrology*, 17(7), pp. 1807–1819. doi: 10.1681/ASN.2006010083.

Leestemaker, Y. and Ovaa, H. (2017) 'Tools to investigate the ubiquitin proteasome system', *Drug Discovery Today: Technologies*. Elsevier Ltd, 26, pp. 25–31. doi: 10.1016/j.ddtec.2017.11.006.

Leist, M. *et al.* (1997) 'Intracellular Adenosine Triphosphate (ATP) Concentration: A Switch in the Decision Between Apoptosis and Necrosis', *The Journal of Experimental Medicine*. The Rockefeller University Press, 185(8), pp. 1481–1486. doi: 10.1084/jem.185.8.1481.

Liou, H. H. *et al.* (1996) 'Effects of paraquat on the substantia nigra of the wistar rats: neurochemical, histological, and behavioral studies.', *Toxicology and applied pharmacology*, 137(1), pp. 34–41. doi: 10.1006/taap.1996.0054.

Van Loo, G. *et al.* (2002) 'The role of mitochondrial factors in apoptosis: A Russian roulette with more than one bullet', *Cell Death and Differentiation*. Nature Publishing Group, pp. 1031–1042. doi: 10.1038/sj.cdd.4401088.

Lopes, F. M. *et al.* (2010) 'Comparison between proliferative and neuron-like SH-SY5Y cells as an in vitro model for Parkinson disease studies', *Brain Research*, 1337, pp. 85–94. doi: 10.1016/j.brainres.2010.03.102.

Lopes, F. M. *et al.* (2017) 'Mimicking Parkinson's Disease in a Dish: Merits and Pitfalls of the Most Commonly used Dopaminergic In Vitro Models', *NeuroMolecular Medicine*, 19(2–3), pp. 241–255. doi: 10.1007/s12017-017-8454-x.

Lotharius, J. *et al.* (2005) 'Progressive degeneration of human mesencephalic neuron-derived cells triggered by dopamine-dependent oxidative stress is dependent on the mixed-lineage kinase pathway', *Journal of Neuroscience*, 25(27), pp. 6329–6342. doi: 10.1523/JNEUROSCI.1746-05.2005.

Van Maele-Fabry, G. *et al.* (2012) 'Occupational exposure to pesticides and Parkinson's disease: A systematic review and meta-analysis of cohort studies', *Environment International*. Pergamon, 46, pp. 30–43. doi: 10.1016/J.ENVINT.2012.05.004.

Mahajani, S. *et al.* (2019) 'Homogenous generation of dopaminergic neurons from multiple hiPSC lines by transient expression of transcription factors', *Cell Death and Disease*. Springer US, 10(12). doi: 10.1038/s41419-019-2133-9.

Marino, B. L. B. *et al.* (2019) 'Parkinson's disease: A Review from the Pathophysiology to Diagnosis, New Perspectives for Pharmacological Treatment', *Mini-Reviews in Medicinal Chemistry*, 19. doi: 10.2174/1389557519666191104110908.

Martinez-Martin, P. *et al.* (2019) 'The long-term direct and indirect economic burden among Parkinson's disease caregivers in the United States', *Movement Disorders*, 34(2), pp. 236–245. doi: 10.1002/mds.27579.

Martins, L. M. and Sood, P. (2016) 'Paraquat-induced metabolic stress signature in human foetal mesencephalic cells', *Matters*, pp. 1–7. doi: 10.19185/matters.201611000025.

McCormack, A. L. et al. (2002) 'Environmental risk factors and Parkinson's disease: Selective degeneration of nigral dopaminergic neurons caused by the herbicide paraquat', Neurobiology of Disease. Neurobiol Dis, 10(2), pp. 119–127. doi: 10.1006/nbdi.2002.0507.

McNaught, K. S. . and Jenner, P. (2001) 'Proteasomal function is impaired in substantia nigra in Parkinson's disease', *Neuroscience Letters*. Elsevier, 297(3), pp. 191–194. doi: 10.1016/S0304-3940(00)01701-8.

McNaught, K. S. P. et al. (2003) 'Altered proteasomal function in sporadic Parkinson's disease', Experimental Neurology, 179(1), pp. 38–46. doi: 10.1006/exnr.2002.8050.

McNaught, K. S. P. *et al.* (2004) 'Systemic exposure to proteasome inhibitors causes a progressive model of Parkinson's disease', *Annals of Neurology*. John Wiley & Sons, Ltd, 56(1), pp. 149–162. doi: 10.1002/ana.20186.

Meiser, J. et al. (2016) 'Loss of DJ-impairs antioxidant response by altered glutamine and serine metabolism', Neurobiology of Disease. The Authors, 89(March), pp. 112–125. doi: 10.1016/j.nbd.2016.01.019.

Miksys, S. and Tyndale, R. F. (2013) 'Cytochrome P450-mediated drug metabolism in the brain', *Journal of Psychiatry and Neuroscience*, 38(3), pp. 152–163. doi: 10.1503/jpn.120133.

Mochizuki, H. *et al.* (1996) 'Histochemical detection of apoptosis in Parkinson's

disease', *Journal of the Neurological Sciences*. Elsevier, 137(2), pp. 120–123. doi: 10.1016/0022-510X(95)00336-Z.

Mohammadzadeh, L. *et al.* (2018) 'Neuroprotective potential of crocin against malathion-induced motor deficit and neurochemical alterations in rats', *Environmental Science and Pollution Research*, 25(5), pp. 4904–4914. doi: 10.1007/s11356-017-0842-0.

Moreno, A. J. and Madeira, V. M. (1990) 'Interference of parathion with mitochondrial bioenergetics.', Biochimica et biophysica acta. Netherlands, 1015(2), pp. 361–367. doi: 10.1016/0005-2728(90)90041-2.

Mortensen, A. *et al.* (2017) 'Safety of the proposed amendment of the specifications for the food additive polyvinyl alcohol-polyethylene glycol-graft-co-polymer (E 1209)', *EFSA Journal*, 15(6). doi: 10.2903/j.efsa.2017.4865.

Mostafalou, S. *et al.* (2012) 'Protective effect of NAC against malathion-induced oxidative stress in freshly isolated rat hepatocytes.', *Advanced pharmaceutical bulletin*. Tabriz University of Medical Sciences, 2(1), pp. 79–88. doi: 10.5681/apb.2012.011.

Moyano, P. *et al.* (2019) 'Proteasome 20S and Rab5 Alteration after 24 h and 14 Days Chlorpyrifos Exposure Lead to β-Amyloid and Tau Protein Level Increases and SN56 Neuronal Cell Death', *Chemical Research in Toxicology*. American Chemical Society, 32(10), pp. 1920–1924. doi: 10.1021/acs.chemrestox.9b00216.

Narayan, S. *et al.* (2017) 'Occupational pesticide use and Parkinson's disease in the Parkinson Environment Gene (PEG) study', *Environment International*, 107, pp. 266–273. doi: 10.1016/j.envint.2017.04.010.

Nicklas, W. J. *et al.* (1987) 'IV. MPTP, MPP+ and mitochondrial function', *Life Sciences*. Pergamon, 40(8), pp. 721–729. doi: 10.1016/0024-3205(87)90299-2.

Nimtz, L. *et al.* (2020) 'Characterization and application of electrically active neuronal networks established from human induced pluripotent stem cell-derived neural progenitor cells for neurotoxicity evaluation', *Stem Cell Research*. Elsevier, 45, p. 101761. doi: 10.1016/J.SCR.2020.101761.

Ntzani, E. E. et al. (2013) 'Literature review on epidemiological studies linking exposure to pesticides and health effects', EFSA Supporting Publications, 10(10), pp. 1–159. doi: 10.2903/sp.efsa.2013.en-497.

Ockleford, C. *et al.* (2017) 'Investigation into experimental toxicological properties of plant protection products having a potential link to Parkinson's disease and childhood leukaemia†', *EFSA Journal*, 15(3). doi: 10.2903/j.efsa.2017.4691.

OECD (2015) 'OECD Style Guide', *OECD Style Guide*. doi: 10.1787/9789264243439-en.

Oertel, W. H. (2017) 'Recent advances in treating Parkinson's disease.', *F1000Research*. Faculty of 1000 Ltd, 6, p. 260. doi: 10.12688/f1000research.10100.1.

Overk, C. R. and Mufson, E. J. (2010) 'Dopamine Transporter: Aging and Parkinson's Disease', in *Encyclopedia of Movement Disorders*. Academic Press, pp. 330–332. doi: 10.1016/B978-0-12-374105-9.00237-9.

Pamies, D. *et al.* (2018) 'Rotenone exerts developmental neurotoxicity in a human brain spheroid model', *Toxicology and applied pharmacology*. NIH Public Access, 354, p. 101. doi: 10.1016/J.TAAP.2018.02.003.

Park, J. H. *et al.* (2013) 'Autophagy regulates chlorpyrifos-induced apoptosis in SH-SY5Y cells', *Toxicology and Applied Pharmacology*. Elsevier B.V., 268(1), pp. 55–67. doi: 10.1016/j.taap.2013.01.013.

Parkinson, J. (2002) 'An Essay on the Shaking Palsy', *The Journal of Neuropsychiatry and Clinical Neurosciences*, 14(2), pp. 223–236. doi: 10.1176/jnp.14.2.223.

Pinheiro, M. V. S. *et al.* (2005) 'The effect of different sweeteners in low-calorie yogurts - A review', *International Journal of Dairy Technology*, 58(4), pp. 193–199. doi: 10.1111/j.1471-0307.2005.00228.x.

Poewe, W. (2008) 'Non-motor symptoms in Parkinson's disease', *European Journal of Neurology*, pp. 14–20. doi: 10.1111/j.1468-1331.2008.02056.x.

Pöltl, D. *et al.* (2012) 'Uncoupling of ATP-depletion and cell death in human dopaminergic neurons', *NeuroToxicology*, 33(4), pp. 769–779. doi: 10.1016/j.neuro.2011.12.007.

Pouchieu, C. *et al.* (2018) 'Pesticide use in agriculture and Parkinson's disease in the AGRICAN cohort study', *International Journal of Epidemiology*. Oxford University Press, 47(1), pp. 299–310. doi: 10.1093/ije/dyx225.

Presgraves, S. P. *et al.* (2003) 'Terminally differentiated SH-SY5Y cells provide a model system for studying neuroprotective effects of dopamine agonists', *Neurotoxicity*

Research, 5(8), pp. 579–598. doi: 10.1007/BF03033178.

Qiao, D., Seidler, F. J. and Slotkin, T. A. (2001) 'Developmental neurotoxicity of chlorpyrifos modeled in vitro: comparative effects of metabolites and other cholinesterase inhibitors on DNA synthesis in PC12 and C6 cells', *Environ Health Perspect*. 2001/10/24, 109(9), pp. 909–913.

Raha, S. and Robinson, B. H. (2000) 'Mitochondria, oxygen free radicals, disease and ageing', *Trends in Biochemical Sciences*. Elsevier Current Trends, 25(10), pp. 502–508. doi: 10.1016/S0968-0004(00)01674-1.

Ramachandiran, S. *et al.* (2007) 'Divergent Mechanisms of Paraquat, MPP+, and Rotenone Toxicity: Oxidation of Thioredoxin and Caspase-3 Activation', *Toxicological Sciences*. Oxford Academic, 95(1), pp. 163–171. doi: 10.1093/toxsci/kfl125.

Rampersad, S. N. (2012) 'Multiple applications of alamar blue as an indicator of metabolic function and cellular health in cell viability bioassays', *Sensors (Switzerland)*, 12(9), pp. 12347–12360. doi: 10.3390/s120912347.

Ramsay, R. R. *et al.* (1986) 'Inhibition of mitochondrial NADH dehydrogenase by pyridine derivatives and its possible relation to experimental and idiopathic parkinsonism', *Biochemical and Biophysical Research Communications*. Academic Press, 135(1), pp. 269–275. doi: 10.1016/0006-291X(86)90972-1.

Ren, Y. *et al.* (2005) 'Selective vulnerability of dopaminergic neurons to microtubule depolymerization', *Journal of Biological Chemistry*, 280(40), pp. 34105–34112. doi: 10.1074/jbc.M503483200.

Rhodes, S. L. *et al.* (2013) 'Pesticides that inhibit the ubiquitin-proteasome system: Effect measure modification by genetic variation in SKP1 in Parkinson[U+05F3]s disease', *Environmental Research*. NIH Public Access, 126, pp. 1–8. doi: 10.1016/j.envres.2013.08.001.

Roser, M. (2020) 'Pesticides', *Our World in Data*. Available at: https://ourworldindata.org/pesticides (Accessed: 13 May 2020).

Rösler, T. W. *et al.* (2018) 'K-variant BCHE and pesticide exposure: Gene-environment interactions in a case–control study of Parkinson's disease in Egypt', *Scientific Reports*. Nature Publishing Group, 8(1), p. 16525. doi: 10.1038/s41598-018-35003-4.

Ryan, S. D. *et al.* (2013) 'Isogenic Human iPSC Parkinson's Model Shows Nitrosative

Stress-Induced Dysfunction in MEF2-PGC1α Transcription', *Cell*. Cell Press, 155(6), pp. 1351–1364. doi: 10.1016/J.CELL.2013.11.009.

Salama, M. *et al.* (2012) 'Colchicine Protects Dopaminergic Neurons in a Rat Model of Parkinson ' s Disease', pp. 1–8.

Salama, M. *et al.* (2014) 'Mitochondrial complex I inhibition as a possible mechanism of chlorpyrifos induced neurotoxicity', *Annals of Neurosciences*, 21(3), pp. 85–89. doi: 10.5214/ans.0972.7531.210303.

Schapira, A. H. V. *et al.* (1990) 'Anatomic and Disease Specificity of NADH CoQ 1 Reductase (Complex I) Deficiency in Parkinson's Disease', *Journal of Neurochemistry*. Wiley/Blackwell (10.1111), 55(6), pp. 2142–2145. doi: 10.1111/j.1471-4159.1990.tb05809.x.

Schildknecht, S. *et al.* (2009) 'Requirement of a dopaminergic neuronal phenotype for toxicity of low concentrations of 1-methyl-4-phenylpyridinium to human cells', *Toxicol Appl Pharmacol*, 241(1), pp. 23–35. doi: 10.1016/j.taap.2009.07.027.

Schildknecht, S. *et al.* (2013) 'Generation of genetically-modified human differentiated cells for toxicological tests and the study of neurodegenerative diseases', *Altex*, 30(4), pp. 427–444. doi: 10.14573/altex.2013.4.427.

Schmidt, W. J. and Alam, M. (2006) 'Controversies on new animal models of Parkinson's disease Pro and Con: the rotenone model of Parkinson's disease (PD)', in *Parkinson's Disease and Related Disorders*. Vienna: Springer Vienna, pp. 272–276. doi: 10.1007/978-3-211-45295-0_42.

Scholz, D. *et al.* (2011) 'Rapid, complete and large-scale generation of post-mitotic neurons from the human LUHMES cell line', *Journal of Neurochemistry*, 119(5), pp. 957–971. doi: 10.1111/j.1471-4159.2011.07255.x.

Sekowski, J. W. *et al.* (2014) 'Metabolomic Analysis of the Secretome of Human Embryonic Stem Cells Following Methyl Parathion and Methyl Paraoxon Exposure, Phase I: Initial Nontargeted LC-MS', (January), pp. 1–17. Available at: http://oai.dtic.mil/oai/oai?verb=getRecord&metadataPrefix=html&identifier=ADA594768.

Shamoto-Nagai, M. *et al.* (2003) 'An Inhibitor of Mitochondrial Complex I, Rotenone, Inactivates Proteasome by Oxidative Modification and Induces Aggregation of

Oxidized Proteins in SH-SY5Y Cells', *Journal of Neuroscience Research*, 74(4), pp. 589–597. doi: 10.1002/jnr.10777.

Sharma, A. *et al.* (2019) 'Worldwide pesticide usage and its impacts on ecosystem', *SN Applied Sciences*. Springer, 1(11), p. 1446. doi: 10.1007/s42452-019-1485-1.

Shi, Y. *et al.* (2017) 'Induced pluripotent stem cell technology: a decade of progress', *Nature reviews. Drug discovery*. NIH Public Access, 16(2), p. 115. doi: 10.1038/NRD.2016.245.

Shimizu, K. *et al.* (2001) 'Carrier-mediated processes in blood–brain barrier penetration and neural uptake of paraquat', *Brain Research*. Elsevier, 906(1–2), pp. 135–142. doi: 10.1016/S0006-8993(01)02577-X.

Siekevitz, P. (1957) 'Powerhouse of the Cell', *Scientific American*. Scientific American, a division of Nature America, Inc., pp. 131–144. doi: 10.2307/24940890.

Somayajulu-Niţu, M. *et al.* (2009) 'Paraquat induces oxidative stress, neuronal loss in substantia nigra region and Parkinsonism in adult rats: Neuroprotection and amelioration of symptoms by water-soluble formulation of Coenzyme Q10', *BMC Neuroscience*, 10(1), p. 88. doi: 10.1186/1471-2202-10-88.

Sparling, D. W. and Fellers, G. (2007) 'Comparative toxicity of chlorpyrifos, diazinon, malathion and their oxon derivatives to larval Rana boylii', *Environmental Pollution*. Elsevier, 147(3), pp. 535–539. doi: 10.1016/J.ENVPOL.2006.10.036.

Stefanis, L. (2012) 'a -Synuclein in Parkinson ' s Disease', Cold Spring Harb Perspect Med, pp. 1–24. doi: 10.1101/cshperspect.a009399.

Stenesh, J. (1998) 'The Citric Acid Cycle', in *Biochemistry*. Boston, MA: Springer US, pp. 273–291. doi: 10.1007/978-1-4757-9427-4_11.

Sui, W. *et al.* (2012) 'A proton nuclear magnetic resonance-based metabonomics study of metabolic profiling in immunoglobulin a nephropathy', *Clinics*. Hospital das Clinicas da Faculdade de Medicina da Universidade de Sao Paulo, 67(4), p. 363. doi: 10.6061/CLINICS/2012(04)10.

Sun, C. *et al.* (2019) 'Activation of the immunoproteasome protects SH-SY5Y cells from the toxicity of rotenone', *NeuroToxicology*. Elsevier, 73(107), pp. 112–119. doi: 10.1016/j.neuro.2019.03.004.

Suzuki, S. *et al.* (2017) 'Efficient induction of dopaminergic neuron differentiation from

induced pluripotent stem cells reveals impaired mitophagy in PARK2 neurons', *Biochemical and Biophysical Research Communications*. Elsevier Ltd, 483(1), pp. 88–93. doi: 10.1016/j.bbrc.2016.12.188.

Swistowski, A. *et al.* (2010) 'Efficient Generation of Functional Dopaminergic Neurons from Human Induced Pluripotent Stem Cells Under Defined Conditions', *STEM CELLS*. John Wiley & Sons, Ltd, 28(10), pp. 1893–1904. doi: 10.1002/stem.499.

Takahashi, K. *et al.* (2007) 'Induction of pluripotent stem cells from fibroblast cultures', *Nature Protocols*. Nature Publishing Group, 2(12), pp. 3081–3089. doi: 10.1038/nprot.2007.418.

Talpade, D. J. *et al.* (2008) 'In Vivo Labeling of Mitochondrial Complex I (NADH:UbiquinoneOxidoreductase) in Rat Brain Using [3H]Dihydrorotenone', *Journal of Neurochemistry*. Wiley/Blackwell (10.1111), 75(6), pp. 2611–2621. doi: 10.1046/j.1471-4159.2000.0752611.x.

Tanner, C. M. *et al.* (2011) 'Rotenone, paraquat, and Parkinson's disease', *Environmental Health Perspectives*, 119(6), pp. 866–872. doi: 10.1289/ehp.1002839.

Terron, A. *et al.* (2018) *An adverse outcome pathway for parkinsonian motor deficits associated with mitochondrial complex I inhibition*, *Archives of Toxicology*. Springer Berlin Heidelberg. doi: 10.1007/s00204-017-2133-4.

Tofoli, F. A. *et al.* (2019) 'Midbrain Dopaminergic Neurons Differentiated from Human-Induced Pluripotent Stem Cells', in, pp. 97–118. doi: 10.1007/978-1-4939-9007-8_8.

Tong, Z. B. *et al.* (2017) 'Characterization of three human cell line models for high-throughput neuronal cytotoxicity screening', *J Appl Toxicol*. 2016/05/05, 37(2), pp. 167–180. doi: 10.1002/jat.3334.

Toulouse, A. and Sullivan, A. M. (2008) 'Progress in Parkinson's disease—Where do we stand?', *Progress in Neurobiology*. Pergamon, 85(4), pp. 376–392. doi: 10.1016/J.PNEUROBIO.2008.05.003.

Tufi, S. (2016) *Metabolomics to investigate pesticide-induced neurotoxicity in non-target species*. Available at: https://core.ac.uk/display/43409391?recSetID=a79fc3e9d3ca241e8ab6ea224244db06::5ac7eca29d72c6.39427957%0Ahttp://core.ac.uk/download/pdf/43409391.pdf.

Turton, N. *et al.* (2020) 'The Effect of Organophosphate Exposure on Neuronal Cell

Coenzyme Q10 Status', *Neurochemical Research*. Springer US, (0123456789). doi: 10.1007/s11064-020-03033-y.

Ullrich, C. and Humpel, C. (2009) 'Rotenone induces cell death of cholinergic neurons in an organotypic co-culture brain slice model', *Neurochemical Research*, 34(12), pp. 2147–2153. doi: 10.1007/s11064-009-0014-9.

Venkatesan, R. *et al.* (2017) 'Gnetol, a Resveratrol Derivative Ameliorates Malathion-Induced Neurotoxicity through Modulating Lysosomal Membrane Permeabilization in N2a Cells', *Journal of Alzheimer's Disease & Parkinsonism*, 07(06). doi: 10.4172/2161-0460.1000388.

Villeneuve, D. L. *et al.* (2014) 'Adverse Outcome Pathway (AOP) Development I: Strategies and Principles', *Toxicological Sciences*. Oxford Academic, 142(2), pp. 312–320. doi: 10.1093/toxsci/kfu199.

Wang, C. and Youle, R. J. (2009) 'The Role of Mitochondria in Apoptosis', *Annual Review of Genetics*, 43(1), pp. 95–118. doi: 10.1146/annurev-genet-102108-134850.

Wang, Y. *et al.* (2019) 'Cytotoxic effects of parathion, paraoxon, and their methylated derivatives on a mouse neuroblastoma cell line NB41A3', *Fundamental Toxicological Sciences*, 6(2), pp. 45–56. doi: 10.2131/fts.6.45.

Wani, W. Y. *et al.* (2017) 'Cell cycle activation in p21 dependent pathway: An alternative mechanism of organophosphate induced dopaminergic neurodegeneration.', *Biochimica et biophysica acta*. Netherlands, 1863(7), pp. 1858–1866. doi: 10.1016/j.bbadis.2016.05.014.

Winklhofer, K. F. and Haass, C. (2010) 'Mitochondrial dysfunction in Parkinson's disease', *Biochimica et Biophysica Acta (BBA) - Molecular Basis of Disease*. Elsevier, 1802(1), pp. 29–44. doi: 10.1016/J.BBADIS.2009.08.013.

Xicoy, H. *et al*. (2017) 'The SH-SY5Y cell line in Parkinson's disease research: a systematic review', *Molecular Neurodegeneration*. Molecular Neurodegeneration, 12(1), pp. 1–11. doi: 10.1186/s13024-017-0149-0.

Xu, M. Y. *et al.* (2015) 'Metabolomics Analysis and Biomarker Identification for Brains of Rats Exposed Subchronically to the Mixtures of Low-Dose Cadmium and Chlorpyrifos', *Chemical Research in Toxicology*, 28(6), pp. 1216–1223. doi: 10.1021/acs.chemrestox.5b00054.

Yang, W. and Tiffany-Castiglioni, E. (2007) 'The bipyridyl herbicide paraquat induces proteasome dysfunction in human neuroblastoma SH-SY5Y cells', *Journal of Toxicology and Environmental Health - Part A: Current Issues*, 70(21), pp. 1849–1857. doi: 10.1080/15287390701459262.

Yu, J. *et al.* (2007) 'Induced pluripotent stem cell lines derived from human somatic cells', *Science*, 318(5858), pp. 1917–1920. doi: 10.1126/science.1151526.

Zeisel, S. H. (2006) 'Choline: Critical Role During Fetal Development and Dietary Requirements in Adults', *Annual Review of Nutrition*. NIH Public Access, 26(1), pp. 229–250. doi: 10.1146/annurev.nutr.26.061505.111156.

Zhang, P., Xia, N. and Reijo Pera, R. A. (2014a) 'Directed Dopaminergic Neuron Differentiation from Human Pluripotent Stem Cells', *Journal of Visualized Experiments*, (91), pp. e51737–e51737. doi: 10.3791/51737.

Zhang, X. M., Yin, M. and Zhang, M. H. (2014b) 'Cell-based assays for Parkinson's disease using differentiated human LUHMES cells', *Acta Pharmacologica Sinica*. Nature Publishing Group, 35(7), pp. 945–956. doi: 10.1038/aps.2014.36.

Zhao, R. Z. *et al.* (2019) 'Mitochondrial electron transport chain, ROS generation and uncoupling (Review)', *International Journal of Molecular Medicine*, 44(1), pp. 3–15. doi: 10.3892/ijmm.2019.4188.

Zhu, H. *et al.* (2001) 'Effects of single or repeated dermal exposure to methyl parathion on behavior and blood cholinesterase activity in rats', *Journal of Biomedical Science*, 8(6), pp. 467–474. doi: 10.1159/000046168.

6 Appendix

6.1 List of Figures

6.2 List of Tables

Acknowledgments

I greatly thank my academic tutors for their help and support in the development of my Ph.D. thesis.

I would like to express my gratitude to Prof. Dr. Ellen Fritsche for providing the topic of PhD, which is both very interesting and future-proof, and for offering comprehensive care, continuous support throughout the entire PhD period, discussions about experimental settings, scientific questions, and the other issues that evolve with my project for Ph.D. thesis.

I would like to greatly thank Prof. Dr. Vlada Urlacher for the co-supervision that made my dissertation possible and for taking on the mentorship.

I would like to express my thankfulness to the Egyptian Ministry of Higher Education and Scientific Research (MHESR) and the German Academic Exchange Service (DAAD) for providing me with the German-Egyptian Research Long Term Scholarship (GERLS), Heinrich Heine University Düsseldorf for offering me with the STIBET Completion of Studies Grant and Bayer CropScience company for funding the current work.

Also, I greatly appreciate and thank Stefan, Katharina and Ines who I could count on for long time in the lab and for their extensive work with me and for all the proofreading. They always supported me competently and warmly with all respects, especially in the last phases of my work.

Additionally, I thank all lab members for a great working atmosphere. Thanks, Arif, Eike, Etta, Farina, Gaby, Georgea, Jördis, Julias, Kevin, Kristina, Lynn, Mats, Saskia and Ulrike.

I would like to extend thanks to Dr. Jessica Gätjens, the scientific coordinator for this PhD program for providing advice and support during the whole PhD period. Also, I thank the PhD committee in the Medical Faculty, HHU, for offering this well-structured program with many beneficial lectures and workshops which allow me to foster my knowledge, improve my soft skills and extend my network.

Last, but not least I would like to express my greatest gratitude to my family and friends, in first line to my parents, wife, children and sisters. Thank you for your support, encouragement, backing, criticisms, reality, discussions, and unlimited love.